Abstract

PATERNAL DIET AND EXERCISE EPIGENETICALLY PROGRAM ENERGY EXPENDITURE AND GLUCOSE METABOLISM IN MOUSE OFFSPRING (Under the direction of Dr. Alexander K. Murashov) Department of Physiology, August 2013.

It is currently estimated that a third of Americans suffer from metabolic syndrome, which is an obesogenic disease shown to increase risk for developing type 2 diabetes (T2DM) by five-fold (Diabetes Care, 2012). The pervasiveness of obesity and T2DM is largely the result of unbalanced nutrition and lack of physical activity. Epidemiological investigations are now finding the detrimental effects of poor lifestyle choices, such as consuming a high-fat diet, have heritable consequences that persist transgenerationally by way of epigenetic modifications.

The epigenome is yet another tier of genetic regulation, one that is capable of producing heritable changes in gene expression without altering the underlying sequence of nucleotides. In an effort to better understand the pathogenesis of these overly prevalent diseases (i.e. obesity and T2DM) researchers have now set their sights on faulty epigenetic machinery. To date, research has primarily focused on epigenetic modifications associated with maternal descent, mainly because of the significant influence had by lifestyle and the environment during 9-months *in utero*. Consequently, the roles of paternal lifestyle choices, like diet and activity, have not received adequate attention.

Using a C57BL/6J mouse model we examined the transgenerational effects of a paternal high fat-diet and prolonged exercise on male offspring's susceptibility to glucose intolerance. Founder fathers (F_0) were randomly divided into three groups: control-diet fathers (CF) // high-fat fathers (FF); 60% of energy derived from fat // control-diet fathers with exercise wheel (EF). After 12 weeks of a high-fat diet (HFD) or free-wheel running F_0 males from each group were mated with control females. At 4 weeks of age their male offspring (F_1) were assigned to either a

HFD or control diet (CD) for a duration of 12 weeks. Metabolic profiles were assessed via indirect calorimetry (i.e. metabolic cages), glucose tolerance testing (GTT), fasting plasma insulin, eMRI imaging (fat/lean body composition), as well as monitoring of developmental milestones. A comparison between cohorts of offspring on post-natal day 7 revealed a significantly lower mean birth weight in the HFD-father offspring (FFO); a factor shown in humans to be predictive of obesity and impaired glucose tolerance in adulthood (Bhargava et. al. 2004). Additionally, when challenged with a HFD only exercise father offspring (EFO) exhibited diabetic traits, such as fasting hyperglycemia, fasting hyperinsulinemia, lower energy expenditure, as well as increased body weight and adiposity.

To better understand the molecular mechanisms driving these observations quantitative real-time PCR was utilized to examine the methylation profile and gene expression within insulin sensitive tissues like the liver, pancreas, and gastrocnemius muscle. Data show intriguing differences in expression of several metabolic genes such as: *Ogt, Oga, Pdk4, Glut4, Ptpn1, Igf2, H19*, and *FoxO1*. Furthermore, with the exception of *Glut4*, methylation patterns in fathers were preserved within male offspring. These novel findings suggest that offspring have a phenotype that is epigenetically programmed to thrive under the same experimental conditions as their respective fathers.

PATERNAL DIET AND EXERCISE EPIGENETICALLY PROGRAM ENERGY EXPENDITURE AND GLUCOSE METABOLISM IN MOUSE OFFSPRING

A Thesis

Presented To the Faculty of the Department of Physiology

East Carolina University

In Partial Fulfillment of the Requirements for the Degree

Master of Science in Biomedical Science

by

Michael K. Koury

August 2013

PATERNAL DIET AND EXERCISE EPIGENETICALLY PROGRAM ENERGY EXPENDITURE AND GLUCOSE METABOLISM IN MOUSE OFFSPRING

by

Michael K. Koury

DIRECTOR OF THESIS: _____
Alexander K. Murashov, M.D., Ph.D.

COMMITTEE MEMBER: _____
P. Darrell Neufer, Ph.D.

COMMITTEE MEMBER: _____
Richard A. Franklin, Ph.D.

COMMITTEE MEMBER: _____
Dianne Walters, Ph.D.

CHAIR OF THE DEPARTMENT OF PHYSIOLOGY: _____
Robert Lust, Ph.D.

DEAN OF THE GRADUATE SCHOOL: _____
Paul J. Gemperline, Ph.D.

Acknowledgements

I want to first express my deepest gratitude to my thesis director and mentor, Dr. Alexander Murashov, for encouraging and facilitating all of my research endeavors. Without his guidance, support, and expertise, this project never would have been possible.

I would also like to thank the other members of my thesis committee, Dr. Darrell Neufer, Dr. Dianne Walters, and Dr. Richard Franklin, for all of their helpful advice and wisdom along the way. They always made themselves available to provide valuable and constructive feedback - for that I am grateful.

Elena Pak played an invaluable role in the quality and scope of my education. I am indebted to her for being so patient during the time spent teaching me several different proteomics assays, which were not only cornerstone to completing this study but they are also skills I can use in my future endeavors to better clinical medicine through research.

I want to thank all of the other faculty at the Brody School of Medicine as well whose contributions made this research possible. In addition to Dr. Dianne Walters, Dr. Jamie DeWitt and Dr. Kevin O'Brien were also kind enough to lend their advice on data analysis. Dr. Brian Shewchuk's help was indispensable to my education in primer design and methods for epigenetic analyses.

Finally, I want to thank all of the administrative personnel working in the Department of Physiology, as well as those in other supporting departments, for creating such a supportive and friendly learning environment.

Last, but certainly not least, I want to sincerely thank my friends, my family, and especially my wife Emily, for being so understanding and supportive during my academic pursuit to earn a Masters in Biomedical Sciences.

Table of Contents

List of Figures

List of Tables

List of Abbreviations

NTC ----------No Template Control

5’ ICDMR ----------5 Prime Imprint Control Differentially Methylated Region

AKT ----------Protein Kinase B

BSA ---------- Bovine Serum Albumin

CARM1 ---------- Coactivator-associated arginine methyltransferase 1

CF ---------- Control Father

CFO ---------- Control Father Offspring

DEPC ---------- Diethyl pyrocarbonate

dH_2O ---------- Distilled Water

DMR ---------- Differentially Methylated Region

DNA ---------- Deoxyribonucleic Acid

EDTA ----------Ethylenediaminetetraacetic acid

EF ---------- Exercise Father

EFO ---------- Exercise Father Offspring

eNOS ---------- Endothelial Nitric Oxide Synthase

ER ---------- Endoplasmic Reticulum

EtBr ---------- Ethidium Bromide

FF ---------- Fat Father (high-fat diet)

FFO ---------- Fat Father Offspring

FoxO1 ---------- Forkhead box class O 1

GFAT ----------D-fructose-6-phosphate amidotransferase 1

GFPT1 ----------Glucose-fructose phosphatase 1

Glut4 ----------Glucose transporter type 4

GTT ----------Glucose Tolerance Test

HAT Domain --------- Histone Acetyltransferase domain

HBP ----------Hexosamine Biosynthetic pathway

HCF1 ----------Host Cell Factor 1

Ins2 ----------Insulin II

IRS1 ----------Insulin receptor substrate-1

MALDI-TOF ---------Matrix-assisted laser desorption time-of-flight

MBD-cap ----------Methyl-Binding Domain Capture

MBD2 ----------Methyl-CpG Binding Domain Protein 2

Mgea5 ----------Meningioma-expressed antigen 5

MLL5 ----------Mixed-linease leukemia 5 (MLL5),

mOGT ----------Mitochondria-OGT

ncOGA ----------Nucleocytoplasmic-OGA

ncOGT ----------Nucleocytoplasmic-OGT

NeuroD1 ----------Neurogenic differentiation 1

NFκB ----------Nuclear factor kappa-light-chain-enhancer of activated B cells

nOGA ----------Nuclear OGA

O-GlcNAc ----------Beta-linked-ortho-acetylglucosamine

Oga ----------Peptide O-GlcNAc-beta-N-acetylglucosaminidase

Ogt----------Uridine diphospho-N-acetylglucosamine:peptide β-N acetylglucosaminyltransferase or O-GlcNAc Transferase

PBS ----------Phosphate buffered saline

PBST ----------Phosphate buffered saline-tween

PcG ----------Polycomb Group

PCG-1α----------Peroxisome proliferator-activated receptor gamma coactivator 1-alpha

PCR ----------Polymerase chain reaction

PDC ----------Pyruvate dehydrogenase complex

PDK4 ----------Pyruvate dehydrogenase lipoamide kinase isozyme 4

PDX-1 ----------Pancreatic and duodenal homeobox 1

PMSF ----------Phenylmethanesulfonyl fluoride

PP1c ----------Protein phosphatase 1

Ptpn1 ----------Tyrosine-protein phosphatase non-receptor type 1

PVDF ---------- Polyvinylidene difluoride

RIPA Buffer ----------Radioimmunoprecipitation assay

RNA ----------Ribonucleic acid

ROS ----------Reactive oxygenated species

SDS ----------Sodium dodecyl sulfate

SNP ----------Single Nucleotide Polymorphism

sOGT ----------Short OGT

Sxc ----------Super sex combs

T2DM ----------Type 2 Diabetes Mellitus

TBE ----------Tris-borate-EDTA

TBS ----------Tris buffered saline

TBST ----------Tris buffered saline-tween

TPR ----------Tetratricopeptide repeat

TSS----------Transcriptional start site

UDP-GlcNAc ---------Uridine diphosphate N-acetylglucosamine

XCI ----------X-Chromosome Inactivation

1.0 Introduction

1.1 Importance of Study

The United States has become one of the most overfed, yet undernourished, nations in the world with an estimated two-thirds of adults now considered to be over-weight (BMI≥25) and approximately 35.7% obese (BMI≥30) [1]. In addition to the staggering rates of obesity observed in the adult population, over the last 30 years its prevalence among children and adolescents (aged 2-19) has more than tripled (Figure 1) [2]. The pervasiveness of obesity, both in children and adults, largely stems from consuming a high calorie diet while living a sedentary lifestyle [3]. A proper balance between dietary intake and energy expenditure is crucial not only for maintaining a healthy weight but also for preserving normal glucose metabolism.

The onset of obesity has been shown to usher in an array of other metabolic dysfunctions such as Type II Diabetes Mellitus (T2DM), a disease which currently affects more than 25 million people in the United States and is seen to occur five- to six- times more often among obese individuals [4]. These two ailments alone have placed an enormous burden on the Nation's health care system, and in 2012 were found to account for nearly $366 billion in total medical costs [5-7]. In an effort to combat this ongoing obesity epidemic, and the co-morbidities inextricably tied to it, researchers have begun exploring new avenues of intervention within the developing field of epigenetics.

1.2 Statement of Problem

While both genetic and non-genetic environmental factors are known to contribute to the heritability of obesity and type II diabetes mellitus (T2DM), a change within the population gene pool during the past three decades doesn't account for such a rapid increase in the prevalence of obesity and diabetes in children [8]. Instead, such changes are likely a product of epigenetic modifications, which alter genomic transcription in a manner that affects the metabolic phenotype of successive generations [8]. Previous studies, which largely focused on epigenetic factors of maternal descent, successfully established there to be a link between maternal metabolism and that of their offspring [9,10]. However, paternal influences on the next generation are still poorly understood. Therefore, the following study used a mouse model to explore how paternal diet and exercise can epigenetically program the metabolism of male progeny.

1.3 Specific Aims

1) Evaluate differences between the metabolic profiles of male offspring born to fathers that consumed a HFD or to fathers given free access to an exercise wheel. Comparative analysis will be performed on data obtained by indirect calorimetry, glucose tolerance testing, magnetic resonance imaging, as well as measures of plasma insulin.

2) Identify any disparities in the gene expression or methylation profile between offspring cohorts (F_1 males) that are attributable to paternal exercise or paternal consumption of a HFD.

A

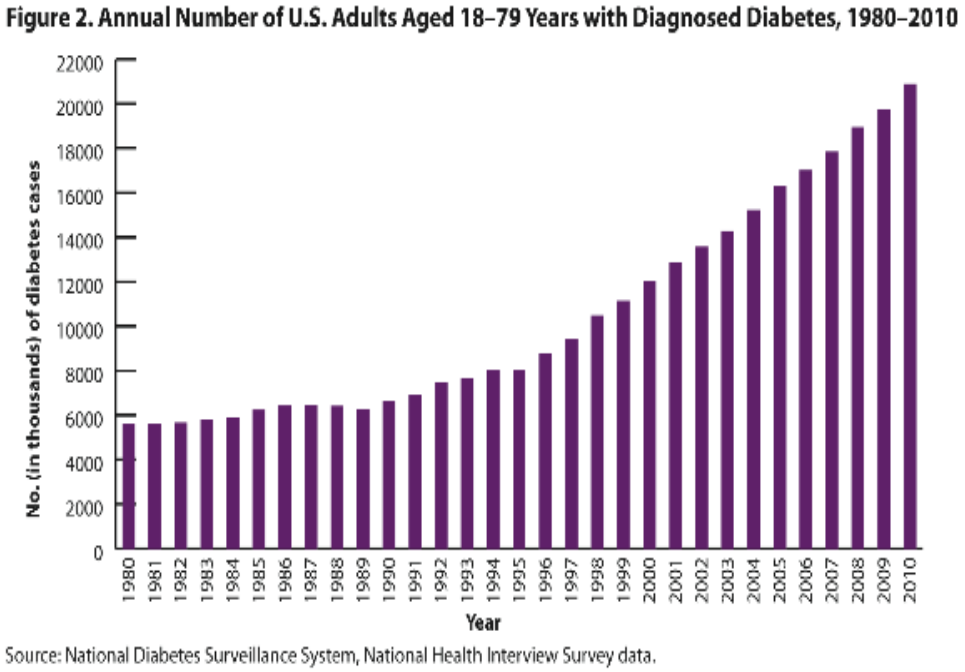

B

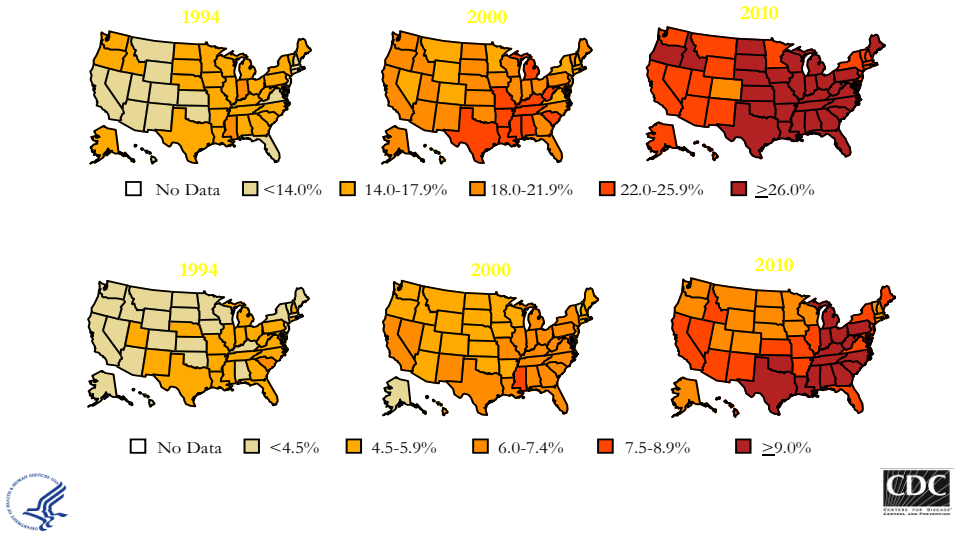

Figure 1. A – Number of newly diagnosed cases of T2DM in the United States. B – Correlation between increases in obesity and T2DM

	Overweight or Obese (BMI ≥ 85th percentile)	Obesity (BMI ≥ 95th percentile)
All	31.8%	16.9%
2-5 year olds	26.7%	12.1%
6-11 year olds	32.6%	18.0%
12-19 year olds	33.6%	18.4%

Table 1. U.S. Prevalence of Childhood Overweight and Obesity (NHANES 2009-2010)

Data Reproduced from: Ogden, C. L., Carroll, M. D., Kit, B.K., & Flegal, K. M. (2012). Prevalence of obesity and trends in body mass index among U.S. children and adolescents, 1999-2010. Journal of the American Medical Association, 307(5), 483-490

2.0 Literature Review

2.1 Epigenetics: Bridging the Gap between Diet and Genetics

The term 'epigenetics' was first coined in the 1940s by developmental biologist Conrad Waddington who defined it as "the interactions of genes with their environment, which bring the phenotype into being" [11]. However, over the past seven decades Waddington's description has slowly evolved into the modern definition, which characterizes epigenetics as being heritable changes in gene expression that occur without any underlying change in the gene sequence [12].

The epigenome is a complex stratum of environmentally regulated mechanisms, capable of producing rapid and enduring changes in genomic activity. Such changes in the genome are potentially transgenerational, and primarily occur through histone modification, chromatin remodeling, and DNA methylation [13-16].

Environmental factors such as a sedentary lifestyle or having poor dietary habits (i.e. high in calories), are known for their catalytic role in the transgenerational etiology of Type 2 Diabetes (T2DM) [17-19]. Although the exact mechanisms are not yet fully understood T2DM is thought to influence epigenetic programming within the germ line, which can have deleterious effects that persist for several generations [15,17,18,20].

In addition to T2DM, to date investigators have identified a broad spectrum of pathologies thought to be directly associated with abnormal epigenetic programming. Other diseases found to exhibit unusual epigenetic profiles include the methylation patterns observed in cancerous tissues [21]. The genes residing in a metastatic tumor are typically found to be in a hypomethylated state. The tumor suppressor genes within these cancerous cells, however, are

primarily found to be hypermethylated [21]. Furthermore, epigenetic dysfunction has been implicated in the etiology of multiple diseases through its involvement in fetal programming. That is, if deregulated epigenetic modifications occur during embryonic development the changes made are often permanent, and consequently affect the susceptibility for certain individuals to contract diseases later on in adulthood [22]. The growing body of evidence linking dysfunctional epigenetic mechanisms to the etiology of complex metabolic diseases is compelling, and one day soon may offer clinical benefits in the form of novel drug developments as well as predictive biomarkers.

2.2 The Etiology of Metabolic Syndrome

It was nearly a century ago that pioneers working in the field of medical sciences first described the convoluted signs of a metabolic-like syndrome, which they recognized after observing an incoincidental coexistence of diseases. Since that time names such as 'syndrome X', 'insulin resistance syndrome', and 'metabolic syndrome' have been used interchangeably for describing a condition that, until recently, lacked any constitutive guidelines of classification [16,23,24]. Over the past decade, however, the term 'metabolic syndrome' has finally gathered enough traction to evolve from an ambiguous idiom into a well-defined medical syndrome; one that is estimated to affect nearly 25% of the adults in America [25].

Although several risk factors are used for the purpose of making a clinical diagnosis of metabolic syndrome, apart from diet and exercise there still are no suitable treatments available. Efforts to develop pharmacological therapies have proven to be difficult, primarily because no unified origin has been found to account for the pathogenesis of metabolic syndrome. Currently, mandates established by the World Health Organization (WHO), the American Association of

Clinical Endocrinologists (AACE), and the National Cholesterol Education Program Adult Treatment Panel II (NCEP ATP III) are used for diagnosing metabolic syndrome [26,27]. Although in most respects they are the same, the WHOs slightly more stringent criterion are more commonly used in clinical settings [26]. This model dictates that patients must present with fasting hyperglycemia or hyperinsulinemia in addition to exhibiting at least two of the following risk factors: centralized obesity (BMI $\geq$ 30), fasting hyperlipidemia (triglycerides $\geq$ 150 mg/dl), chronic hypertension (blood pressure $\geq$ 130/85 mm Hg), below average high density lipoprotein cholesterol (HDL $\leq$ 40 and 50 mg/dl for men and women respectively), or microalbuminuria [26]. Those who suffer from three or more of these comorbidities are on the precipice of developing diseases like type II diabetes mellitus (T2DM) or cardiovascular disease (CVD), both of which are maladies known to catalyze a kaleidoscopic array of other dysfunctions [26]. The following sections will serve to elaborate on glucose and insulin metabolism, which are cornerstone elements that often trigger or potentiate the other comorbidities listed.

2.3 The Tissue Specific Pathology of Glucose Impairment

Glucose is the primary source of energy used by the human body and is therefore, to no surprise, tightly regulated by a myriad of homeostatic mechanisms. Typically, the fasting glucose concentration for a euglycemic individual ranges between 70-100 mg/dl, whereas those who suffer from T2DM exhibit values in excess of 126 mg/dl [28]. Hyperinsulinemia is often seen to occur concomitantly to hyperglycemia, and together they serve as the hallmark traits for a T2DM phenotype [29]. Unfortunately, their clinical manifestations only become apparent long after their pathogenic mechanisms have been at work. It is now widely accepted that impaired glucose and insulin signaling are concordant pathologies, their origins of dysfunctions, however,

are still under debate. Current evidence has implicated the pathology to result from a set of complex dysfunctions, which occurs in several metabolic tissues like the pancreas, the liver, and the muscle [4,16,24,29-32].

2.3.1 Pancreas

The pancreas has been linked to the pathology of type 2 diabetes for a multitude of reasons. The endocrine function of pancreatic tissue, specifically the beta cells of the Islets of Langerhans, are responsible for secreting the hormone insulin to counteract high concentrations of peripheral glucose [29]. However, in T2DM the insulin producing beta cells are unable to keep up with the demand imposed by a hyperglycemic state [29]. As a result of the pancreatic beta cells working over-time a hyperinsulinemic state manifests that ultimately facilitates the onset of insulin resistance, which is a condition characterized by the inability of peripheral tissues (e.g. muscle, liver, adipose) to respond to insulin [29]. After prolonged and unsuccessful efforts to produce an adequate supply of insulin the pancreas begins to suffer from the toxic effects of chronic hyperglycemia [33]. This glucose-induced damage to beta cells further impairs the pancreas's ability to produce sufficient levels of insulin, which both exacerbates and perpetuates metabolic dysfunction [33].

2.3.2 Liver

The liver is situated at a key juncture point where all nutrient intake and insulin are first passed through its hepatocellular network prior to entering systemic circulation. It is theorized that obesity is a leading contributor in the development of insulin resistance, a pathology that subsequently promotes hepatic hyperglycemia [34]. In addition to excessive blood glucose,

dyslipidemia is also seen to occur in the form of elevated triglycerides, elevated free fatty acids (FFA) and reduced levels of HDL cholesterol [35].

Liver disease is one of the most common causes of death associated with T2DM [30]. In fact, virtually every subset of liver dysfunction is found to occur more often in diabetic patients including such pathologies as hepatocellular carcinoma, nonalcoholic fatty liver disease, cirrhosis, abnormal liver enzymes, and acute liver failure [30,31]. Based on these criteria T2DM clearly is not a disease only associated with hyperglycemia and insulin resistance.

Until recently it was thought that hepatic glucose production (HGP) was at the heart of fasting hyperglycemia [36]. However, research efforts have proven this theory to be false by demonstrating basal HGP in T2DM patients closely resembles that of normal euglycemic individuals [31]. This observation indicates the problem is instead likely to occur during the postprandial state, and potentially involves elevated FFA and triglyceride release, which sustains the insulin resistant state of peripheral tissues.

2.3.3 Skeletal Muscle

Insulin resistance occurring at the level of the skeletal muscle is a complex defect thought to occur years before other clinical manifestations appear [37]. Skeletal muscle is the primary site of glucose uptake and has been shown to utilize approximately 80-90% of glucose under normal euglycemic conditions [37].

Although multitudes of genetic factors have been implicated as causative agents of muscular insulin resistance, the broad array of evidence compiled to date would suggest that rather than a single culprit it's more likely to be a combinatorial effect of much deeper

complexity. In the current study, gene expression for several different transcripts were examined, all of which are known participants in glucose and insulin homeostasis.

2.4 Molecular Mechanisms Implicated in Glucose Impairment

As previously stated, researchers have compiled an enormous amount of data to substantiate the link suspected to exist between epigenetic programming and Type 2 Diabetes [12,13,38-40]. These data have shown that an array of different molecular pathways are participatory in transgenerational glucose impairment via indirect mechanisms that alter the germ line and begin in insulin sensitive tissues like the pancreas, the liver, adipose tissue, as well as skeletal muscle [13,31,37,41].

In an effort to contrive more effective treatments for glucose impairment occurring in these tissues it is essential to have a solid understanding of the constitutive elements causing dysfunction. Therefore, the following sections will offer a comprehensive review of the mechanisms known to be fundamental in the onset of glucose impairment, as well as those that facilitate its transgenerational persistence.

2.4.1 CpG Methylation

The most common form of epigenetic modification studied is DNA methylation, which is an event found to occur in all vertebrate animals [42]. Methylation is a fairly stable repressive marker for gene expression that is characterized by the addition of a methyl group to the 5th carbon of cytosine's pyrimidine ring, via the enzymatic actions of methyltransferases [11,18].

Although DNA methylation is not exclusive to cytosines, and can also be found to occur on adenine bases, it is unquestionably most prevalent on repetitive strings of cytosines bound to guanine nucleotides (CpG Islands) [42]. The acronym 'CpG' simply reflects adjacent cytosine and guanine nucleotide bases, bound together by a phosphodiester linkage. The frequency of methylated CpG's that occurs within a defined range of DNA (length > 200bp) is the classifying proponent used to distinguish two separate categories of CpG's termed islands and CpG and deserts [43]. CpG islands are defined as having a GC content greater than 50%, with an observed-to-expected CpG ratio exceeding 60% [43]. CpG islands are a prevalent feature of gene promoters, especially in humans where high CpG content is found in approximately 70% of all promoters [43]. This characteristic situates DNA methylation in a prime position to block transcriptional initiation complexes, and therefore prevent gene activity.

As stated, DNA methylation is an essential factor involved with normal embryonic development [44]. However, the dynamic sequences of events that occur upon zygote fertilization have made elucidating parental specific pathology a challenging task. It is well known that nearly all methylated marks acquired over the lifetime of both parents are wiped clean, or hydroxylated, at the time of zygote formation [45,46]. Subsequent to erasing the parental methylation patterns the epigenetic memory that resides within the maternal lineage is used as a template for re-methylating the genome of the developing embryo [47]. It is crucial to note however that certain genes existing within both paternal and maternal lineages are located in protected regions called Imprint Control Regions (ICR) [47]. These sequences are shielded from de-methylation, and thus are able to reflect a parent specific methylation pattern.

Due to the nature of cytosine biosynthesis the level of methylation is highly dependent on the availability of several cofactors and micronutrients (e.g. folic acid, choline, etc.) [48]. This

notion, in combination with the methylation erasure previously described, serve to partially illustrate the justification used by those researchers whose investigations are confined to the maternal contributions made during 9 months of gestation, which is a time when a nutritional diet is *sine qua non* to embryonic development.

2.4.2 Chromatin and histone modification

In addition to DNA methylation both chromatin remodeling and histone modifications are vital to epigenetic programming [14,49]. These names are umbrella terms used to describe, in addition to methylation, a myriad of specific mechanisms such as: acetylation, phosphorylation, ubiquitylation, sumoylation, biotinylation, and O-GlcNAcylation [11,49].

The human genome packs an unfathomable amount of information into a highly organized storage network that is readily accessible at a moments notice. This feat begins with DNAs affinity for a cheese wheel shaped cluster of eight proteins known as a histone, which DNA has a natural tendency for wrapping itself around while not in use [49]. However, when cellular functions demand additional gene transcripts the respective coding sequences are lured away from the histone core by proteins possessing an even greater electrostatic attraction for DNAs phosphodiester backbone, thereby releasing it from a tightly wrapped and dormant state. Upon severing the transient bond formed with epigenetic factors, gene transcription terminates and DNA returns to a tightly wrapped state around its designated histone. At this stage histones themselves begin to condense and twist into a packed arrangement forming what are known as nucleosomes [14]. The condensation process is repeated yet again on the chains of newly formed nucleosomes, at which time the structure known as chromatin makes its debut. Chromatin is the

constitutive element for chromosomes, and represents the densest level of DNA compression [14].

As was briefly illustrated here epigenetic regulation is a multifactorial process adding exponential diversity to genomic regulation, and it can be found to offer both extraordinary advantage as well as extraordinary risk. In many respects epigenetic control promotes a merger of Darwinian and Lamarkian evolutionary theories by allowing for immediate adaptation at the genomic level. Contrary to such a benefit, however, are the severe risks presented by any dysfunction in activity, which have potential to be maintained for several generations.

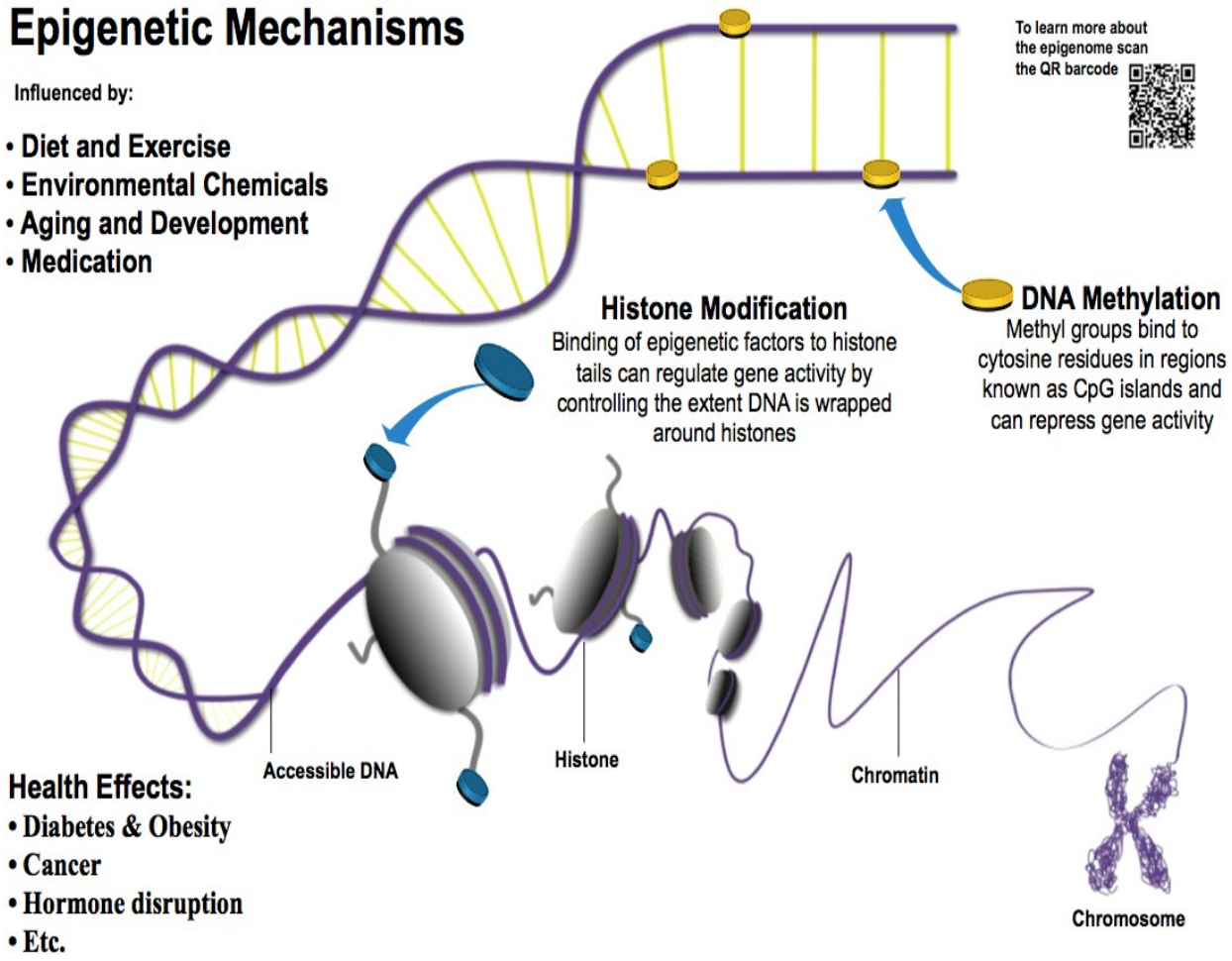

Figure 2. Genomic storage and epigenetic modifications

2.4.3 Evidence of transgenerational glucose impairment

Several recent lines of evidence, collected from both humans and mice, have confirmed transgenerational inheritance does occur by route of the paternal germ line [13,50,51]. As previously mentioned epigenetic changes are the product of environmental exposures, which includes toxins and dietary habits alike. One study performed by Skinner et. al. (2010) painted a clear picture on the transgenerational effects had by maternal exposure to the toxin vinclozolin, which is an endocrine disruptor found to carry its toxic effects through the paternal lineage, even managing to alter promoter methylation patterns within the sperm of F_3 rat offspring [52]! While another study conducted by Carone et. al. (2010) demonstrated that a low protein diet fed to male mice altered the methylation patterns within their offspring (F_1), which consequently resulted in a dysfunctional lipid metabolism [38]. These findings and others have implicated numerous non-genetic factors, like cytosine methylation and changes in microRNA, as the origin of fetal programming because both are capable of shaping the development of soon-to-be fertilized zygotes [53].

One investigation by Sheau-Feng Ng, et. al. (2010), using Sprague-Dawley rats, showed that a paternal high-fat diet directly contributes to β-cell dysfunction in F_1 female offspring [40]. Upon examining the pancreatic tissues of adult female offspring they found expressions for 642 islet genes to be significantly different than those offspring sired by control fathers ($p<0.01$). Furthermore, a paternal HFD contributed to an overall reduction in total islet area within female offspring (-23%; $p<0.04$) [40]. Interestingly the impaired glucose tolerance and insulin secretion experienced in F_1 females was observed in the absence of obesity or any changes in energy metabolism, indicating that metabolic dysfunction was likely the product of an endocrine disruption that interfered with pancreatic β-cell function [40]. Although this particular study

failed to investigate molecular changes occurring within the father's sperm they believed it to be the likely mode of transmission for which the differentially methylated promoter of *Il13ra2 (*hypomethylated; 1.76-fold resulting increase in expression*)*, a gene heavily involved in islet development and function, was able to facilitate metabolic impairment in the pancreas of offspring.

The findings made by Sheau-Feng Ng, et. al. have been substantiated by a handful of other studies that specifically focused on changes occurring at the level of the sperm. One such example can be seen in a study hosted by Fullston et. al. (2013), which demonstrated that paternal HFD was associated with a 25% reduction in DNA methylation within sperm that was not only linked to metabolic impairment (e.g. adiposity and insulin resistance) within F_1 males and females, but was also found to affect offspring metabolism in the F_2 generation [54]. Dunn GA and Bale TL (2011) further showed a maternal HFD reduced insulin sensitivity and increased body size in two successive generations of offspring "via both maternal and paternal lineages" [9]. Additional findings gathered in the Newborn Epigenetics Study by Soubry et. al. (2013) revealed that in humans (n=79) paternal obesity does in fact reprogram "imprint marks during spermatogenesis" [51]. This was seen as severe hypomethylation at the DMR of *Igf2*, which is a trait that also happens to be a known risk factor for several types of malignant cancers (e.g. rectal cancer, ovarian cancer etc.) [51].

Despite the fact that, to date, the vast majority of diet-centered transgenerational research has focused on F_1 and F_2 female progeny, the observations discussed here clearly demonstrate paternal diet plays a significant role in epigenetically shaping the metabolic phenotype of male offspring. Results gathered in the current study will hopefully serve to partially fill the void of

information that exists on the epigenetic effects had by paternal diet and exercise on male offspring within the F_1 generation.

2.4.4 *H19* & *Igf2 Cis* acting regulation

H19 and *Igf2* are imprinted genes that have recently come into the lime light of research because of their suspected roles in transgenerational metabolic impairment [13,51,55-58]. Monoallelic expression (i.e. parent-specific) of imprinted genes like *H19* and *Igf2* is a phenomenon that transpires from epigenetic modifications that occur within differentially methylated regions (DMR) [13,59]. The *H19* gene is a maternally inherited allele responsible for transcribing a noncoding RNA of unknown function, while insulin-like growth factor 2 (*Igf2*) is a paternally derived allele that encodes an embryonic mitogen responsible for promoting tissue-specific growth during gestation [56].

The series of mechanisms that regulate *Igf2* and *H19* genomic imprinting, in addition to the genes themselves, are highly conserved from rodents to humans which has allowed them to be thoroughly investigated using established mouse models [55,56]. Imprinting at *Igf2/H19* is particularly relevant to the current topic of discussion for two reasons. First, despite still having much to learn about the exact regulatory mechanisms involved, the *Igf2/H19* imprinting scheme offers a well-characterized example of paternally inherited epigenetic dysfunction [51,55,58-61]. Secondly, it is a paradigm that has been subject to extensive investigation in humans, where studies have demonstrated a clinical correlate between hypomethylation and low birth weight, which is a trait well-supported as a predictor of adult onset T2DM [62].

The syntenic genes *H19* and *Igf2,* located on human chromosome 11, are separated by an intronic sequence that spans roughly ~80 Kb [59]. The *cis* acting regulatory zone shared by *H19*

and *Igf2* is located approximately ~2 Kb to ~4 Kb upstream from *H19*'s transcriptional start site (TSS) in a domain referred to here as the 5' differentially methylated imprint control region (5' DMICR) [56,60]. This sequence serves a dual role, one function of which is to bind CTCF insulator proteins on the maternal chromosome (CCCTC-binding factor). It is also particularly important to note that in both mice and humans alike these insulating CTCF proteins are typically unable to bind on the fathers DMICR, primarily due to the hypermethylated state of resident CpGs. Hypermethylation within this region protects the developing zygote from exhibiting biallelic expression for both maternal and paternal *H19*. (Figure 3)

The second primary function of the CTCF proteins on the maternal chromosome is to act as a barrier that prevents enhancers from binding inside the *H19* promoter, thereby allowing them to travel further upstream where they instead promote the monoallelic expression of paternal *Igf2* [60]. The transcriptional activity of *H19* occurs on the maternal chromosome where the DMIC region its self serves as the docking site for the enhancers described above, all four of which are located ~10 kb downstream from *H19*'s TSS [60]. Irregular methylation occurring at the DMICR affects the transcription of both *H19* and *Igf2*, an occurrence recently identified to be a potential contributor to impaired islet function within offspring [13].

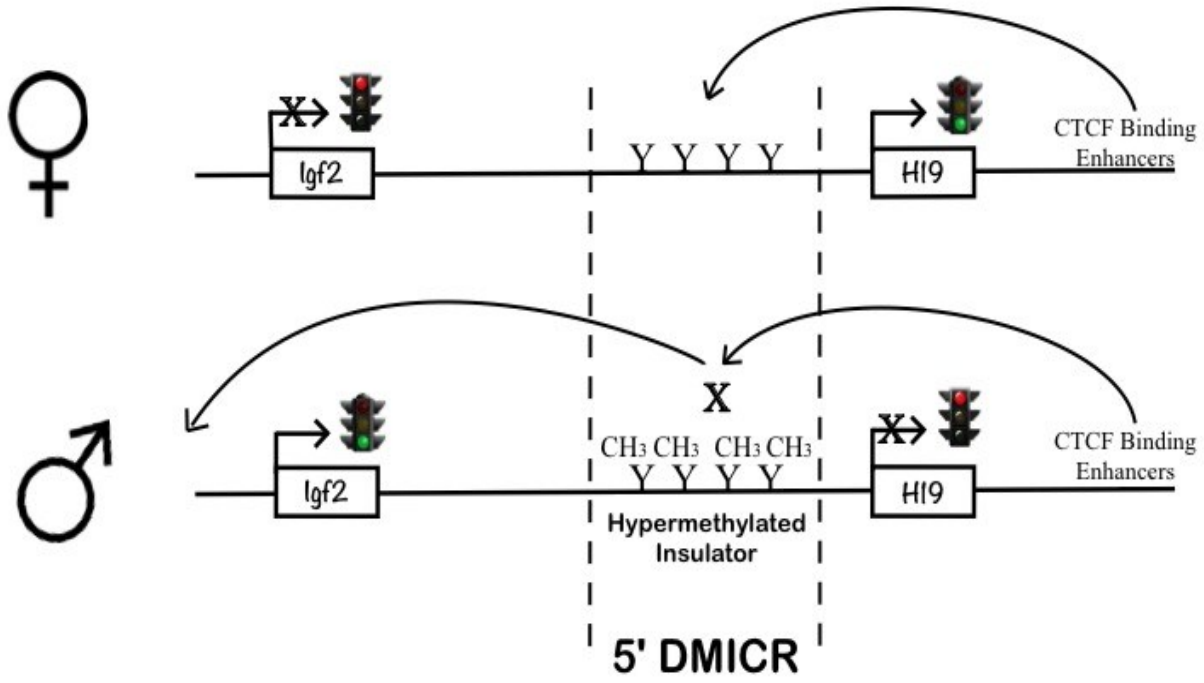

Figure 3. *Cis*-acting regulation of *H19* and *Igf2.*

2.4.5 Glucose homeostasis by *Pdk4*

The pyruvate dehydrogenase complex (PDC) plays a pivotal role in the metabolic state of pancreatic islets, the liver, and also the muscle [63,64]. PDC is responsible for glucose oxidation (i.e. breakdown). Its level of activity, however, is primarily dependent on the negative regulation imposed by pyruvate dehydrogenase kinases 1-4 (PDK) [63]. Of interest here is the PDK4 isoform, which shows the highest level of basal activity among the PDKs [63].

The action of PDK4 under normal circumstances is suppressed by insulin action. Starving conditions on the other hand promote the opposite trend, which is seen as a marked increase in *Pdk4* transcript levels occurring 48 hours after food deprivation [63]. In T2DM the ability of insulin to suppress PDK4's activity becomes hindered, which has devastating consequences that result in exacerbated hepatic glucose release. The capacity of insulin to regulate *Pdk4* expression is thought to occur through an intermediary protein called FOXO1 [36]. This dysfunctional series of events, involving PDK4, perpetuates pre-existing hyperglycemia and therefore hyperinsulinemia as well.

2.4.6 Hepatic glucose release by *FoxO1*

The forkhead transcription factor known as forkhead box class O 1 (FOXO1) was investigated here because of the keystone role it plays in energy metabolism and insulin signaling [65]. FOXO1 is typically in an unphosphorylated state and localized within the nucleus where it's niche as a transcription factor serves as a prerequisite for the expression of several genes, including the aforementioned *Pdk4* [65]. However, upon insulin stimulation (as well as by IGFs) a molecular cascade is initiated, via the phosphatidylinositol 3-kinase (PI3K)-Akt

pathway, which ultimately phosphorylates nuclear FOXO1 [64,65]. Phosphorylated FOXO1 is exported from the nucleus, effectively terminating the transcription of all FOXO-dependent genes [65]. The deleterious effects of insulin resistance become readily apparent upon examination of the genes whose transcriptions are FOXO1 dependent. Insulin resistant tissues fail to deliver the inhibitory message to FOXO1, allowing it to remain in the 'on' state within the nucleus where it actively promotes gene transcription for several gluconeogenic proteins [65].

Overactive FOXO1 (and its associate PCG-1α/PPARGC1) in the liver can be found to have profoundly negative consequences [36,65]. As mentioned above, several of the genes that undergo FOXO-mediated transcription are gluconeogenic factors that when activated facilitate glycogen breakdown, and yet again serve to further increase blood glucose concentration [65]. This only perturbs the ongoing pathological dichotomy happening between hyperglycemia and hyperinsulinemia/insulin resistance. Contrary to the negative role FOXO1 potentially plays in the diabetic liver, studies performed using mice have demonstrated in the pancreas it can actually reverse beta cell failure through interactions with Pdx-1 [66]. The actions of FOXO1 are therefore understandably often described as being a double-edged sword.

2.4.7 *Ptpn1*: Insulin signaling antagonist

The Protein tyrosine phosphatase N1 (*Ptpn1*) gene was examined in the current study because of the significant role it plays as a negative regulator of insulin signaling. It is located on the long arm of human chromosome 20, a region that has been strongly implicated in the heritability of T2DM [67, 68], which has placed it under heavy investigation by researchers as a potential therapeutic target in the treatment of insulin resistance [67]. To date 6 different naturally occurring haplotypes of *Ptpn1* have been identified, each possessing a unique pattern of

SNPs. One of these haplotypes is expressed by approximately 35% of people living in the United States. Interestingly, 30% (1.3-fold increase in risk) of these carriers go on to develop full-blown T2DM, a percentage that sadly equates to roughly 3.6 million people (calculation based on 18 million diagnosed) [68].

The gene *Ptpn1* encodes a ubiquitously expressed phosphatase called protein tyrosine phosphatase 1B (PTP1B) [68]. The role of PTP1B is to dephosphorylate the tyrosine residues on active insulin receptors (e.g. IRS-1) [68]. This activity disrupts insulin signaling on a global level, drastically increasing the severity of an insulin resistant state [68].

Current research efforts have demonstrated that PTP1B-deficient mice, subjected to diet-induced obesity and diabetes, experienced significantly better glycemic control and also had reduced plasma insulin levels compared to wild-type mice [67, 68]. This evidence further supports *Ptpn1* as a candidate for therapeutic intervention.

2.4.8 *Slc2A4* (GLUT4): Glucose sensitivity

One of the main purposes served by the acute response phase of insulin is to promote cellular uptake of free glucose [69]. One primary mechanism for accomplishing this task is mediated by GLUT4 translocation, which at the level of muscle is solely responsible for as much as 70% of total glucose uptake [70]. GLUT4 is one isoform of glucose transporters transcribed by the *Slc2A4* gene that is directly regulated by insulin signaling [69]. GLUT4 is temporarily recruited to the plasma membrane, where it serves the crucial role of translocating free blood glucose into the cell via facultative diffusion [70]. Interestingly, GLUT4 receptors have been shown to be internalized up to twenty-times faster than they are recruited to the membrane,

which allows for a rapid correction in cellular metabolism [[70]]. The relative density of GLUT4 receptors at the cell surface is primarily what dictates the extent of glucose uptake (i.e. glucose sensitivity and glucose tolerance).

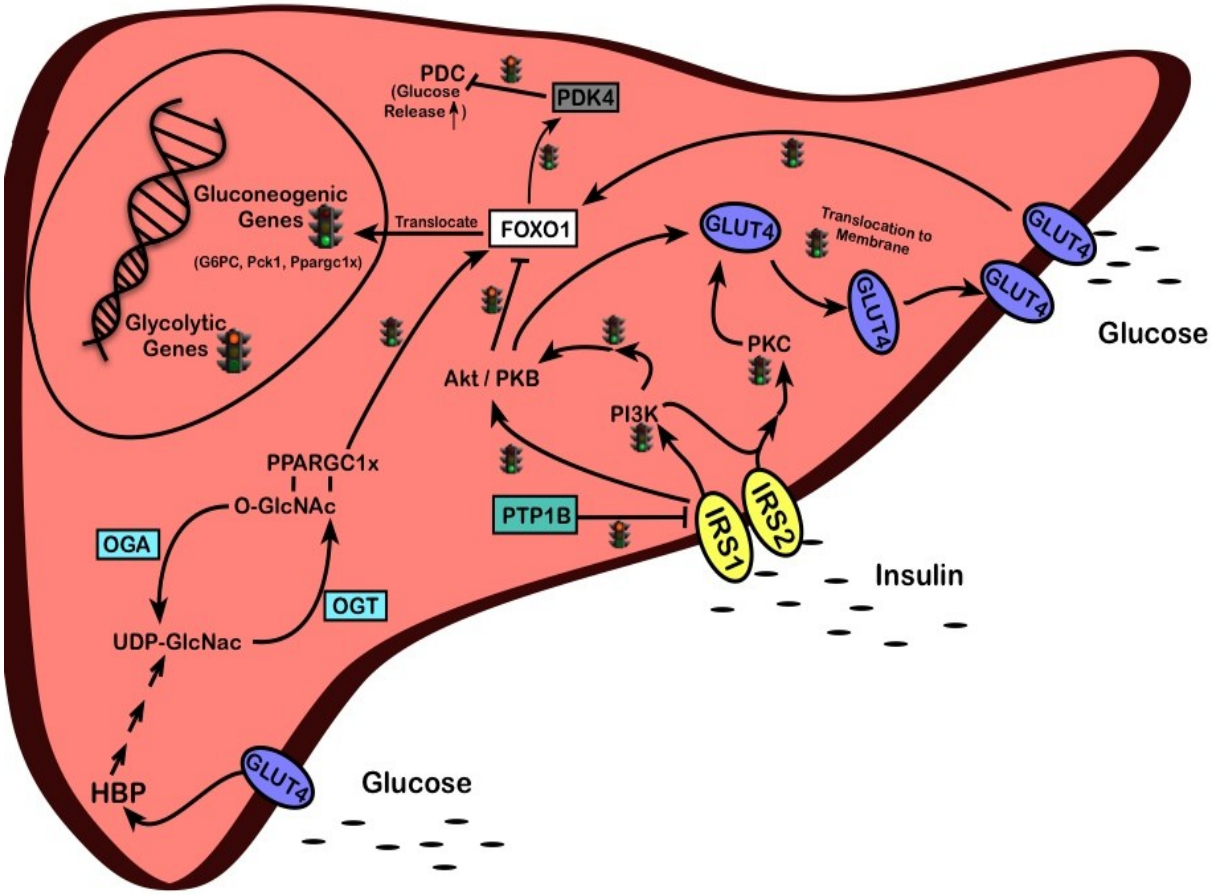

Figure 4. Generalized overview of molecular mechanisms involved in glucose and insulin metabolism

*Note: The liver is portrayed for illustrative purposes only; the mechanisms shown don't necessarily represent hepatic pathways (e.g. GLUT2 is primarily expressed in hepatic and pancreatic tissue, while GLUT4 is found in skeletal muscle and adipose tissue)

2.5 O-GlcNAc: The Chief Nutrient Sensor

In 1983 Torres and Hart made the profound discovery of a post-translational modification by β-O-linked N-acetylglucosamine (O-GlcNAc) [71]. Investigators have since demonstrated its actions are vital to maintaining a broad number of cellular functions, and that aberrant O-GlcNAc cycling is likely to be involved in the pathogenesis of human illnesses such as T2DM, cardiovascular disease, X-linked Dystonia Parkinsonism, Alzheimer's disease, as well as several other neurodegenerative and metabolic ailments [71]. These observations have made O-GlcNAc, and the two enzymes that facilitate its cycling, alluring targets for novel drug therapies. Even more intriguing, however, is their strong potential to be used as predictive biomarkers of disease [72].

As of today researchers have identified well over 3,000 proteins that undergo modification by O-GlcNAc, including a myriad of different regulatory elements such as transcription factors, methyltransferases, RNA polymerase II, histone cores and tails, nuclear pore receptors, steroid receptors, phosphatases and kinases, as well as oncogenes and tumor suppressors (figure 5) [71]. This vast and diverse catalogue of O-GlcNAc modified proteins continues to grow, strengthening support for the ubiquitous and pivotal role it plays not only in glucose metabolism but also cellular signaling, protein transport and stability, as well as chromatin remodeling and gene transcription [71].

2.5.1 What makes O-GlcNAc so different?

O-GlcNAc modification is a process very different from all other forms of glycosylation that, oddly enough, shows more similarity to protein phosphorylation [71]. O-GlcNAc is

considered to be one of the most abundant post-translational modifications within the nucleus, the cytoplasm, as well as the inner membrane of the mitochondria [71,73,74]. This attribute distinguishes O-GlcNAc from other N- and O- glycans, which are typically confined to the lumen of the endoplasmic reticulum or golgi apparatus [71]. Additionally, mature O-GlcNAc is generally unmodified and has a half-life that extends for a duration long enough to cycle on and off target proteins several times [71].

2.5.2 Detecting the elusive β-O-GlcNAc

Although nearly three decades have passed since Hart and Torres' first discovered O-GlcNAcylation (i.e. modification by O-GlcNAc) it still remains among researchers, more often than not, an esoteric form of post-translational modification. The general lack of awareness is an understandable product for any molecular event capable of eluding some of the most advanced screening techniques used in the field of proteomics, including both mass spectrometry and SDS-PAGE (sodium dodecyl sulfate–polyacrylamide gel electrophoresis) [71].

The inconspicuous nature of O-GlcNAc modification is primarily a result of three fundamental attributes. First, unlike modifications by phosphate the cycling of O-GlcNAc has virtually no effect on the net charge of it's host species and is therefore unlikely to produce any noticeable change in migration during SDS-PAGE [71]. Secondly, techniques that physically irradiate samples, including electrospray mass spectrometry and matrix-assisted laser desorption time-of-flight (MALDI-TOF), are unable to detect the substoichiometric amount of peptide-bound O-GlcNAc because it is quickly lost during the ionization step [71]. Third, cell lysis or damage causes ubiquitously high levels of hydrolases (e.g. lysosomal hexosaminidases and

nucleocytoplasmic β-N-acetylglucosaminidases), which are present in all cells, to promptly remove O-GlcNAc [71].

However, in recent years these obstacles have been overcome with improvements made to mass spectrometry as well as by using newly developed monoclonal antibodies [against O-GlcNAc] and potent inhibitors for β-N-acetylglucosaminidases [71]. During the two decades preceding these developments progress was sluggish, but with their arrival the productivity of researchers catapulted forward and our understanding of the role played by O-GlcNAc sharply improved.

2.5.3 Overview of O-GlcNAc cycling

Approximately 2-5% of all incoming cellular glucose is shunted towards the 'nutrient sensing' Hexosamine Biosynthetic Pathway (HBP), where the terminal product is the high-energy sugar donor for O-GlcNAc called Uridine diphosphate N-acetylglucosamine (UDP-GlcNAc) [71,73,74]. The initial flux of glucose towards the HBP is the trigger that primes a molecular cascade of events that all eventually become subject to a bottleneck effect created by the enzyme called D-fructose-6-phosphate amidotransferase 1 (GFPT1), or simply GFAT [71,74]. Glucose becomes fully committed to the Hexosamine pathway after enzymatic modification by GFAT, a role that has branded GFAT as the primary regulator for UDP-GlcNAc synthesis and key component involved in governing total cellular O-GlcNAcylation [71,74].

Protein modification by O-GlcNAc occurs when the N-acetylglucosamine moiety of UDP-GlcNAc is enzymatically transferred onto a serine or threonine residue, forming a glycosidic link that lasts anywhere from seconds to minutes [71]. This heavily investigated

process lead researchers to take notice of O-GlcNAc's high potential for dynamically interacting with serine/threonine phosphorylation, making its role much more complex than was ever previously anticipated [71,73,74].

2.5.4 Dynamic interactions with protein phosphorylation

In many respects O-GlcNAcylation and phosphorylation exhibit a yin-yang type relationship, which can be seen by their tendency to cycle in reciprocity on-and-off adjacent, if not the same, residues. In fact, nearly every phosphorylation site undergoing active cycling is influenced by O-GlcNAcylation [75]. Protein phosphatase 1 (PP1c) for instance has been shown to form a complex with OGT, in which they act in unison to simultaneously facilitate the replacement of O-phosphate with O-GlcNAc [71]. There are however distinctive characteristics separating the two enzymatic processes, the hallmark being that unlike protein phosphorylation, which utilizes hundreds of different kinases and phosphatases, protein O-GlcNAcylation is an event mediated by just two enzymes: uridine diphospho-N-acetylglucosamine:peptide β-N-acetylglucosaminyltransferase (O-GlcNAc Transferase; OGT), and N-Acetyl-D-glucosaminidase (O-GlcNAcase; OGA) [71,73,74]. The concerted action between these enzymes dictates the rate at which N-acetylglucosamine is added and removed from proteins, respectively, and any disruption that off sets their delicate balance has potential for causing system-wide catastrophe.

2.5.5 O-GlcNAc cycling enzymes

O-GlcNAc cycling is mediated by two highly conserved enzymes, which to date have been found in nearly every multi-cellular organism examined [71]. In animals the enzymes that

facilitate this process are called OGT (O-GlcNAc Transferase) and OGA (O-GlcNAcase), each of which is encoded by a single gene [71,73]. The only exception to this is found to occur in *Arabidopsis*, which appear to have two genes responsible for encoding OGT [76]. The precise and concerted activity between OGT and OGA is momentously important for dozens of signaling pathways and a broad range of other cellular functions (figure 5). Gene transcription for instance is an event arbitrated by the O-GlcNAc moiety, which can be seen cycling on- and off- the transcriptional initiation complex of RNA Polymerase II; the former acting to block transcription [71,73].

The role played by OGT and OGA is one that if dysfunctional has a high potential to not only disrupt insulin signaling but also cause unabated cellular proliferation [71,73,74]. A thorough explanation of OGT and OGA's complex biology would require volumes of information. Therefore, the following sections will briefly address the key structural and chemical features of each enzyme, providing insight into why their involvement has been implicated in the pathogenesis of T2DM.

2.5.5.1 O-GlcNAc Transferase

Recombinant gene studies (e.g. Cre-recombinase technologies like Cre-loxP) and conditional knockouts of O-GlcNAc transferase have proven it to be an unassailable requisite for embryogenesis and stem cell viability [77,78]. In addition to the essential role it plays for mouse ontogeny, researchers have demonstrated that deletion of *Ogt* is lethal in all organisms except for *Caenorhabditis elegans* (*C. elegans),* who instead are found to become lethargic [79].

The solitary gene that encodes for OGT shows over 99% homology between mice and humans, and it spans a distance of ~42 Kb on the long arm of the X chromosome (human Xq13.1) [80,81]. Its 23 exons are so far known to encode for three separate isoforms that can be found in varying concentrations within all human tissues, although pancreatic α/β cells and the brain are known to be the most abundant [71,82-84].

Each isoform is comprised of three parts: a C-terminal catalytic domain, a linker region, and finally an N-terminus containing a tetratricopeptide repeat motif (TPR), which differs in length for each transcript [80]. The longest isoform is a ~110-116 kDa nucleocytoplasmic protein encoded by all 23 exons, and is found to have an optimum pH existing around ~6.8 [85]. To no coincidence this also happens to be a pH that falls in close proximity to the acidotic environment common to pathologies like obesity and cancer.

At ~103 kDa the next longest transcript, termed mOGT, contains a unique mitochondrial-directing N-terminus that is encoded by exons 5-23 [86]. Interestingly, unlike its counterparts the overexpression of mOGT has been found to cause notable levels of cytotoxicity, and is therefore considered a pro-apoptotic isoform [87]. In contrast, the last and shortest transcript, sOGT (~78 kDa), appears to exhibit anti-apoptotic tendencies [87]. Just like ncOGT, sOGT is a ubiquitously active protein localized within both the nucleus and cytoplasmic compartments [67, 80].

Several regulatory mechanisms have been identified that mediate the transcriptional activity of *Ogt*. Such examples include enzyme-activating tyrosine phosphorylation (e.g. CaMKIV transcriptional feedback loop) as well as self-induced O-GlcNAcylation (whose role is not yet fully understood) [88]. The most notable means of regulation, however, is thought to involve negative feedback imposed by free UDP that is released upon the transfer of GlcNAc to

target proteins [82].

2.5.5.2 O-GlcNAcase

O-GlcNAcase, or OGA, is a pH neutral enzyme that is primarily found within the cytosolic compartment of cells and shares 97.8% identity between mice and human gene [81]. The gene that encodes for OGA was cloned and found to be identical to the hyaluronidase gene meningioma-expressed antigen 5 (*MGEA5)* [89]. It's composed of a glycosidase domain located at the N-terminus, with a histone acetyltransferase (HAT) domain at the opposite carboxyl terminal [90]. The HAT domain shows remarkable homology to the GCN5 HAT family, which allows OGA to serve the dual purpose of removing the O-GlcNAc moiety from modified proteins while also having the capacity to acetylate histones thereby activating gene transcription [89,91]

Oga resides on the human locus 10q24.1, which is a region juxtaposed to the insulin-degrading enzyme that has been implicated in the pathology of both Alzheimer's disease as well as the etiology of transgenerational T2DM [78,81,92-94]. A specific example can be seen among individuals of Mexican American ethnicity who are known to exhibit a uniquely high susceptibility to developing a T2DM phenotype [95]. The elevated risk experienced in this population of people may be due to a point mutation that causes an early termination of OGA during translation, which leads to an enzyme deficiency that is quickly outmatched by OGTs activity.

Furthermore, O-GlcNAcase offers a high potential for use as a biomarker to detect T2DM [96,97]. Although both OGA and OGT are expressed in human erythrocytes, only OGA exhibited

statistical significance for its ability to outperform HbA1c as a test for detecting pre-diabetes and diabetes (two and three fold increases in the expression levels, respectively; n=13/14 $p \leq 0.01$) when compared against HbA1c levels [97]. The HbA1c is a sensitive and specific test commonly used for diagnostic purposes when screening for T2DM. However, the study referenced here found OGA to be a more sensitive and reliable method for detecting pre-diabetes [97].

2.5.6 A Word on epigenetic regulation by O-GlcNAcylation

In many respects O-GlcNAcylation is a process that generates continuity in a nutrient-based molecular circuit, designed to interface our dietary habits to the transcriptional activity of our genome. O-GlcNAc was officially inducted into the "Histone Code" after several investigations witnessed its cycling activity directly influenced epigenetic machineries like acetylation, ubiquitylation, and methylation [71,78,91,92,94]. Sakabe et al. (2010) additionally found O-GlcNAc to interact with polycomb group proteins (PcG), and alter higher order chromatin structures on all four histone cores including H2A, H2B, H3 and H4 [91].

In addition to OGA's histone acetyltransferase domain described in the previous section, the O-GlcNAc moiety has also been shown to interact with several methyltransferases including mixed-linease leukemia 5 (MLL5), coactivator-associated arginine methyltransferase 1 (CARM1), and Whc1 (92). One additional example recently discovered by Chen et. al. (2012), was O-GlcNAc's propensity to interact with ten eleven translocation enzymes (TET) [98]. Specifically, they found OGT-dependent histone O-GlcNAcylation to be facilitated by TET2 and TET3 enzymes. Moreover, these enzymes appeared to target O-GlcNAc to transcriptional start sites on histone 2B. Although the facts presented here only reflect a small portion of the

evidence compiled to date, they are an effective demonstration of the significant role O-GlcNAc plays in regulating the epigenome.

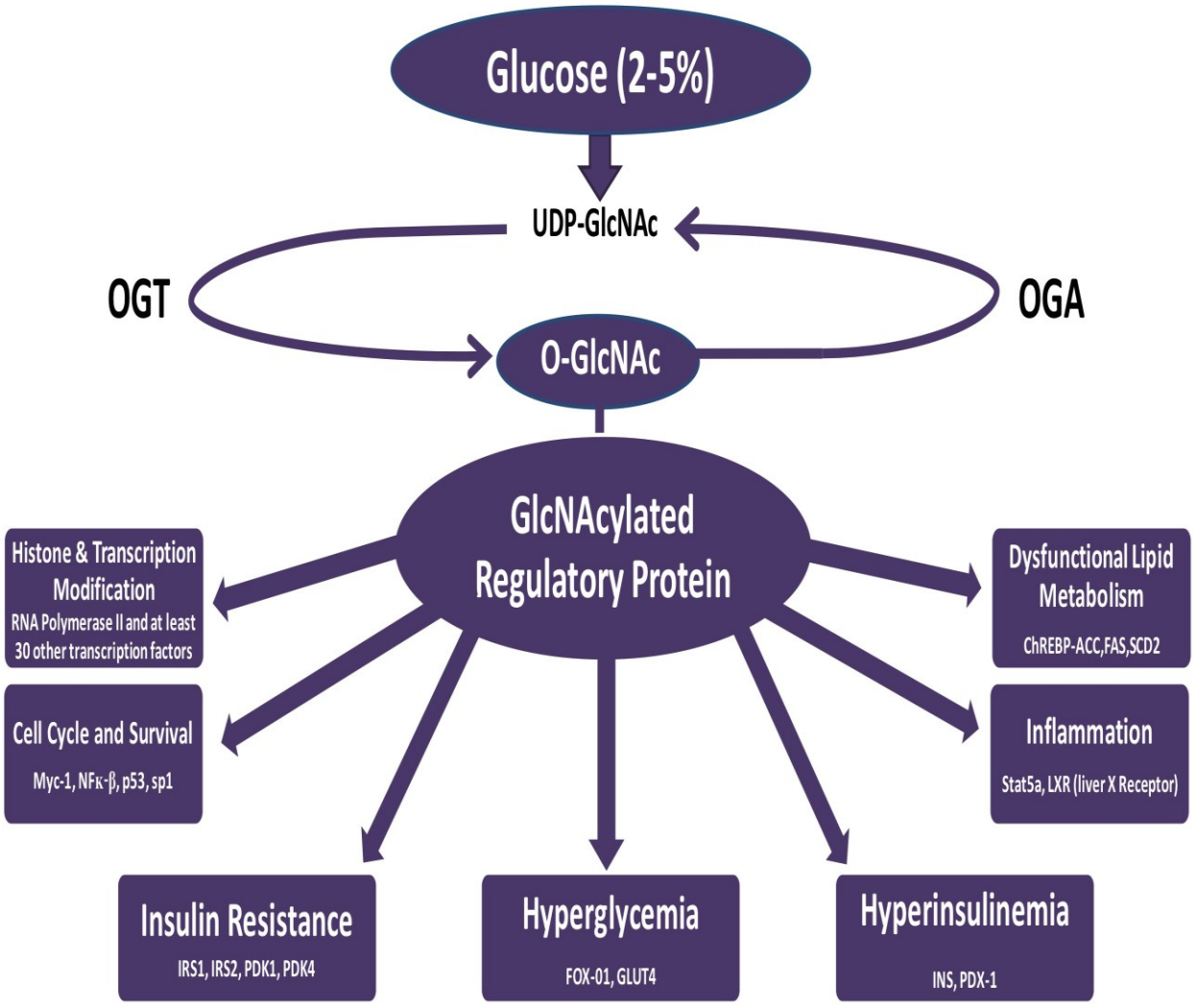

Figure 5. Epigenetic and metabolic regulation by O-GlcNAcylated proteins.

3.0 Materials and Methods

3.1 Approach

An animal model consisting of genetically identical inbred C57BL/6J mice (Jackson Laboratories) was employed to study the epigenetic modifications that contribute to an increased risk of childhood obesity and diabetes. In order to effectively measure epigenetic markers of paternal origin only founder fathers were exposed to experimental conditions, while mothers were maintained on a control diet and used exclusively for breeding purposes. All procedures and tissue collection methods were conducted in a humane manner with the approval of the Institutional Animal Care and Use Committee (IACUC) of East Carolina University.

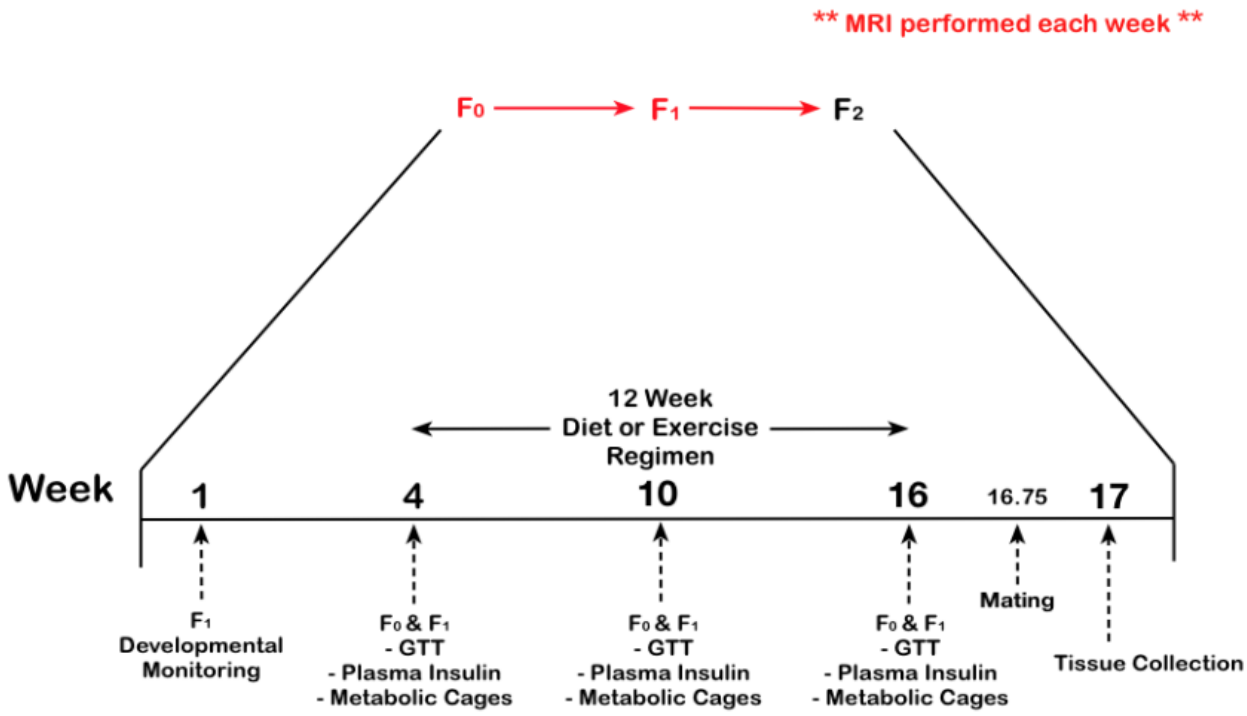

Figure 6. Timeline of experimental design

3.2 Animal Housing Conditions and Diet

C57BL/6J mice were obtained from Jackson Laboratory and bred on site at East Carolina University for two generations to eliminate any confounding variables associated with the transition in living conditions. The third generation of male mice born at East Carolina served as the founder generation (F_0), and at 4-weeks of age were divided into three experimental groups: control-diet fathers (CF), high-fat diet fathers (FF), and control-diet exercise fathers (EF) housed with free access to a running wheel. When F_0 fathers reached 16-weeks of age they were temporarily housed with a pair of control females for a duration of 3 days to produce the F_1 generation of offspring. F_1 mice were weaned at post-natal day 21 and at 4-weeks of age were assigned to either a control diet or high-fat diet for a duration of 12 weeks, at which time they were used to breed an F_2 generation of offspring. After breeding, all male mice were sacrificed for tissue collection. Control diets consisted of 10% energy derived from fat (D12450; Research Diets, Inc., NJ, USA), while high-fat diets were 60% energy derived from fat (D12492I; Research Diets). All animals were fed ad libitum and housed individually in a climate-controlled environment maintained at 24 °C with 50% humidity, on a 12-hour light/dark cycle.

3.3 Wheel Cages and Exercise

Exercise fathers (EF) were housed individually and given free 24-hour access to a running wheel. Cages for exercising fathers were slightly larger than others to accommodate room for their wheel. Revolutions were actively monitored, and transmitted, by sensors connected to an automated computer system designed to tabulate activity. Only the animals found to run an average of 3 miles per day, over the course of the 12-week exercise regimen, were chosen for breeding and for inclusion in other tests.

3.4 Developmental Monitoring

Developmental milestones were recorded on mice during post-natal days 7-14. The following parameters were measured: body weight, the time at which upper and lower incisors erupted, fur appeared, eyes opened, and ear flaps had separated from head. Considerable efforts were made to minimize the length of time spent interacting with pups, and also to preventing scent carry-over between different litters.

3.5 Weight and Adiposity Measurements

At four weeks of age mice were subjected to body composition testing using an EchoMRI-700 machine (EchoMRI, Inc., TX, USA), and each week until mice were sacrificed the following parameters were measured: percent fat, free water, total water and lean mass, which is defined by manufacturer as the total biomass of muscle tissue and all body parts containing water; excluding fat, bone, hair, and claws. As suggested by the manufacturer, before each use of the EchoMRI it was calibrated for mice by using an appropriate volume of canola oil, which has been shown from NMR chemical analysis to accurately reflect the signal recorded from fat molecules.

3.6 Metabolic Profiling

F_0 and F_1 generation animals were temporarily housed in metabolic cages to evaluate the effects of diet and free wheel running. Metabolic performance was measured at 0-, 6-, and 12-weeks, with respect to time of diet assignment, via indirect open-circuit calorimetry (LabMaster

Software; TSE-Systems, MO, USA). At the 0-week time point all mice were consuming the same control diet.

Metabolic chambers (i.e. calorimetric modules) were equipped with the following components: food and water dispensers attached to independent balances, perimeter sensors used to assess total, ambulatory, or fine movement, and lastly each cage included high-speed paramagnetic gas sensing units to monitor respiration. Gas sensors were calibrated prior to each session using primary gas standards containing known concentrations of N_2, O_2, and CO_2. A mass air flow meter was used to validate rate of airflow.

Animals were transferred to clean metabolic cages between the times of 0900-1200 on Thursday and then removed at 0900 the following Monday. The first day served as a period of acclimation, with measurements used for statistical purposes beginning Friday at 0700 and ending Monday at 0700. All mice were weighed upon their removal from metabolic cages.

Parameters measured at 20-minute intervals include the following: total activity (x-, y-, z-axes), food and water consumption, CO_2 production and O_2 consumption (ml/h/kg). Energy expenditure was derived by the following equation: $(((3.941*VO_2)+(1.106*VCO_2))/1000)/(\text{total body weight}/1000)$, which served to adjust the respiration exchange rate by body weight (grams).

3.7 Glucose Tolerance Testing and Plasma Insulin

Glucose metabolism was assessed at 0-, 6, and 12- weeks with respect to time of diet assignment. Mice were transferred to the procedure room four hours prior to testing, at which time their food was removed to simulate fasting conditions (fasting time 0700-1100). Blood was first collected from the tail caudal vein to establish baseline values for glucose and plasma

insulin concentrations. Immediately following the initial blood collection mice were injected intraperitoneally with a 50% dextrose solution (dose dependent on lean body mass). Plasma insulin was measured again 30 minutes after injection while glucose was measured again at 30, 60, and 120 minutes. Glucose concentration was determined with a glucometer (Alpha-Track Glucometer; Abbott Laboratories, CA, USA). All precautions were taken to minimize animals stress level. Additionally, in an effort to reduce variation within data collection processes all personnel assisting on glucose tolerance testing were kept constant.

Quantification of plasma insulin was performed on approximately 50 µl of blood collected by a glass capillary. Plasma was isolated from whole blood by centrifuging for 10 minutes at 10,000 × g (4 °C). Isolated plasma was then processed using the Rat / Mouse Insulin ELISA Kit from Millipore (MA, USA), and absorbances were subsequently read at 450 nm and 590 nm using a LKB Biochrome 4050 Ultrospec II UV/Vis Spectrophotometer (MN, USA).

3.8 Tissue Collections and Processing

After 12-weeks of diet or exercise mice were individually euthanized by isoflurane overdose followed by decapitation. White and brown adipose tissue, liver tissue, pancreatic tissue, and gastrocnemius muscle were collected immediately after death and snap frozen in liquid nitrogen. All samples were later transferred to a -80 °C freezer for permanent storage.

3.9 Protein Extractions and Downstream Processing

Protein was isolated from gastrocnemius muscle, pancreas, and liver to examine OGT and OGA protein expressions. Whole tissue lysates (10% weight/volume) were processed and suspended in the following mixture: 10 µl/ml of protease inhibitor cocktail (P8340; Sigma-Aldrich, MO, USA) and 10 µl/ml of phenylmethanesulfonyl fluoride (PMSF) combined with radioimmunoprecipitation assay buffer (RIPA) - [50mMTris-HCL, 150mMNaCl, 1mM ethylenediaminetetraacetic acid (EDTA), 0.1% SDS, 0.5% Sodium Deoxycholate, and 1% Triton X-100, pH 7.8]. Mechanical disruption and homogenization were performed on ice by 2× 0:15 pulses using a PowerGen 700 polytron set to maximum speed (Fisher Scientific Inc, MA, USA). The homogenate was then centrifuged for 12 minutes at 10,000 × g (4 °C), and the supernatant then transferred to a clean 1.5 ml tube. To determine protein concentration a Bradford assay was performed on a Bio-Rad SmartSpec 3000 spectrometer (Bio-Rad Laboratories, PA, USA). Samples were measured in duplicate and prepared as follows: 750 µl dH_2O, 50 µl diluted protein (1:10), and 200 µl Bio-Rad Protein Assay Dye (Bio-Rad Laboratories). A standard curve was generated at the start of each protein assay using a series of dilutions prepared by adding 200 µl of Bio-Rad Assay Dye to the following pre-mixed tubes containing dH_2O/BSA (µl): 800/0, 798/2, 796/4, 784/16, 760/40, 720/80.

3.9.1 Western Blot Analysis

Protein expression was measured by Western blot analysis. Samples were made western-ready by mixing approximately 15 µg of protein with 4×NuPAGE LDS Sample Buffer, 10× Reducing Agent (Life Sciences, NY, USA), and dH_2O. Sample preparations were then boiled for 5 minutes. Proteins were analyzed under reducing conditions (NuPAGE Reducing Agent)

with MES SDS running buffer on 4-12% Bis-Tris gels (Life Sciences, USA). Samples were transferred to polyvinylidene difluoride membranes (PVDF; Life Sciences, USA) by electroblotting for 7 minutes at 25V using the iBlot Dry Transfer System (Life Sciences). Equal loading of samples was confirmed by Ponceau staining [0.25 g Ponceau-S, 40 ml methanol, 15 ml Acetic Acid, 45 ml dH_2O] and by using the housekeeping protein α-tubulin as an internal control (1:500 dilution). Following transfer, PVDF membranes were blocked at room temperature for 1 hour in a 1:1 mix of PBS and Odyssey Blocking Buffer (LI-COR, NE, USA) and then incubated overnight at 4 °C with primary antibodies. Primary antibodies cocktails were prepared with following ingredients: rabbit polyclonal anti-OGT diluted to 1:2000 (AL25; a kind gift from Dr. Gerald Hart, Johns Hopkins Institute, Baltimore, MD, USA) in a 1:1 mixture of Odyssey blocking buffer and PBST (0.2% Tween). Anti-OGA (C345 isoform; also a generous donation provided by Dr. Gerald Hart of Johns Hopkins Institute) was diluted to 1:6000 in the same manner described for OGT. After incubating membranes with primary antibodies they were washed with 0.1% PBST for 10 minutes (4×) and 20 minutes (1×). Subsequent to washing the membranes were subjected to a second blocking step (30' at room temperature) to reduce potential for non-specific binding of secondary antibodies.

Secondary incubation was carried out at room temperature, for 1 hour, in complete darkness. Two-channel detection for OGT+α-tubulin or OGA+α-tubulin was accomplished using secondary antibodies derived from different host species. Solutions used for secondary incubation were prepared as follows: a 1:1 mix of Odyssey blocking buffer and PBST (0.2% Tween), 0.01% SDS, 1:15,000 goat-anti-mouse [680λ detection of α-tubulin] (LI-COR), and finally either 1:15,000 goat-anti-rabbit [for OGT at 800λ] (LI-COR) or with 1:5,000 donkey-anti-chicken [for OGA at 800λ] (LI-COR). To finish, 5× 5-minute washes and 1× 10-minute wash

were performed using PBST (0.1% Tween). Membranes were kept wet in PBS and visualized by 2-channel chemiluminescence with an Odyssey CLx Infrared Imaging System (LI-COR). Upon initially receiving secondary antibodies their specificity was validated by performing a secondary incubation, as described above, on a negative control PVDF membrane (i.e. protein-loaded PVDF membrane, not previously exposed to primary antibodies)

3.10 RNA Isolation and Downstream Processing

Approximately ~25mg of solid frozen tissue was processed by using the mirVana miRNA Isolation kit (Ambion, CA, USA). Tissues were kept on dry ice until being transferred to the appropriate volume of Lysis/Binding Buffer (1:10 for liver, 1:6 for pancreas and muscle). Samples were kept on ice during mechanical homogenization for a duration of 30 seconds (2×0:15 pulses) using a PowerGen 700 polytron (Fisher Scientific). Organic extraction was then performed using acid-phenol:chloroform (5:1 solution pH 4.5 ± 0.2). All subsequent steps were conducted in accordance to the standard mirVana protocol provided by the manufacturer. RNA was eluted with nuclease-free H_2O (78 °C) and then treated with DNase (Ambion DNA-free kit, Cat. #AM1906) to ensure samples were free of genomic DNA contamination. RNA concentration was determined using a NanoDrop UV-Vis ND-1000 spectrometer (Fisher Scientific) and purity was evaluated by the observed A_{260}/A_{280} ratio (2.00±0.08). Eluted RNA (2 µg) were prepared for RT-PCR with the Superscript Vilo Kit (Invitrogen, NY, USA). Upon completion of cDNA synthesis all samples were adjusted to a final concentration of 5 ng/µl before analyzing by real-time PCR.

3.10.1 Semi-quantitative Real-Time PCR: cDNA

Semi-quantitative real-time PCR was performed on an ABI 7900HT sequence detection system with SDS 2.3 software (Applied Biosystems, CA, USA). Samples were loaded in triplicate and NTCs in duplicate onto Bio-Rad 384-Well PCR plates (Bio-Rad Laboratories, USA; Item #HSR-4805). Each 10 µl reaction consisted of 5µl Power Sybr Green Master Mix (Invitrogen, USA), 3.6 µl nuclease-free H_2O, 200mM forward primer, 200mM reverse primer, and 1 µl cDNA template (5 ng/µl). After loading samples, plates were sealed and centrifuged for 1 minute 900 × g at 4°C. Two-Step PCR cycling conditions used were as follows: 2:00 at 50°C// 10:00 at 95°C// 0:15 at 95°C/1:00 at 60°C (40 cycles)//0:15 at 95°C/0:15 at 60°C. Target gene transcripts were normalized against the reference gene β-actin, and calculated $\Delta\Delta CT^2$ values were used to represent relative gene expression [99].

3.11 DNA Isolation and Downstream Processing

Approximately 20-30 mg of frozen tissue was processed with the Qiagen DNeasy Blood & Tissue Kit (Qiagen Inc., CA, USA). All steps were carried out according to the manufacturer's instructions with three exceptions. Firstly, tissues were optionally disrupted by mechanical homogenization (2 × 10 seconds; PowerGen 700 polytron) prior to digesting with Proteinase K (2:30hr/56 °C). Second, all samples were treated with 4 µL of RNase A to ensure there was no RNA carry over (Qiagen, USA; Item #19101). The last deviation from protocol was made by performing two successive elutions with 50 µL (68 °C) of a TE buffer mix. The TE buffer mixture was a 1:4 composition of Ambion TE (Ambion, USA; AM9849) and Qiagen AE buffer (Qiagen, USA; 19077). This combination of TE buffers offers an optimum pH and EDTA (ethylenediaminetetraacetic acid) concentration to promote DNA stability with minimal risk of

intercalating and sequestering, MgCl ions during active PCR reactions.

3.11.1 Sonication and Agarose Gel Electrophoresis

Isolated DNA samples were subsequently sonicated to obtain an average fragment size of ~150-750bp. Fragmentation was achieved with a Misonex 4000 Sonicator (Misonix, Inc., NY, USA) using a cup-horn attachment. Using indirect sonication via a cup horn (i.e. water bath) was preferred over use of a probe sonicator, as the former reduces risk for cross-contamination (samples are kept sealed) and also allows for batch processing. Samples (100 µl /vial) were floated approximately ~2 mm above the resonating platform, and sonicated for a duration of 10 minutes at maximum amplitude (30 second on/off intervals). The water bath was drained and refilled with ice-cold water every 2 minutes. DNA concentration and purity (A_{260}/A_{280} ratio1.80±0.2) were measured in duplicates using a NanodropND-1000, and then diluted to a final concentration of 15 ng/µl before storing at -80°C.

Gel electrophoresis was used to verify DNA integrity, purity (i.e. RNA contamination) and fragment sizes. Agarose gels were mixed to a concentration of 1.75% with the following components: 0.445 grams of agarose powder dissolved in 32 ml dH_20, 8 ml 10× TBE (1× final), and 0.8 µl ethidium bromide (EtBr). The liquid agarose was poured to a depth of 6 mm in a clean 5 × 8 cm casting tray and allowed to cool for 30 minutes. Running buffer (1× 1M TBE) was prepared with 204 ml dH_20, 51 ml of 10× 1M TBE, and 2 µl EtBr. Upon filling the electrophoresis tank with running buffer an additional 4 µl of EtBr was mixed at the anode terminal. Ethidium Bromide migrates in an opposing direction to that of DNA; therefore this step was performed to increase the potential number of collisions between EtBr and DNA, which effectively increasing the fluorescence of samples. Stock 10× TBE, used for gel and buffer

preparation, was made by dissolving the following ingredients in 1 liter of deionized water: 108 grams Tris-base, 55 grams boric acid, and 7.5 grams EDTA. Lanes were loaded with a 10 µl mix that consisted of 500 ng DNA, 2 µl of 5× sample buffer (Bio-Rad Laboratories, USA), and nuclease-free H_2O used to adjust the final volume. Samples were run for 01:10 hours at constant voltage (100V) and immediately visualized on a UV transilluminator (AlphaEaseFC software; Alpha Innotech, FL, USA). A 100-1000bp molecular ladder was loaded adjacent to samples to assess the extent of DNA fragmentation (Bio-Rad Laboratories, USA).

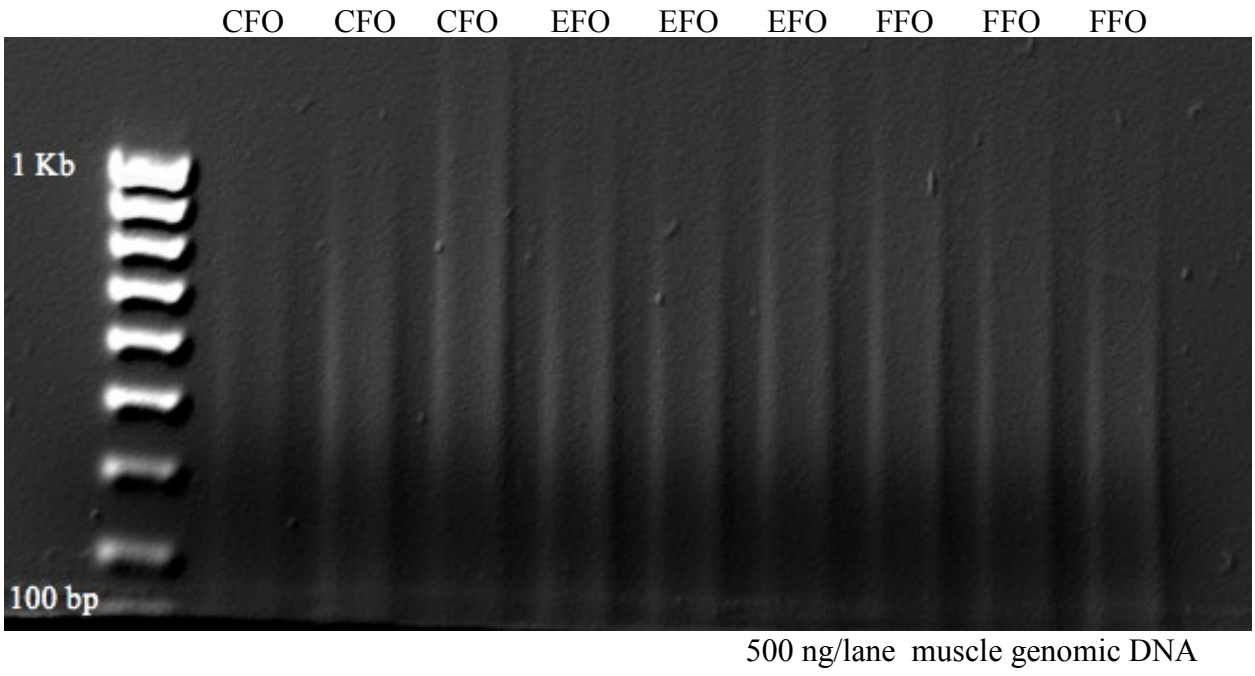

Figure 7. Agarose gel electrophoresis illustrating optimized sonicatication conditions. DNA is fragmented to an average size of 200 – 500 bp.

3.11.2 Methylation Capture

Methylated regions (≥ 4 CpG's) of input DNA were enriched by a capture reaction using the human MBD2 protein (Methyl-CpG Binding Domain Protein 2) coupled to paramagnetic beads via a biotin linker (MethylMiner Kit #ME10025; Invitrogen, USA). MBD-cap (Methylated Binding Domain-Capture) was performed according to the manufacturer's suggested protocol with a few minor adjustments, which are described below. Use of the MethylMiner kit was validated with two synthetic duplex DNAs (non-methylated and methylated DNA) that served as controls and were processed in the same manner as other samples. Approximately 1 µg of input DNA was loaded for methylation enrichment. MBD-protein only recognizes double stranded DNA, thus it was decided to incubate samples overnight at 4°C to reduce any risk of heat-induced DNA dissociation. CpG-methylated DNA was eluted as a single fraction using a high-salt buffer solution (2000mM NaCL), as opposed to a step-wise elution with a series of buffers of increasing NaCl concentration.

Ethanol precipitation was performed to clean up the methylated DNA. This was accomplished by incubating samples at -80 °C for a minimum of 3 hours with the following components: 1.5 µl glygogen (20 µg/µl), 40 µl of 3 M sodium acetate pH 5.2, and 800 µl of 100% ethanol. After incubation, samples were centrifuged for 15 minutes 16,000 × g at 4 °C and the supernatant discarded. Approximately 500 µl of ice-cold 70% ethanol was then added and samples were centrifuged for 5 minutes at 16,000 × g at 4 °C (repeat 1×). Following the third round of centrifugation the supernatant was removed using a sterile glass micropipette attached to a vacuum aspirator. The resulting DNA pellet was air dried for ~10 minutes at room temperature and then resuspended in 80 µl of the same TE buffer mix described above in *Methods for DNA isolation*.

3.11.3 Semi-quantitative Real-time PCR: Genomic DNA

To determine the relative density of methylation (fold enrichment) in promoter sequences, input DNA and MBD-cap DNA for each animal were subjected to PCR on the same ABI 7900HT machine used for gene expression analysis. All preparatory methods described were carried out on ice and in low-light conditions. Reactions were loaded in triplicate onto 384-well PCR plates at a volume of 10 µl. Master Mix preparations consisted of the following components: 5 µl Sybr Select Master Mix (Invitrogen, USA), 250mM forward primer, 250mM reverse primer, and 2.6 µl of nuclease-free H_2O. Approximately 8µl of Master Mix was dispensed to each well and then 2 µl of template DNA subsequently added. NTC (No Template Control) reactions were run in duplicate for each gene by adding 2 µl of nuclease free water in lieu of template DNA. After loading and sealing the PCR plates, they were centrifuged for 1 minute 900 × g at 4 °C. 3-Step PCR cycling conditions used to amplify templates were as follows: 2:00 at 50°C // 2:00 at 95°C // 0:20 at 95°C / 0:25 at 59.5°C / 0:45 at 72°C (40 cycles) // 0:15 at 95°C / 0:15 at 60°C / 0:15 at 95°C. Amplification values were normalized against the house keeping gene β-actin and $\Delta\Delta CT^2$ was calculated for both input and methylated samples [100].

To assess methylated enrichment (i.e. fold change relative to input) of targeted promoter sequence the following equation was used, and then normalized against controls: ((methylated $\Delta\Delta CT^2$/ input $\Delta\Delta CT^2$)*100). Results obtained using this method reflect a general degree of methylation; more precise quantification would necessitate PCR also be run on unbound DNA and multiple wash fractions collected during MethylMiner**.**

3.12 Primer Design and Optimization

All genomic primers were designed to flank a 75-150 bp amplicon within the promoter region of each target gene (table 2). Promoter sequences all consisted of the nucleotides situated within -1200 bp /+200 bp of the transcriptional start site (TSS) or the first exon. The only exception being for the gene *h19* whose primers were designed to flank a unique sequence, referred to here as the Imprint Control/Promoter-Region (IC/P-R), which is located ~2 kb upstream from the first exon. Primers were generated using Primer3 Version 0.4.0 [5] and blasted against the built-in mispriming database for rodents. To verify primer selections all sequences were subsequently screened using Vector NTI software (Life Technologies, USA). Desalted oligonucleotides were purchased from Invitrogen (NY, USA), and optimum annealing temperatures were established by running a PCR thermal gradient (annealing temperature range of 52°C-67°C) on a Bio-Rad C1000 Thermal Cycler (Bio-Rad Laboratories, USA).

Target	Gene Name	Forward Primer Sequence	Reverse Primer Sequence
cDNA	*Ogt*	GACGCAACCAAACTTTGCAGT	TCAAGGGTGACAGCCTTTTCA
	Oga (Mgea5)	GGGTTATGGAGCAGAGAAAAGAG	CCTGGCGAAATAGCATAGATGAA
	Pdk4	AGGGAGGTCGAGCTGTTCTC	GGAGTGTTCACTAAGCGGTCA
	Ptpn1	GGAACTGGGCGGCTATTTACC	CAAAAGGGCTGACATCTCGGT
	Glut4 (Slc2a4)	GTGACTGGAACACTGGTCCTA	CCAGCCACGTTGCATTGTAG
	Ppargc1α	AACCAGTACAACAATGAGCCTG	AATGAGGGCAATCCGTCTTCA
	Igf2	GTGCTGCATCGCTGCTTAC	ACGTCCCTCTCGGACTTGG
	H19	CCTTGTCGTAGAAGCCGTCTG	GGGTAGCACCATTTCTTTCATCT
	FoxO1	AACCAGCTCAAATGCTAGTACCATC	CAGAAGGTTCTCCATGTTTTTCTGGA
	Gfpt1α	GCCGAGCTGTGCAAACTCT	GGCTGCTCAAAAATTTCCTTC
	Ins2	GACCCACAAGTGGCACAAC	TCTACAATGCCACGCTTCTG
Genomic DNA	*Ogt*	CCCATAGGGAGCCCTTAACC	GCGTAACAAGACTACCGACC
	Oga (Mgea5)	GGCGCCCTTTGTCCTTTT	CGCTTCCTGTTTATCCGCAC
	Pdk4	CTCCTCCCTCTCACCCTTTG	AACTTTGGGCTCCTCCCTTT
	Ptpn1	TGGAGAAGGAGTTCGAGGAG	TCTAGGGCGACGAGGATG
	Glut4 (Slc2a4)	TCGGGGCATACACACATACA	TGAAAGGTCGAAGAGGAGGG
	Ppargc1α	GAGTGACAGCCCAGCCTAC	TCCACTCTGACACACAGCAC
	H19	ATAAGGGTCATGGGGTGGT	GGCATCGTCTGTCCATTTAG
	FoxO1	AAAATACCCCACCGCCCC	GCCGAAGCAGCCAATGAAC
	Gfpt1α	AACATTCCCTTCCTCCTCCT	CCAGCATCCGCTTTAGGTTC
	Ins2	TGGCCATCTGCTGACCTAC	GACCAAAGCACCTCCTCTCT
	β-Actin	ATGCTGACCCTCATCCACTT	AATAGCCTCCGCCCTTGT

Table 2. Genomic and cDNA primer sequences used in PCR reactions.

3.13 Statistical Analysis

Data are presented as mean ± standard error. Densitometry analysis was performed on western blot images using Kodak 1D 3.6 software (Eastman Kodak, NY, USA). Gene expression, methylation density, and statistical outliers (interquartile range) were calculated using Microsoft Excel. All project data was grouped and organized within Microsoft Excel and subsequently transferred to Graphpad Prism for statistical analysis (version 5.00, CA, USA; www.graphpad.com). Statistical significance of data were determined using unpaired two-tailed student's t-test or repeated measures one-way ANOVA followed by Bonferroni's Multiple-Comparison post-hoc test. All calculations were performed with a 95% confidence interval. Statistical test used for each data set is indicated in the respective figure legend.

4.0 Presentation of Findings

4.1 Body Weight and Adiposity

Body weight and composition were measured each week in fathers and offspring. As expected, fathers assigned to a high-fat diet were seen to weigh significantly more than both CF and EF at the 12-week time point ($p<0.001$). Additional findings from MRI body composition testing revealed the FF group had a tremendously higher fat content than other fathers ($p<0.001$; $n=5$). Furthermore, CF were found to have a higher total body weight, as well as higher fat percent, than the EF ($p<0.01$; $n=9$).

Statistical differences among offspring were only observed between those groups challenged with a high fat diet. Interestingly, the diet challenged EFO seemed to suffer the greatest insult from consuming a high calorie diet. At the 12-week time point following diet assignment, EFO were found to weigh significantly more than both CFO and FFO ($p<0.01$). Furthermore, EFO had significantly higher fat content than diet challenged CFO and FFO ($p<0.001$ and $p<0.0001$ respectively).

These findings indicate that fathers consuming a high fat diet became obese, while those assigned to a 10% control diet didn't. Furthermore, EFO seem to be the most susceptible to metabolic dysfunction compared to other offspring challenged by a high fat diet. These results indicate potential epigenetic programming by fathers, which prepares the metabolism of offspring to live a lifestyle similar to their own.

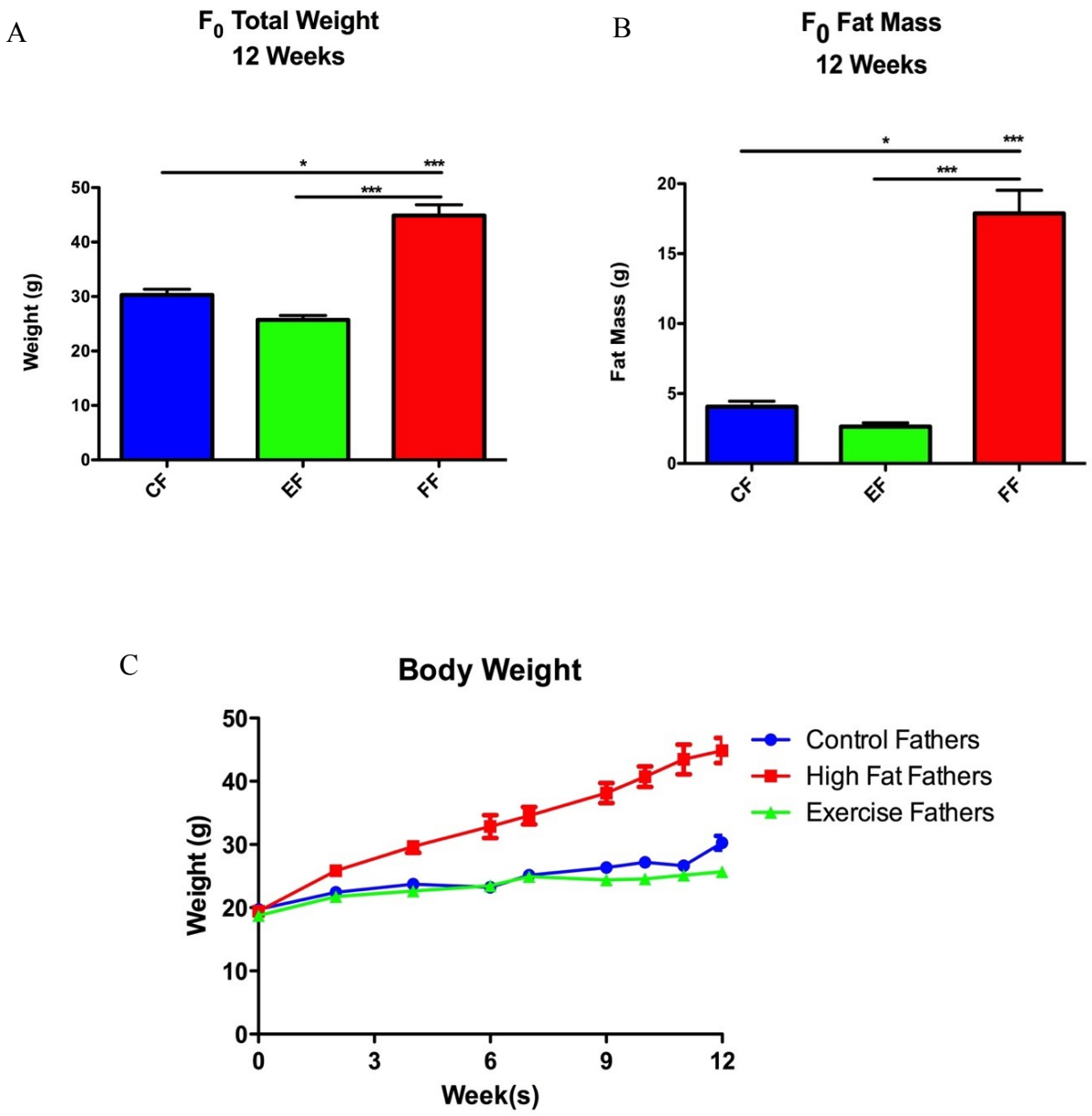

Figure 8. Father's (F_0) body weight and fat mass. A – total body weight measured 12 weeks after time of experimental group assignment (n= 9). B – Total fat mass measured by MRI (n=5). C – Weekly measures of paternal body weight (n=5). Significance calculated by one-way ANOVA with post-hoc Bonferroni ***p<0.001 *p<0.05.

A

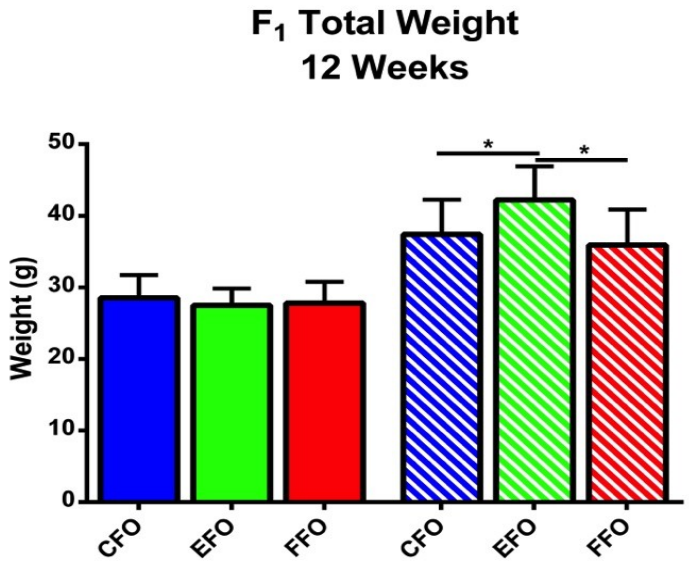

B

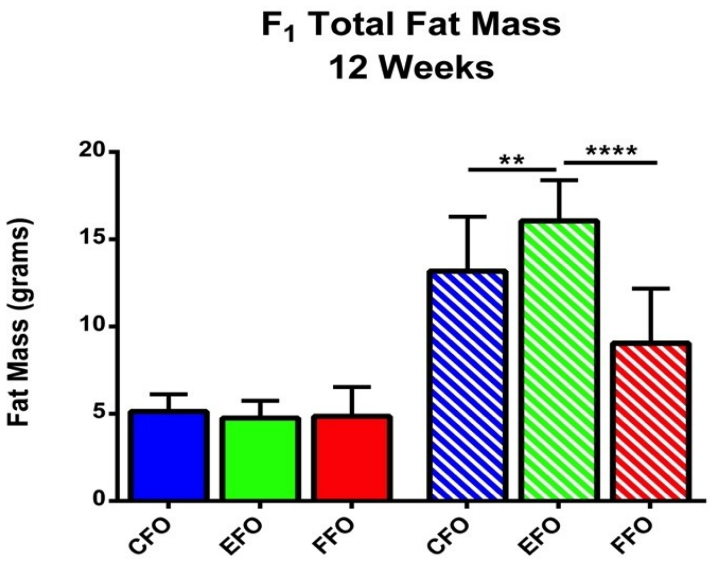

Figure 9. Offspring (F_1) body weight and fat mass. Solid colors represent offspring consuming 10% fat control diet, while striped bars are diet-challenged offspring, consuming a 60% high-fat diet. A – Total body weight measured 12 weeks after time of diet assignment (10%-CFO/EFO/FFO n=9/13/9 respectively // 60%-CFO/EFO/FFO n=10/11/7 respectively). B – Total fat mass measured by MRI (10%-CFO/EFO/FFO n=8/12/9 respectively // 60%-CFO/EFO/FFO n=11/11/8 respectively). Significance calculated by one-way ANOVA with post-hoc Bonferroni ****p<0.0001 **p<0.005 *p<0.05.

4.2 Metabolic Profiling

Metabolic profiles for mice were assessed using computer automated indirect calorimetry (i.e. metabolic cages). This well validated methodology encompasses both physiological and behavioral elements of data collection, which in the current study provided substantiating support for molecular analysis [[101]]. Together these data present for a more comprehensive assessment. Moreover, for a number of reasons only male offspring in the F_1 generation were examined. The primary justification for excluding female offspring stemmed from their high rate of variability. Furthermore, preliminary comparisons revealed distinctly different trends in the data collected from male and female offspring. These gender-based disparities were determined to be confounding variables that would compromise the validity of the study as a whole.

4.2.1 Energy Expenditure

In the current study, energy expenditure was investigated to characterize the acute and potentially transgenerational effects had by diet and exercise on the metabolic performance of male offspring. By evaluating the energy metabolism in physically active mice, as well as those subjected to diet-induced obesity, valuable insight was gained as to whether the onset of obesity was a problem that occurred from excess energy intake or a problem caused by reduced energy expenditure.

Calculations were made using whole body weight rather than lean mass due to higher variability using the latter (both methods reflected same trend). Findings presented here demonstrate that high-fat diet fathers (FF) in the founder generation experienced a significant

reduction in total energy expenditure compared to both exercising fathers (EF), as well as control fathers (CF; $p<0.0001$; figure 10A). Although much less pronounced the same trend was observed at the 0-week time point for high-fat father offspring (FFO; figure 10B) and exercise-father offspring (EFO), which both exhibited reduced energy expenditure in comparison to control father offspring (CFO).

Finally, at 12-weeks the EFO who were challenged with a high-fat diet (60% energy derived from fat) were seen to exhibit a marked decrease in energy expenditure compared to CFOs also challenged by with a high fat diet (HFD). Other data compared from the 12-week time point failed to produce any additional findings with statistical value.

As the following sections will further demonstrate, these findings here show that failure to thrive is most evident in EFO challenged with a HFD. This is the first piece of evidence offered to hint at an unknown mechanism of phenotypic programming, which prepares offspring for living conditions similar to those lived by their respective father.

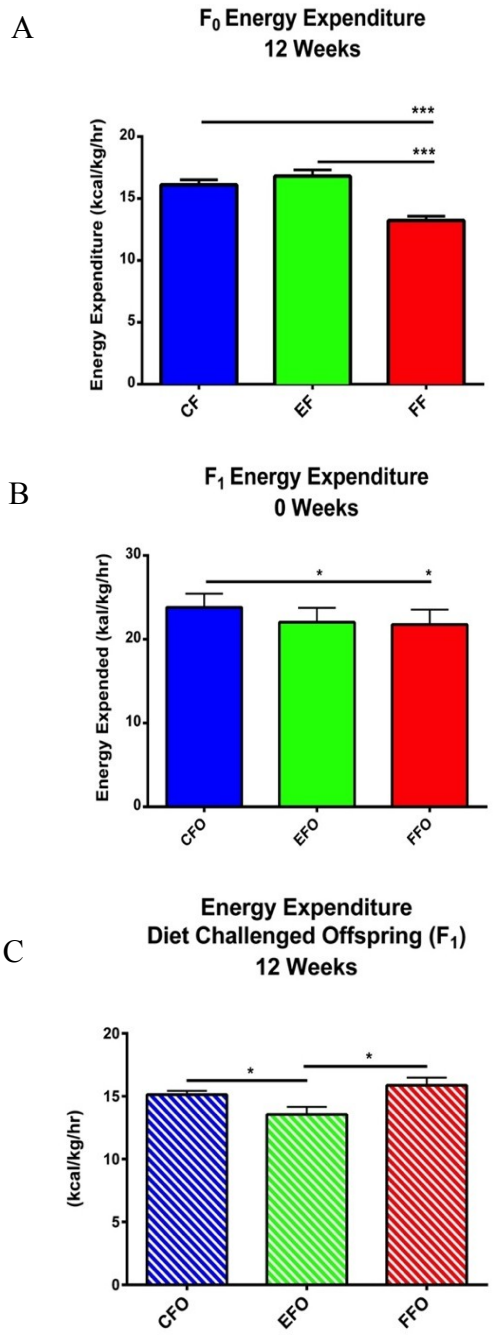

Figure 10. Energy expenditure measured by indirect calorimetry using total body weight. A – Fathers (F_0) energy expenditure measured 12 weeks after experimental group assignment (CF/EF/FF n=26/23/24 respectively). B – Offspring (F_1) energy expenditure measured at the 0-week time point with respect to time of diet assignment (CFO/EFO/FFO n=6/6/5 respectively). C – 60 % Diet challenged offspring (F_1) energy expenditure measured at 12 weeks with respect to time of diet assignment (60% CFO/EFO/FFO n=8). Significance calculated by one-way ANOVA with post-hoc Bonferroni ***p<0.001 *p<0.05.

4.2.2 Activity

Mice activity was monitored for a duration of 72 hours, during which time ambulatory movements were continuously recorded on each plane of orientation (x, y, and z). These data reflect the total number of breaks that occurred between the IR emitter and the IR detector. Findings presented are for total activity, which was the combined count of beam breaks in each plane. At the 12-week period, a significant increase in total activity was seen to occur in EF, which had not been observed previously during time spent in metabolic cages. The markedly increased level of locomotion in EF (n=27) was statistically higher than both FF ($p<0.00001$; n=29) as well as CF ($p<0.001$; n=29). CFs were additionally found to be more active than FF ($p<0.0001$). As stated, no statistical value is seen in a separate comparison of z- oriented motion, however these data are provided for their inference value associated with food and water consumption discussed later.

Similar observations were noted in offspring consuming a 10% fat diet. At the 0-week time point both EFO (n=12) and CFO (n=10) were found to be significantly more active than FFO (n=12; $p<0.001$, $p<0.01$ respectively). These findings between EFO and FFO were again repeated at the 12-week period ($p<0.01$), however no other statistically significant observations were made.

Additionally, as seen in Figure-11C, offspring challenged by a HFD were also included for presentation. Despite there being no statistical difference, the trend shaping between diet-challenged EFO and FFO is indicative of epigenetic modifications that alter their susceptibilities to metabolic impairment.

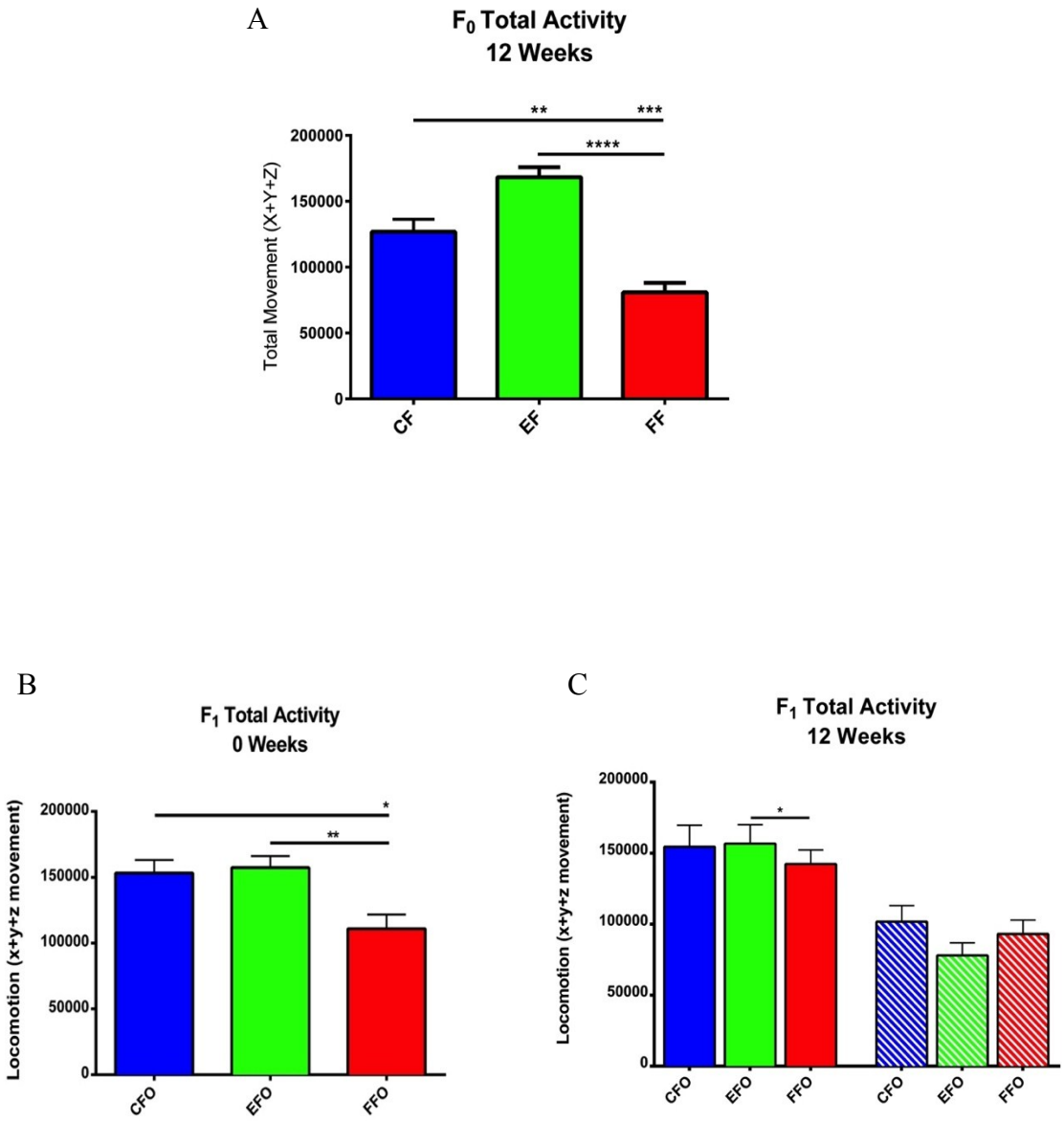

Figure 11. Total activity measured during indirect calorimetry (x+y+z axes). A – Father's (F_0) total activity measured at 12 weeks (CF/EF/FF n=29/27/29 respectively). B – Offspring total activity measured at 0 weeks with respect to time of diet assignment (CFO/EFO/FFO n=10/12/12). C – Total activity of 10% diet offspring (solid) and 60% diet challenged offspring (striped) measured at 12 weeks (10% CFO/EFO/FFO n=8/9/8 respectively // 60% CFO/EFO/FFO n=8/8/8). Significance calculated by one-way ANOVA with post-hoc Bonferroni ****p<0.0001 ***p<0.001 **p<0.005 *p<0.05.

4.2.3 Food and Water Consumption

In addition to energy expenditure and motor activity, both food and water consumption were also recorded during the time spent housed in metabolic cages. To ensure precision and accuracy of these data, food and water sensors were calibrated between each use of the system. Furthermore, cages were inspected daily and notations were made when appropriate to disband any data discrepancies associated to animals that had tendencies to play with their chow rather than eat.

Among fathers, the only statistical differences identified occurred at the 12-week time period. Surprisingly, FFs (n=12) were found to consume substantially less chow than both CF ($p<0.01$; n=13) and EF ($p<0.0001$; n=10). However, it is important to note that these data for fathers were also evaluated with respect to caloric values (figure 12b) and although no statistical significance was found FFs did consume more calories on average than both CF and EF (7.88% and 9.65%, respectively).

Statistically relevant findings between groups of offspring were noted at both 0- and 12-week time points for food and water consumption. Food consumption at 0-weeks was found to relatively similar across groups; FFO (n=9), however, appeared to drink an excessive amount of water ($p<0.01$).

Several disparities between offspring were also found at 12-weeks. The most notable of which includes the excessive amount of water FFO drank compared to CFO and EFO ($p<0.0001$). FFO also consumed substantially more food than EFO ($p<0.01$).

These findings, measured in FFO, are suggestive of what could reasonably be inferred as polydipsia (excessive thirst), a hallmark symptom commonly seen among newly diagnosed type 2 diabetic patients. [102]

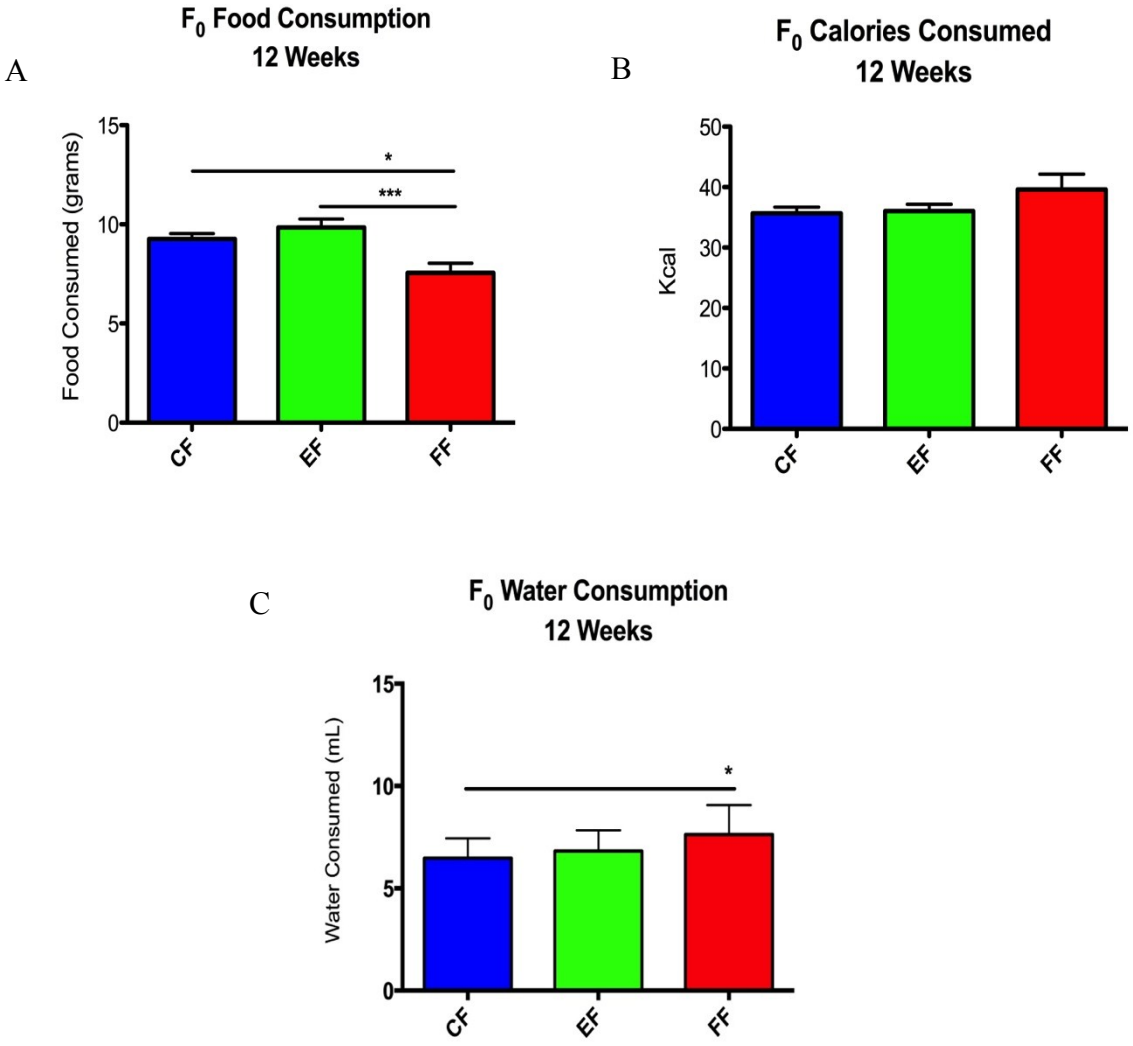

Figure 12. Father's (F_0) food (A), calories (B), and water (C) consumption measured at 12 weeks, with respect to time of experimental group assignment (CF/EF/FF n=14/12/14 respectively). Significance calculated by one-way ANOVA with post-hoc Bonferroni ***p<0.001 *p<0.05.

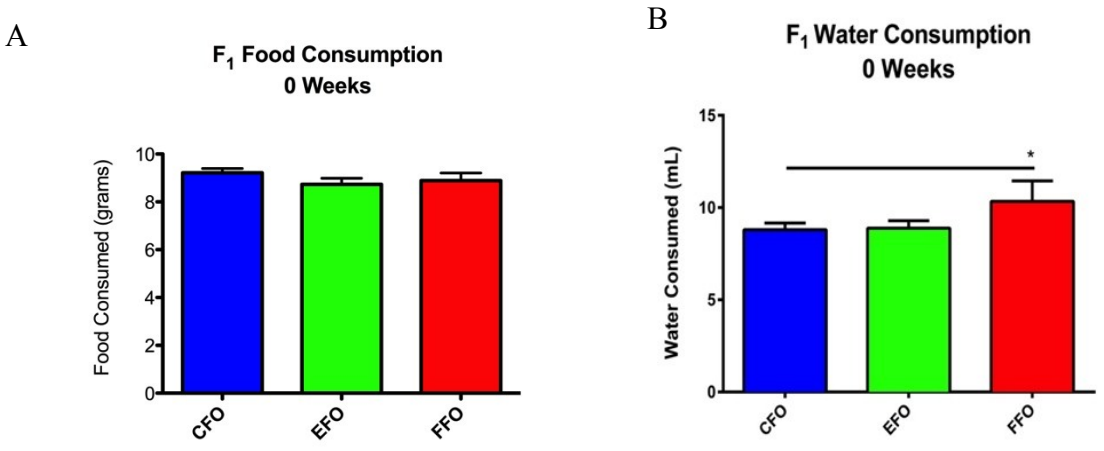

Figure 13. Offspring (F_1) food (A) and water (B) consumption measured at 0 weeks, with respect to time of diet assignment (CFO/EFO/FFO n=9/11/8 respectively). Significance calculated by one-way ANOVA with post-hoc Bonferroni *p<0.05.

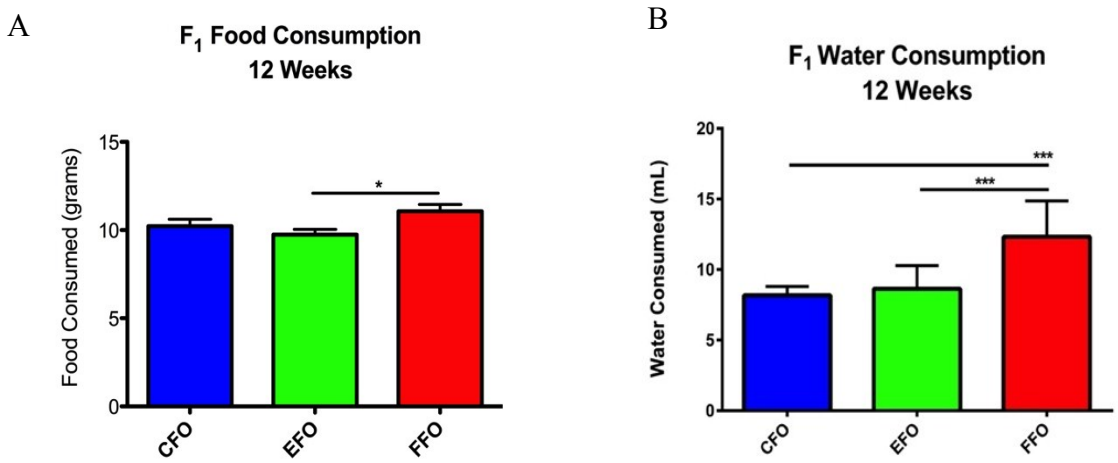

Figure 14. 10% Diet offspring (F_1) food (A) and water (B) consumption measured at 12 weeks, with respect to time of diet assignment (A- CFO/EFO/FFO n=8/9/8 respectively // B – 7/9/7 respectively). Significance calculated by one-way ANOVA with post-hoc Bonferroni ***p<0.001 *p<0.05.

4.3 Glucose Tolerance Test and Plasma Insulin

Glucose tolerance testing (GTT) was performed to gain a temporal perspective on glucose metabolism between different groups of animals. Fathers consuming a high-fat diet were found to have a statistically higher area under the curve (AUC) than CF (n=6) and EF ($p<0.001$; n=5). Furthermore, 12-week insulin concentrations measured in fathers reveal FFs (n=10) became hyperinsulinemic as a result of consuming a high fat diet. Basal insulin, as well as acute phase response insulin (APR; 30 minutes) measured in FFs was significantly higher than CF and EF fathers ($p<0.0001$; n=7 and 10 respectively). Taken together, these findings indicate FFs had developed a diabetic phenotype in response to a high-fat diet.

Analyses performed on offspring GTT data at 0 and 12-weeks revealed a significantly higher AUC in FFO compared to CFO and EFO ($p<0.01$; n=30, 30, 40 respectively). Findings at week 12 revealed the same trend, as seen by a significantly higher AUC measured in FFO compared to CFO and EFO ($p<0.001$; n=9, 6, 9 respectively). All other data collected on offspring, who were consuming a normal control diet, were found to be non-significant.

Furthermore, plasma insulin measured in diet challenged EFO demonstrated, once again, appeared to be most affected by the high fat content. Although basal insulin measures were statistically insignificant between groups, the concentrations seen in EFO (n=8) appeared higher than all other offspring. Insulin measures at the 30-minute APR, however, were found to be statistically significant compared to both CFO and FFO ($p<0.01$ and $p<0.001$ respectively; n=6).

These results demonstrate that FFs developed a diabetic phenotype (i.e. hyperglycemic, hyperinsulinemic) and, to a lesser extent, so did their respective offspring despite the fact they

were consuming a regular control diet. Moreover, diet challenged EFO were again seen to be the most susceptible to the deleterious effects of a HFD; further substantiating paternal-of-origin transgenerational programming.

A

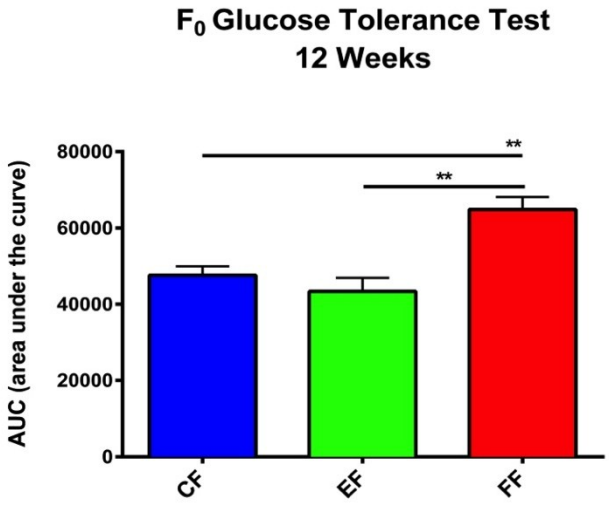

B

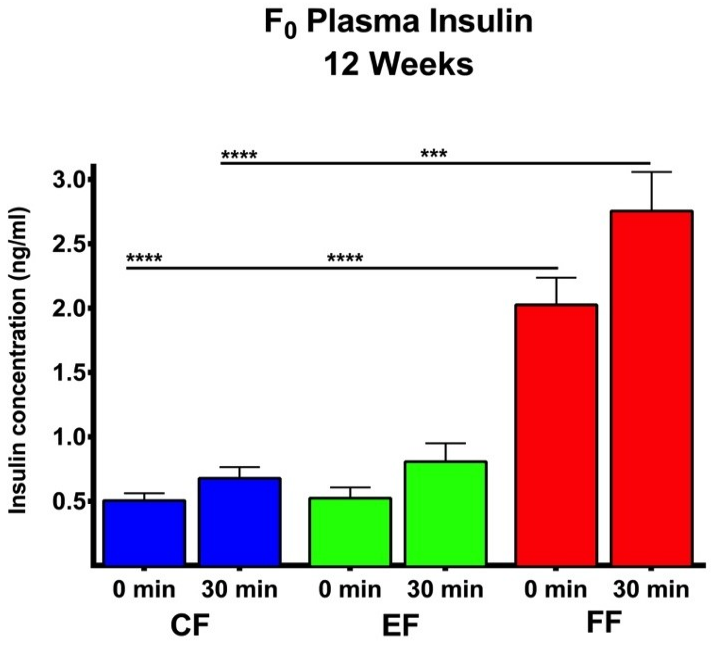

Figure 15. Father's (F_0) glucose (A) and plasma insulin (B) measured at week 12, with respect to time of diet assignment (A – CF/EF/FF n=6/5/6 // B – n=7/6/7 respectively). Significance calculated by two-tailed student's t-test ****p<0.0001 ***p<0.001 **p<0.005 *p<0.05.

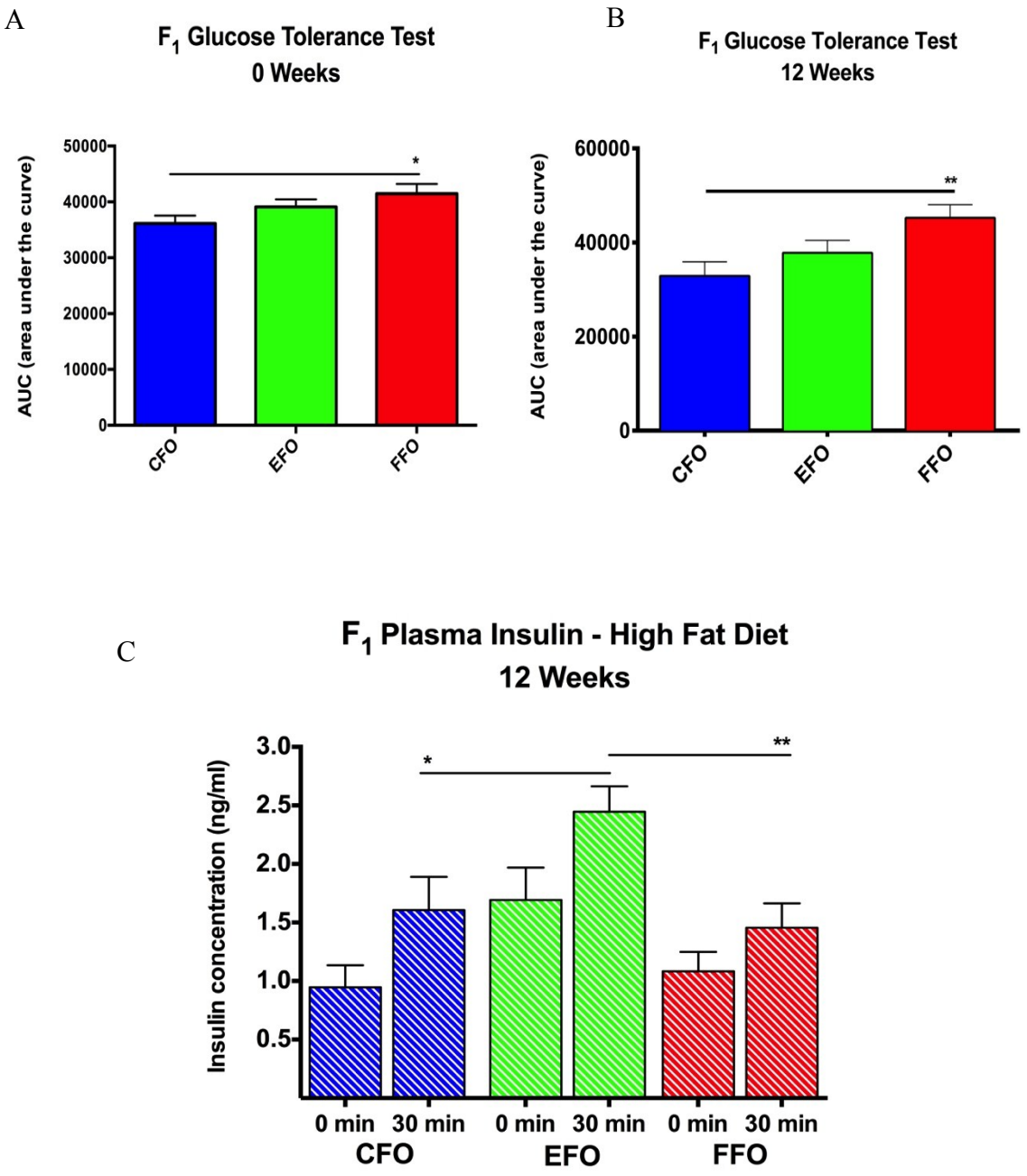

Figure 16. Control diet offspring (F_1) glucose measured at 0 weeks (A – 10% CFO/EFO/FFO n=33/35/28) and 12 weeks (B – 10% CFO/EFO/FFO n=35/40/30). C – Plasma insulin measured in 60% high-fat diet challenged offspring at week 12 (60% CFO/EFO/FFO n=6/7/6 respectively). Significance calculated by two-tailed student's t-test ****p<0.0001 ***p<0.001 **p<0.005 *p<0.05.

4.4 Developmental Monitoring

Analyses of developmental milestones revealed several intriguing differences among groups of offspring (male and female). One of the most notable disparities was seen in the body weights recorded on post-natal day 7 (Figure 17B) Offspring born from fat-diet fathers (FFO) were found to have a significantly lower body weight compared to both control father offspring and exercise father offspring (-10.7% and -13.1% respectively). This curious observation is one also described in several human studies, which identified a powerful correlation between low birth weight and paternal diabetes [10,62,103-105]

In addition to reduced body weights, FFO appeared developmentally delayed in the time at which their eyes first opened, fur appeared, and upper/lower incisors erupted.

Taken together these findings effectively illustrate that paternal diet and exercise play an important role in shaping their progeny's intrauterine development.

A

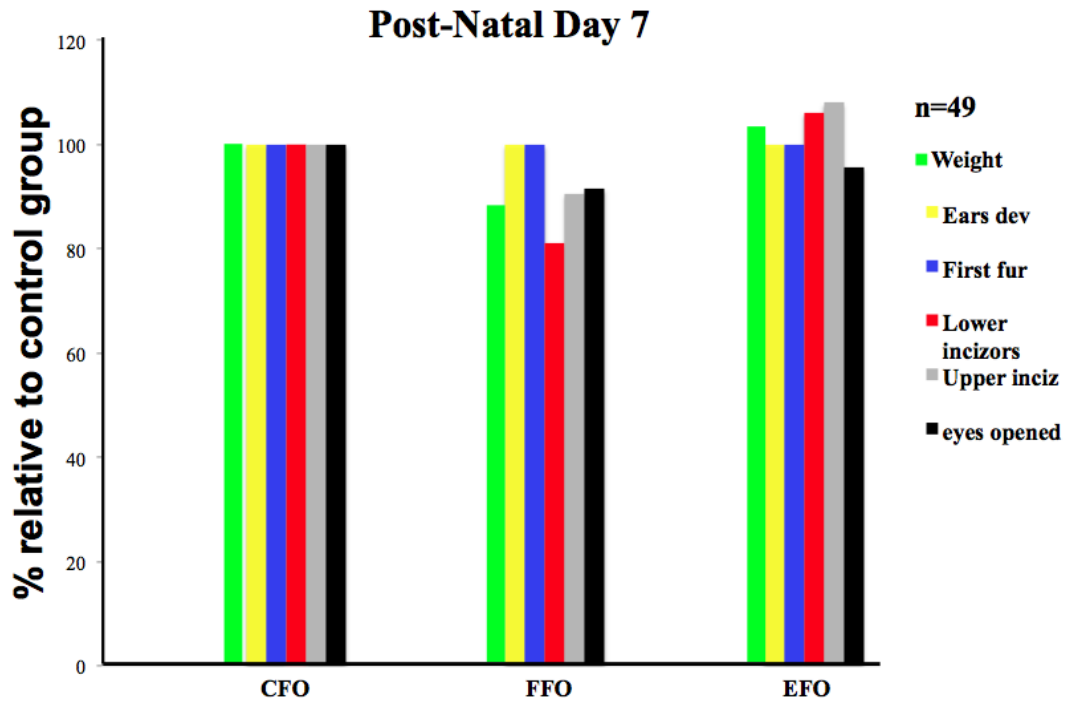

B

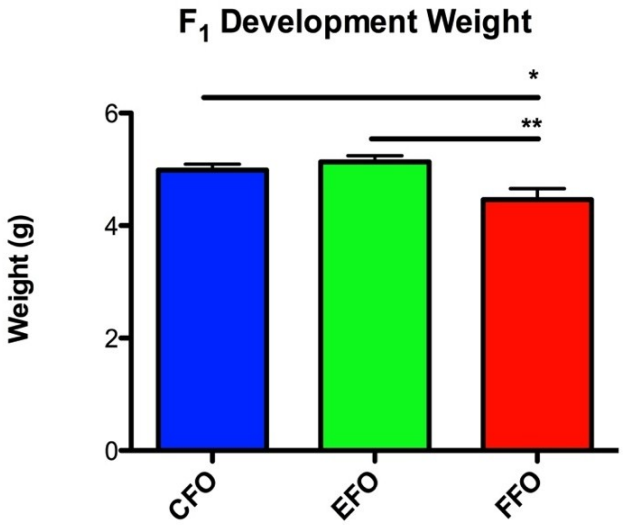

Figure 17. Developmental measurements taken on post-natal day 7. Observations made here did not distinguish between male and female offspring. A - Presentation of all parameters measured, normalized against control offspring. B – Offspring (F_1) weight as measured on post-natal day 7. Sample size: CFO/EFO/FFO n=49/42/31 respectively. Significance calculated by one-way ANOVA with post-hoc Bonferroni **p<0.005 *p<0.05.

4.5 F_0 Protein Expression

OGT and OGA protein expressions were quantified from western blot band intensities. Only father's data are presented here, due to offspring data being unavailable at the time of discussion. However, one implication of these data that is crucial to recognize is they effectively demonstrate OGT and OGA protein expressions are highly correlative to mRNA levels measured by PCR.

Protein expression measured in muscle revealed that FFs (n=3) have significantly higher levels of OGT compared to both CF and EF ($p<0.01$; n=2 and $p<0.005$; n=3 respectively). Furthermore, FFs were found to have significantly less OGA compared to CF ($p<0.01$), while EF's expression was significantly increased relative to both CF and FF ($p<0.01$).

Hepatic tissue demonstrated a similar pattern of OGT and OGA expression. This is seen by a significant reduction in measurable OGT within EF compared to CF and FF ($p<0.01$), in addition to a sharp increase in the levels of OGA within EF compared to CF and FF ($p<0.005$). FFs were also found to have significantly higher OGA compared to CF ($p<0.005$).

Finally, pancreatic tissue exhibited significantly higher amounts of OGT within FF compared to CF ($p<0.05$), while EFs were found to have a marked reduction in OGT compared to CF and FF ($p<0.005$ and 0.01 respectively). Pancreatic OGA expression was not included here due to inconclusive results at the time of authoring this paper.

These findings validate that consumption of a HFD causes an increase in OGT, which is an expected consequence of elevated flux through the hexosamine pathway.

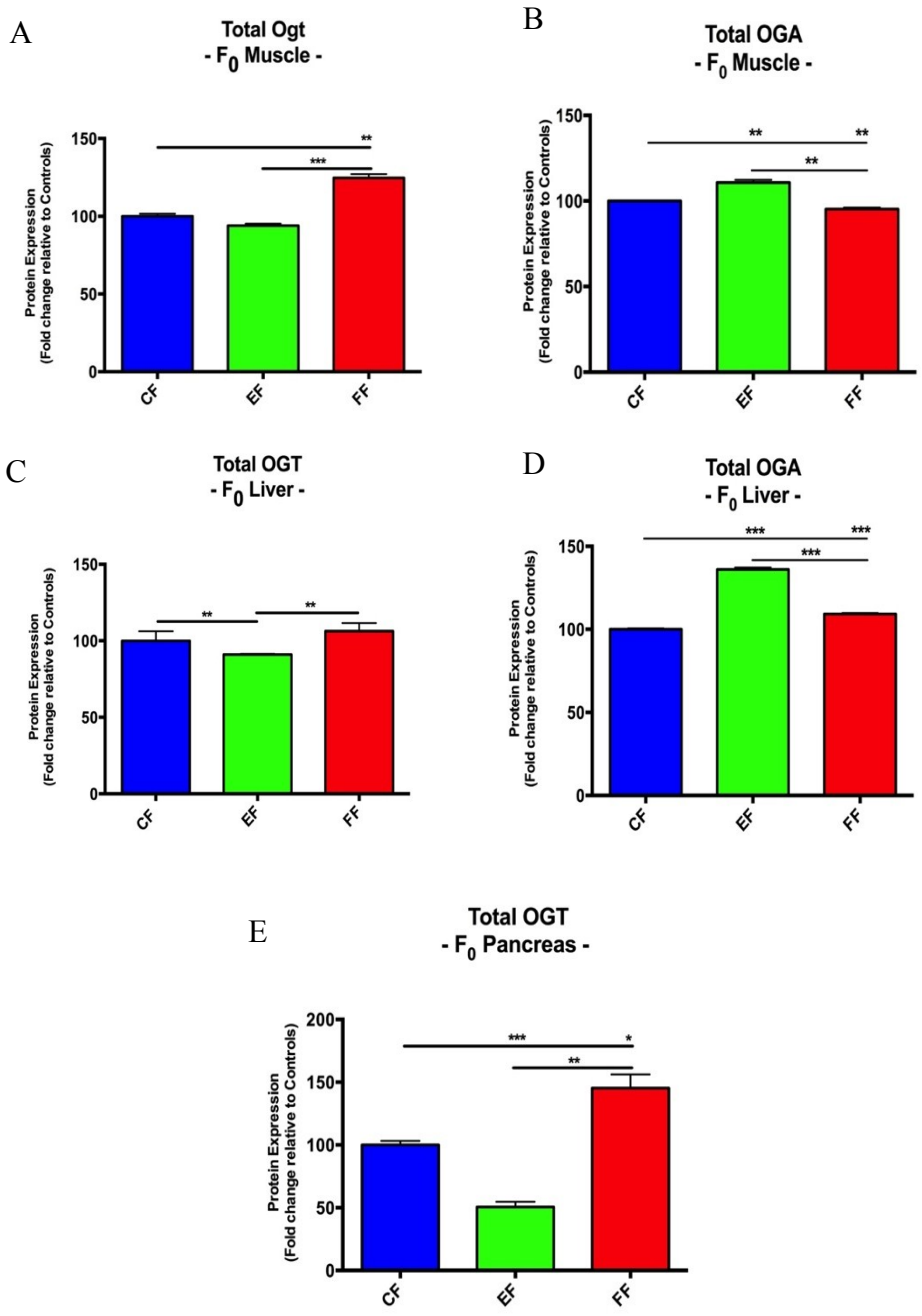

Figure 18. Father's (F_0) OGT and OGA total protein expression measured in insulin sensitive tissues. A – OGT protein expression measured in muscle (n=3). B – OGA protein expression measured in muscle (n=3). C – OGT protein expression measured in liver (n=3). D – OGA protein expression measured in liver (n=3). E – OGT protein expression measured in pancreas (n=3). Significance calculated by two-tailed student's t-test ***p<0.001 **p<0.005 *p<0.05.

4.6 Gene Expression

Messenger RNA (mRNA) transcripts were measured by real-time PCR to assess relative expression of target genes that, to varying extents, have all been implicated in an obese diabetic phenotype. All molecular data for offspring, presented in the subsequent sections, are for those animals assigned to a 10% fat control diet (i.e. no diet-challenged offspring included). Statistical differences were calculated by unpaired student's t-tests.

4.6.1 Skeletal Muscle mRNA

Significant differences were found between several genes examined in both fathers and offspring gastrocnemius muscle. Just like protein expression, gene expression of uridine diphospho-N-acetylglucosamine:peptide β-N-acetylglucosaminyltransferase (*Ogt*) was found to be substantially higher in FFs compared to both CF and EF ($p \leq 0.01$; n=4). Concomitant expression of *Oga* was identified to be statistically lower in FF compared to CF and EF ($p<0.05$). Moreover, *Oga* was statistically elevated in EF compared to CF ($p<0.05$).

These observations were also exhibited in FFO (n=3), where *Ogt* expression was found to be statistically higher than CFO and EFO ($p<0.001$; n=5). Furthermore, expression for Oga in EFO was significantly higher than FFO ($p<0.05$).

The patterns of *Ogt* and *Oga* gene expression, observed here in FF and FFO, are a platform for excessive protein O-GlcNAcylation, which current literature would suggest is a possible cause of T2DM.

A

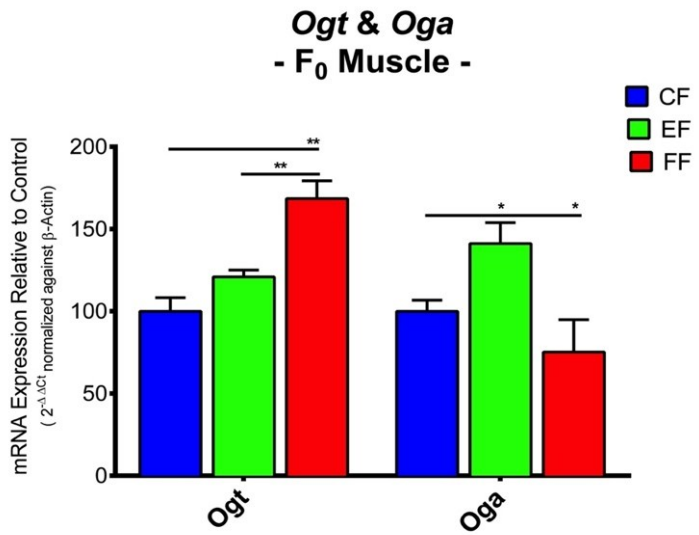

B

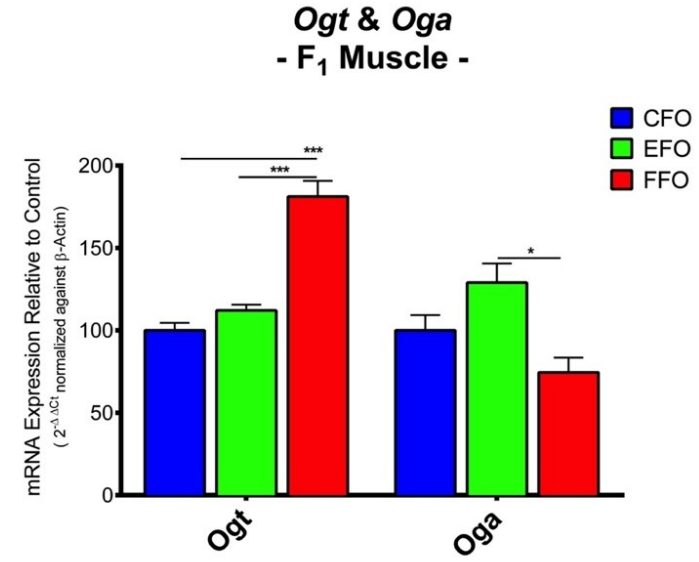

Figure 19. Gene expressions of *Ogt* and *Oga* (mRNA) measured in muscle. A – Father's (F_0) *Ogt* and *Oga* expressions (n=4). B – Offspring (F_1) *Ogt* and *Oga* expressions (CFO/EFO/FFO n=4/3/3 respectively). Significance calculated by two-tailed student's t-test ***p<0.001 **p<0.005 *p<0.05.

The imprinting genes *H19* and *Igf2* also revealed interesting patterns of reciprocity in their expression. Although the expression for *H19* in fathers was not quantified as significant, the trend remains interesting nonetheless. However, a comparison of the monoallelic expression for *Igf2* revealed EF and FF are drastically higher than CF ($p<0.001$ and 0.01 respectively). Furthermore, EF appeared statistically higher than FF ($p<0.05$). While in offspring, the expression for *H19* in EFO (n=5) was discovered to be drastically lower than CFO and FFO ($p<0.0001$ and 0.0005 respectively; n=4)

Igf2 expressions among offspring were highest in EFO ($p<0.05$). Interestingly, the trends seen in Figures 20A and 20B illustrates there is almost perfect chirality between fathers *H19* and offspring *Igf2*. The epigenetic mechanisms responsible for this phenomenon will be further explained in the methylation results.

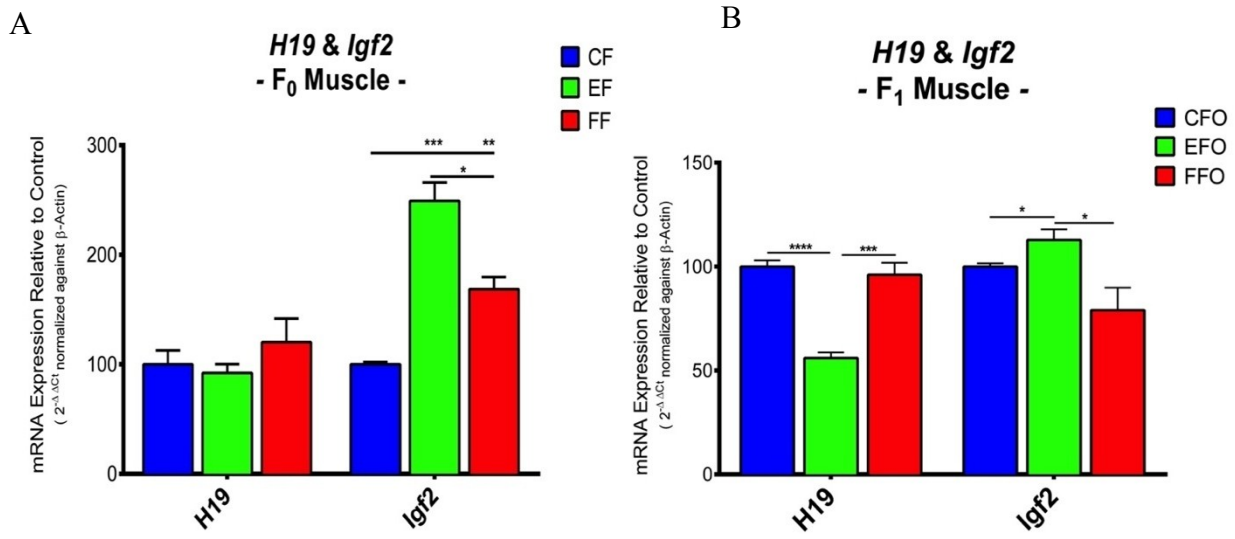

Figure 20. Gene expressions of *H19* and *Igf2* (mRNA) measured in muscle. A – Father's (F_0) *H19* and *Igf2* expressions (CF/EF/FF n=3/4/4 respectively). B – Offspring (F_1) *H19* and *Igf2* expressions (CFO/EFO/FFO n=3/4/4 respectively). Significance calculated by two-tailed student's t-test ****p<0.0001 ***p<0.001 **p<0.005 *p<0.05.

Other genes examined include *Slc2A4* (*Glut4*), *Ptpn1*, and *Pdk4*. In fathers, *Glut4* was found to be statistically higher in EF compared to FF ($p<0.01$); a trend that was further seen in EFO where expression was significantly higher compared to CFO and FFO ($p<0.01$). Overexpression of *Glut4* indicates potential for improved glucose sensitivity, although to confirm such a prediction necessitates protein expression and activity also be investigated, which is the case for each of the genes examined here.

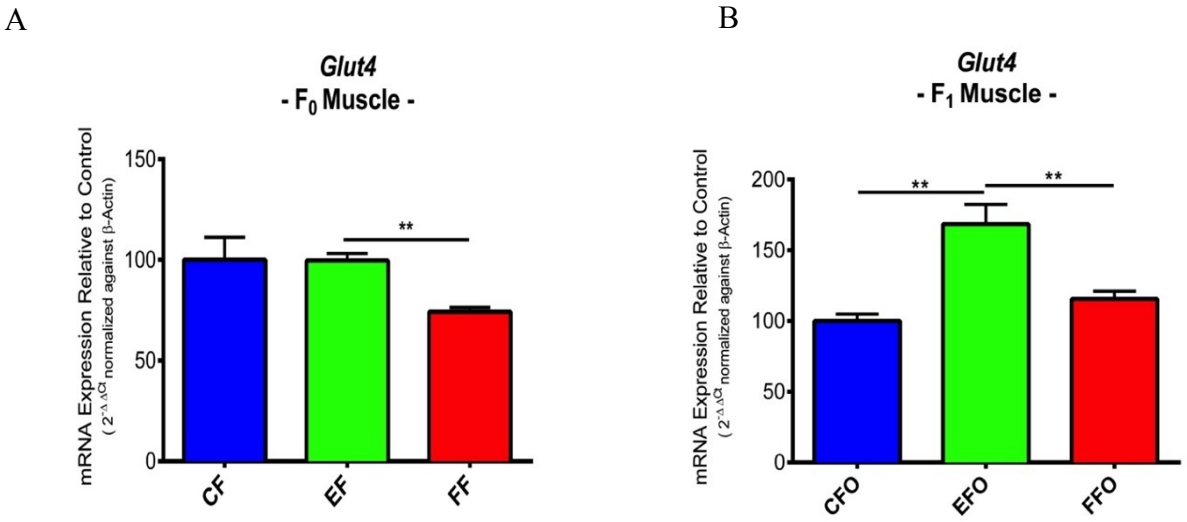

Figure 21. Gene expression for *Glut4* (mRNA) measured in muscle. A – Father's (F_0) expression (CF/EF/FF n=5/3/3 respectively). B – Offspring (F_1) expression (CFO/EFO/FFO n=4/6/4 respectively). Significance calculated by two-tailed student's t-test **p<0.005.

Ptpn1, which encodes the insulin receptor antagonist PTP1B, was observed to be statistically higher in FF compared to CF and EF ($p<0.005$ and $p<0.01$ respectively). FFO were also seen to be statistically higher than EFO and CFO ($p<0.005$ and $p<0.05$ respectively), in addition to CFO expression also being statistically higher than EFO ($p<0.01$). These findings indicate FF and FFO (assigned to a normal control diet) have a much higher risk of becoming insulin resistant compared to other groups of mice.

Finally, *Pdk4* expression in FF muscle was found to be statistically higher than both CF and EF ($p<0.005$). Among offspring, *Pdk4* transcripts measured in FFO were identified as statistically increased compared to EFO ($p<0.05$), which again is indicative of a diabetic phenotype.

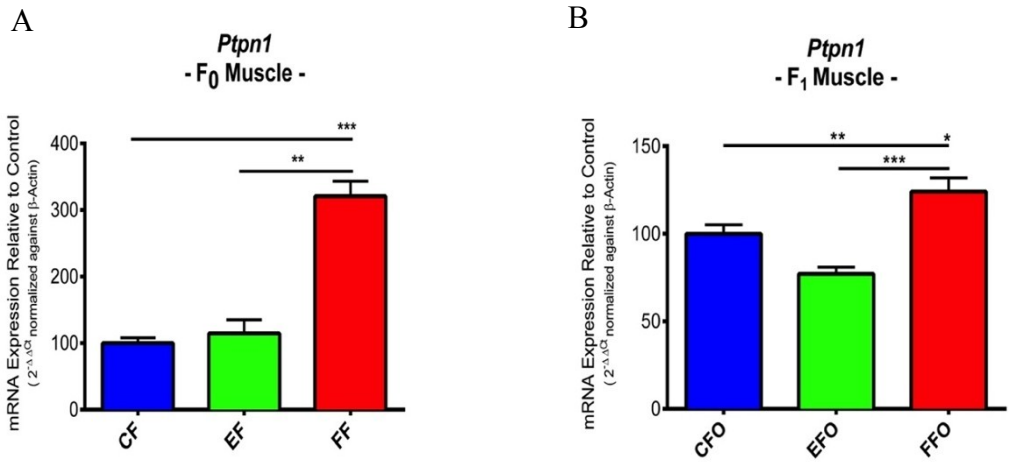

Figure 22. Gene expression for *Ptpn1* (mRNA) measured in muscle. A – Father's (F_0) expression (CF/EF/FF n=5/3/3 respectively). B – Offspring (F_1) expression (CFO/EFO/FFO n=4/6/4 respectively). Significance calculated by two-tailed student's t-test ***p<0.001 **p<0.005 *p<0.05.

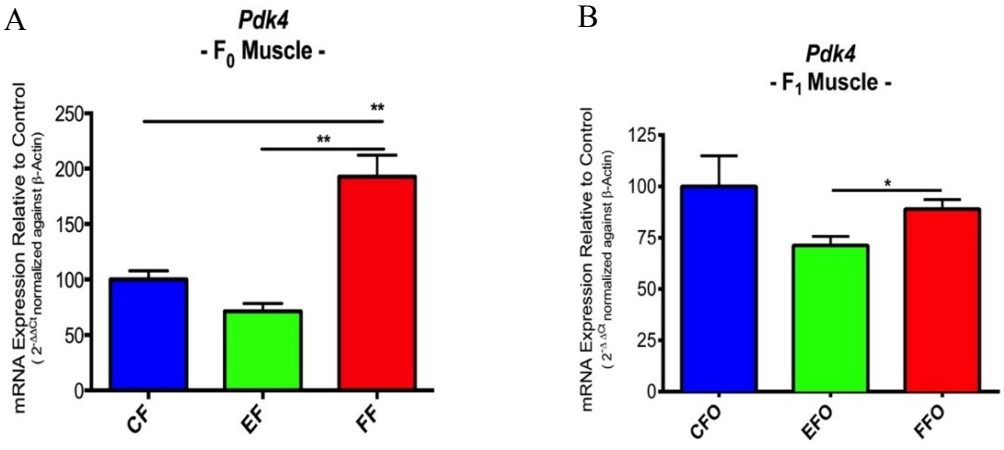

Figure 23. Gene expression for *Pdk4* (mRNA) measured in muscle. A – Father's (F_0) expression (CF/EF/FF n=5/3/3 respectively). B – Offspring (F_1) expression (CFO/EFO/FFO n=4/6/4 respectively). Significance calculated by two-tailed student's t-test **p<0.005 *p<0.05.

4.6.2 Pancreatic mRNA

In fathers the trends between Ogt and Oga were similar to the results presented for muscle. Ogt expression in FF was statistically elevated compared to CF and EF ($p<0.005$), while for Oga EF had the highest expression to both CF and FF ($p<0.005$). These patterns of expression were further carried over to offspring, where Ogt was highest in FFO compared to CFO and EFO. In addition, EFO and CFO were demonstrated significantly higher than FFO ($p<0.05$). These findings were also observed in skeletal muscle, and again are reflective of T2DM.

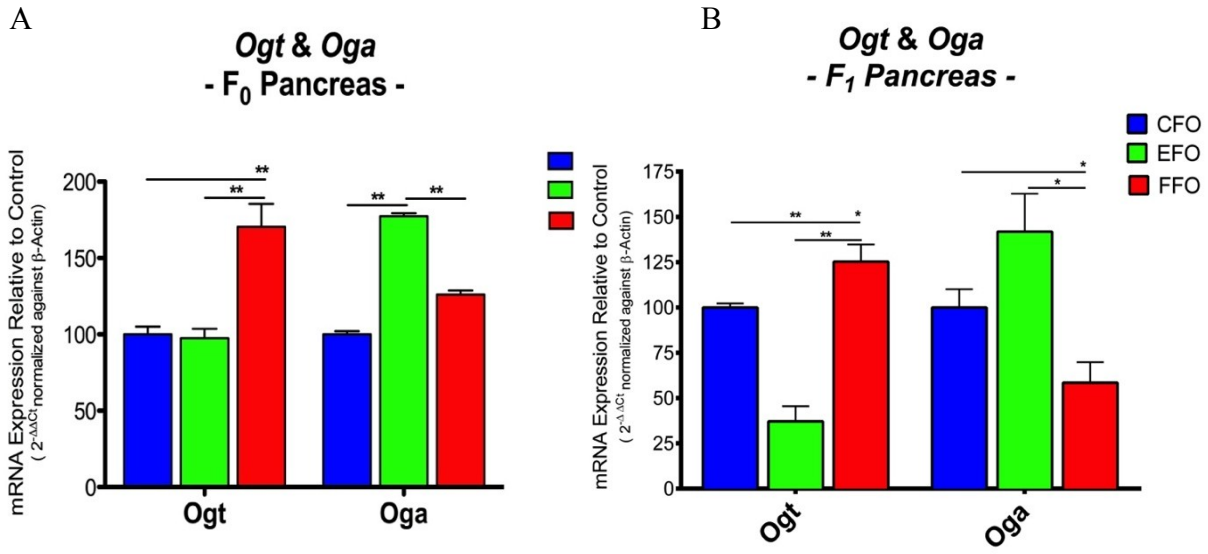

Figure 24. Gene expressions of *Ogt* and *Oga* (mRNA) measured in the pancreas. A – Father's (F_0) *Ogt* and *Oga* expressions (n=4). B – Offspring (F_1) *Ogt* and *Oga* expressions (CFO/EFO/FFO n=4/3/3 respectively). Significance calculated by two-tailed student's t-test **p<0.005 *p<0.05.

In fathers, there was no significant difference identified between CF and EF *H19*, however FF were found to be significantly higher than both father groups ($p<0.005$). Moreover, an increase in *Igf2* gene expression within EF was found to be statistically significant compared to FF ($p<0.05$).

In offspring, *H19* expression in EFO was statistically higher compared to CFO and FFO ($p<0.005$). Expression of *H19* measured in CFO was additionally found to be higher than that of FFO ($p<0.05$). These results contradict findings seen in other tissues. However, this is likely the product of methylation patterns within *H19's* 5' DMICR (discussed in the following section). The developmental programming of *H19* and *Igf2*, experienced by FF offspring, is likely to promote an enlargement of the pancreas. This is perhaps a preparatory mechanism, conferred by their respective fathers to facilitate increased insulin production. These findings are yet another example of paternal programming, preparing offspring for a similar life style.

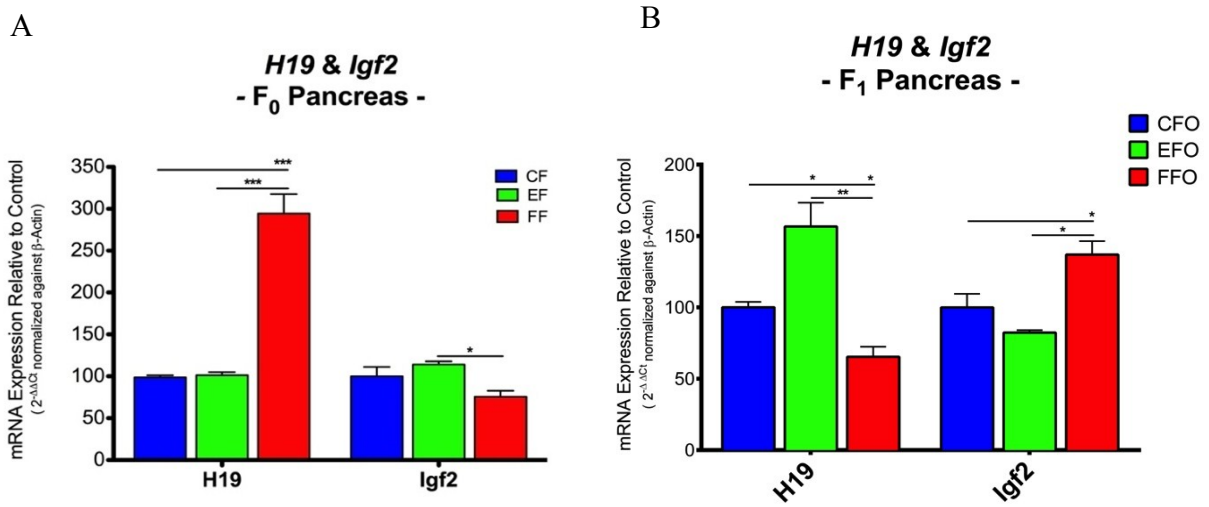

Figure 25. Gene expressions of *H19* and *Igf2* (mRNA) measured in the pancreas. A – Father's (F_0) *H19* and *Igf2* expressions (CF/EF/FF n=3/4/4 respectively). B – Offspring (F_1) *H19* and *Igf2* expressions (CFO/EFO/FFO n=3/4/4 respectively). Significance calculated by two-tailed student's t-test ***p<0.001 **p<0.005 *p<0.05.

Analysis of gene expression in fathers further revealed *Glut4* was statistically elevated in EF compared to CF and FF ($p<0.0005$). Additionally, differences between CF and FF were found to be statistically relevant ($p<0.0005$). Interestingly, this shortage of *Glut4* in FF was reversed in FFO, who were shown to have statistically higher levels than CFO ($p<0.05$). These findings indicate a severe deficit in glucose sensitivity occurring in FF pancreatic tissue

Pdk4 expressions in fathers and offspring were highly similar to one another. FFs were found to have significantly higher levels of *Pdk4* mRNA compared to CF and EF ($p<0.05$). In addition, expression measured in CF was statistically higher than EF ($p<0.05$). In offspring, EFO had significantly lower levels of *Pdk4* transcript compared to CFO and FFO ($p<0.0005$ and 0.001 respectively).

Similar to *Pdk4*, the expression of *FoxO1* between fathers and offspring were highly similar. FFs were shown to have the highest level of expression compared to CF and EF ($p<0.001$), while CF was even lower than EF (0.005). Although the trend in offspring was not as pronounced as in fathers, FFO were found to have a significantly higher amount of *FoxO1* transcript compared to CFO ($p<0.05$).

Finally, *Ptpn1* was not differentially expressed in fathers, however in FFO its transcriptional activity was significantly higher than that measured in CFO ($p<0.05$).

The findings presented here demonstrate that FFO experienced the same detrimental trends observed within the skeletal muscle tissue. One notable difference, however, was the substantial increase of *Igf2* expression in FFO. This only occurred in pancreatic tissue, indicating perhaps that FFO were epigenetically programmed by their fathers to have a higher capacity for insulin production.

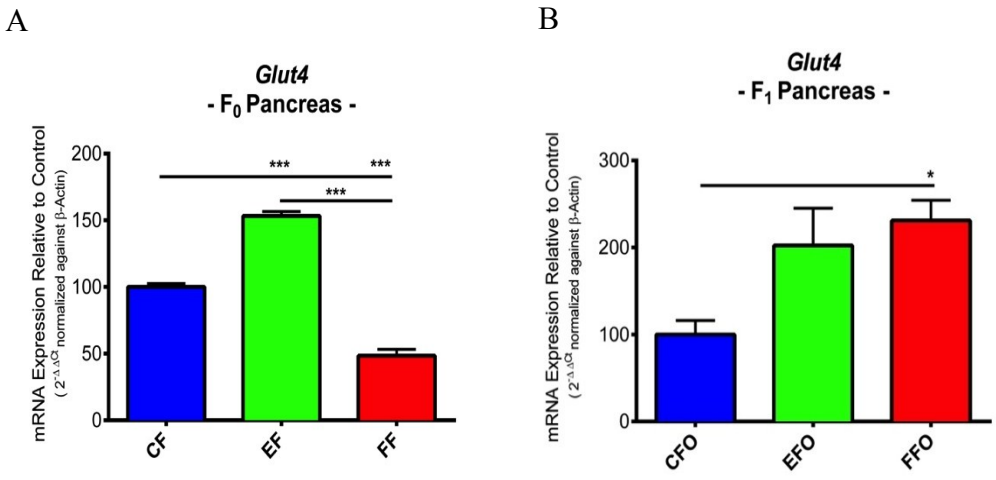

Figure 26. Gene expression for *Glut4* (mRNA) measured in the pancreas. A – Father's (F_0) expression (CF/EF/FF n=3/3/4 respectively). B – Offspring (F_1) expression (CFO/EFO/FFO n=3/3/3 respectively). Significance calculated by two-tailed student's t-test ***p<0.001 *p<0.05.

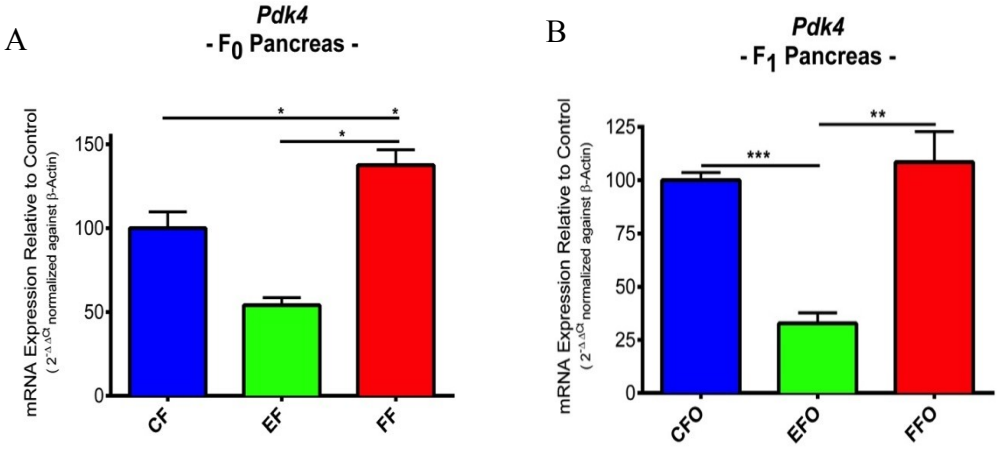

Figure 27. Gene expression for *Pdk4* (mRNA) measured in the pancreas. A – Father's (F_0) expression (CF/EF/FF n=3/3/3 respectively). B – Offspring (F_1) expression (CFO/EFO/FFO n=3/3/3 respectively). Significance calculated by two-tailed student's t-test ***p<0.001 **p<0.005 *p<0.05.

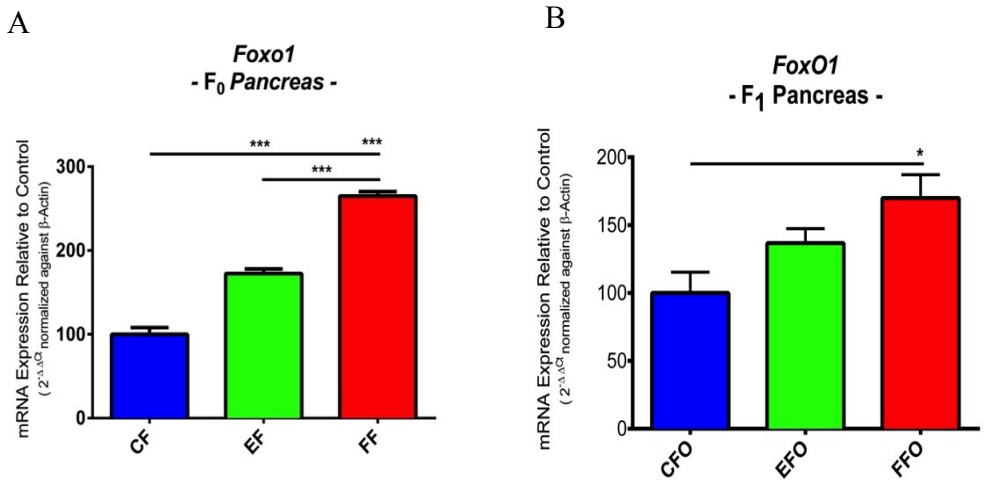

Figure 28. Gene expression for *FoxO1* (mRNA) measured in the pancreas. A – Father's (F_0) expression (CF/EF/FF n=3/3/3 respectively). B – Offspring (F_1) expression (CFO/EFO/FFO n=4/3/3 respectively). Significance calculated by two-tailed student's t-test ***p<0.001 *p<0.05.

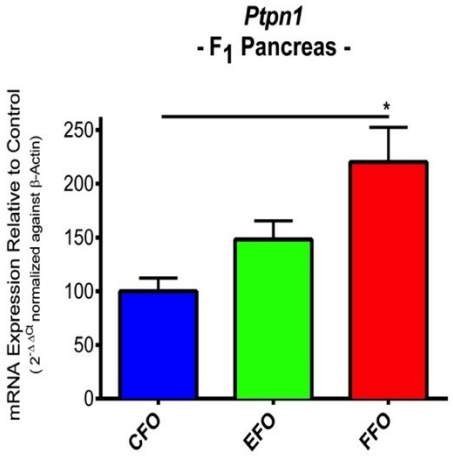

Figure 29. Gene expression for *Ptpn1* (mRNA) measured in the pancreas of offspring (F_1) (CFO/EFO/FFO n=3/3/4 respectively). Significance calculated by two-tailed student's t-test *p<0.05.

4.6.3 Hepatic mRNA

In hepatic tissue collected from fathers, the FF group had significantly elevated expression for Ogt compared to CF and EF ($p<0.05$ and 0.01), while their respective level of Oga was found to be statistically lower than EF ($p<0.05$). This pattern was repeated to a lesser extent among offspring, where EFO showed lower levels of Ogt mRNA compared to CFO ($p<0.05$), and additionally were seen to have the highest level of Oga expression compared to CFO and FFO ($p<0.05$ and 0.01). CFO were additionally found to have higher Oga expression compared to FFO ($p<0.01$).

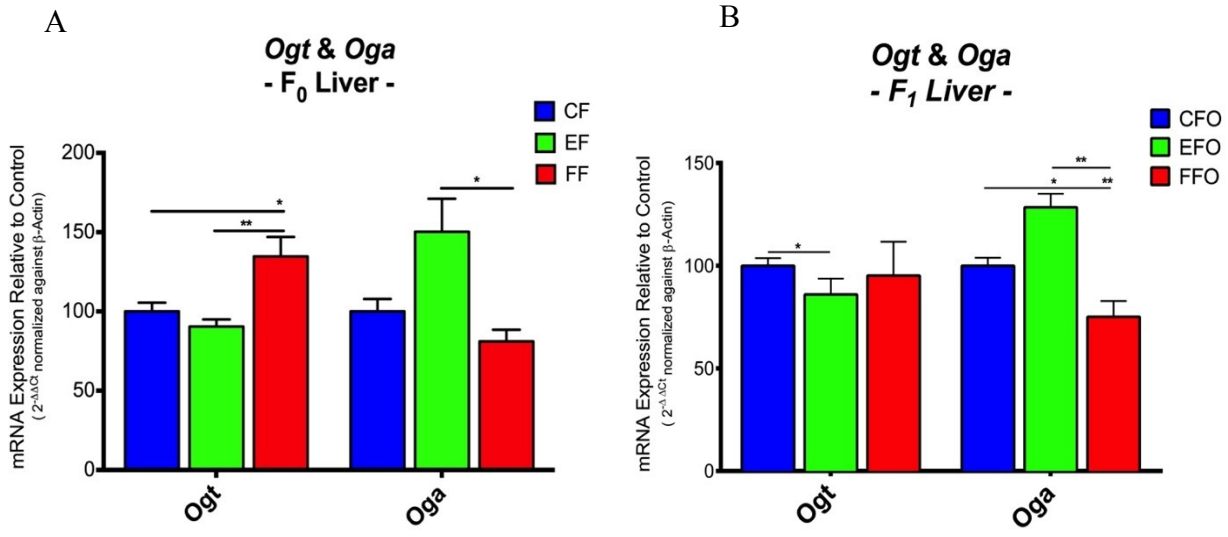

Figure 30. Gene expressions of *Ogt* and *Oga* (mRNA) measured in the liver. A – Father's (F_0) *Ogt* (CF/EF/FF n=5/4/4) and *Oga* expressions (CF/EF/FF n=4/3/4 respectively). B – Offspring (F_1) *Ogt* and *Oga* expressions (CFO/EFO/FFO n=5/4/4 respectively). Significance calculated by two-tailed student's t-test **p<0.005 *p<0.05.

A

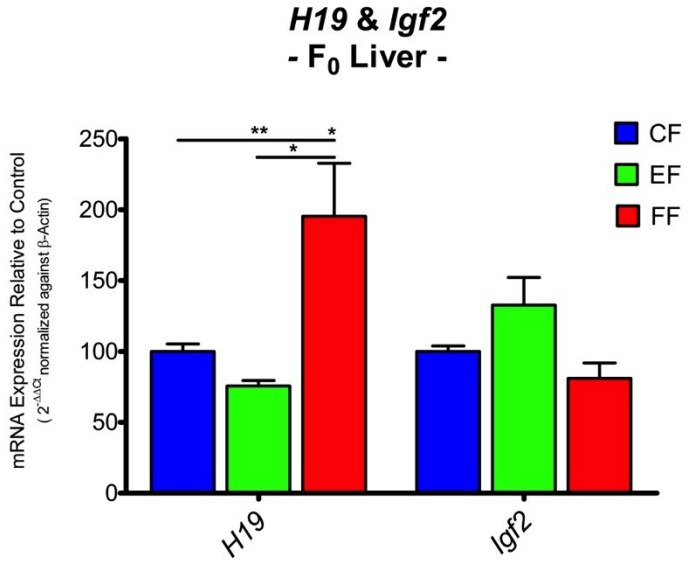

B

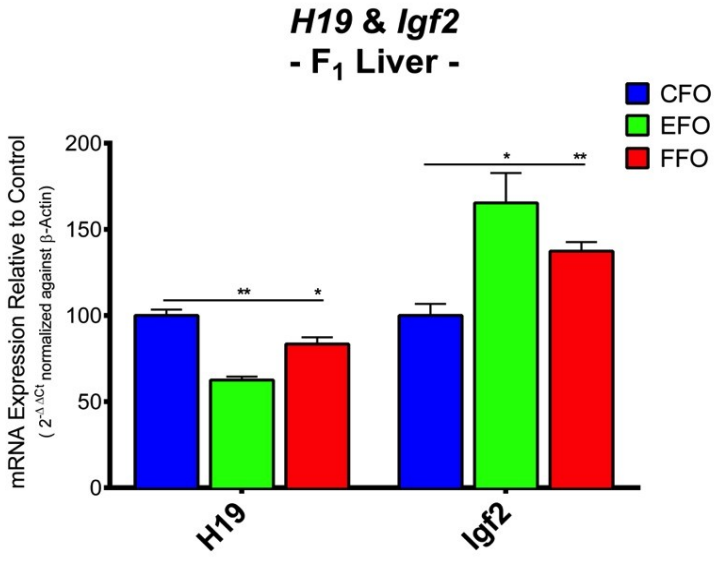

Figure 31. Gene expressions of *H19* and *Igf2* (mRNA) measured in the liver. A – Father's (F_0) *H19* and *Igf2* expressions (CF/EF/FF n=5/4/4). B – Offspring (F_1) *H19* and *Igf2* expressions (CFO/EFO/FFO n=3/3/3 respectively). Significance calculated by two-tailed student's t-test **p<0.005 *p<0.05.

Differential gene expression was seen to occur in several additional genes including *Glut4* (an isoform typically only assessed in skeletal muscle), where EF showed the greatest level of expression compared to CF and FF ($p<0.005$). Strangely, these findings were observed in reverse among offspring, where EFO had a statistically lower amount of *Glut4* mRNA compared to CFO and FFO ($p<0.05$).

Ptpn1 gene product was highest in FF, compared to both CF and EF ($p<0.05$). This observation was also seen to a lesser degree in offspring, where FFO were shown to have statistically higher levels of *Ptpn1* transcript compared to CFO ($p<0.05$).

Finally, *Pdk4* gene expression was found highly conserved from fathers to offspring. Measurements from EFs were significantly lower than CF and FF ($p<0.01$ and 0.05), while among offspring groups FFO were observed to be significantly higher than both CFO and EFO ($p=0.0001$ and $p<0.0001$ respectively).

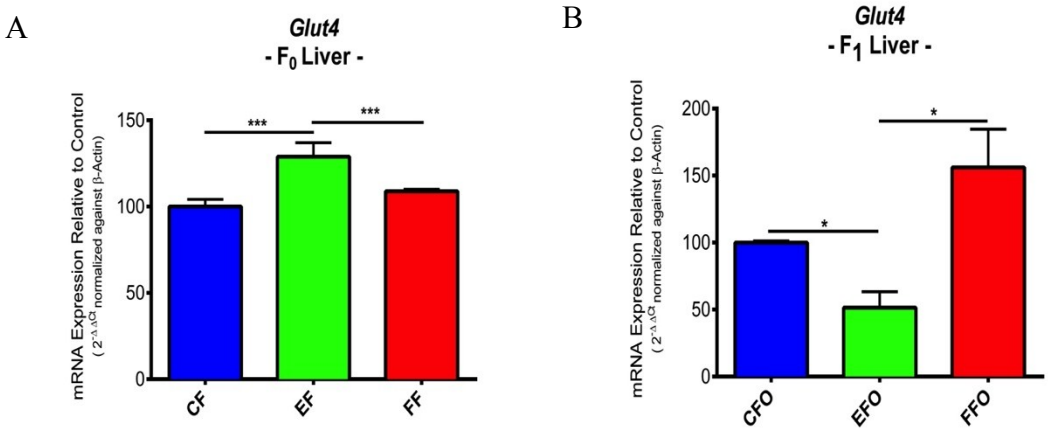

Figure 32. Gene expression for *Glut4* (mRNA) measured in the liver. A – Father's (F_0) expression (CF/EF/FF n=3/4/3 respectively). B – Offspring (F_1) expression (CFO/EFO/FFO n=3/3/3 respectively). Significance calculated by two-tailed student's t-test ***p<0.001 *p<0.05.

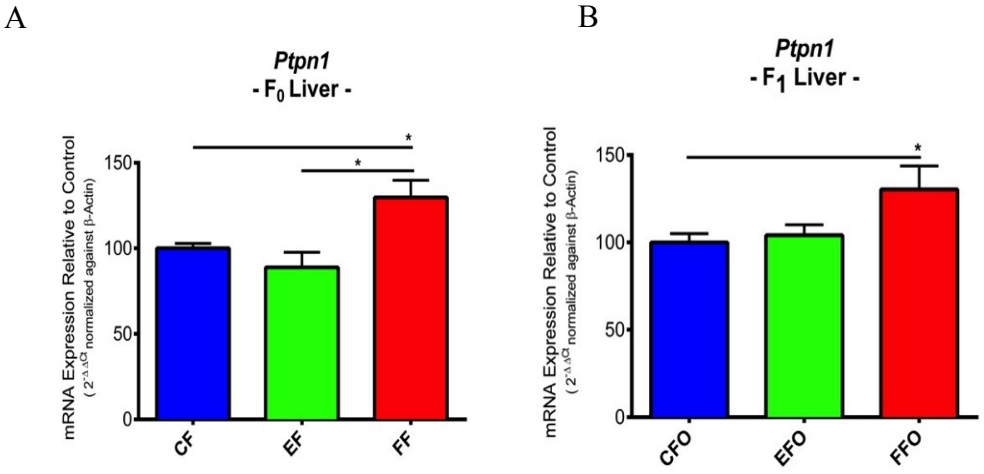

Figure 33. Gene expression for *Ptpn1* (mRNA) measured in the liver. A – Father's (F_0) expression (CF/EF/FF n=4/4/4 respectively). B – Offspring (F_1) expression (CFO/EFO/FFO n=5/4/4 respectively). Significance calculated by two-tailed student's t-test *p<0.05.

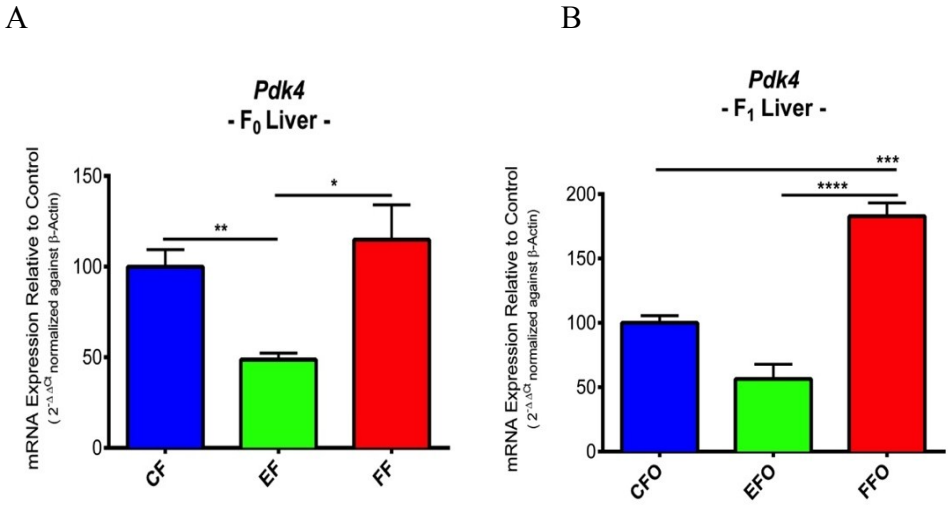

Figure 34. Gene expression for *Pdk4* (mRNA) measured in the liver. A – Father's (F_0) expression (CF/EF/FF n=5/4/3 respectively). B – Offspring (F_1) expression (CFO/EFO/FFO n=5/5/4 respectively). Significance calculated by two-tailed student's t-test ****p<0.0001 ***p<0.001 **p<0.005 *p<0.05.

4.7 Methylation Analysis

Epigenetic programming was assessed in terms of the methylation patterns occurring at gene promoters, which were conserved from fathers to offspring. Several differences were observed between animals, although the most interesting findings were the seemingly opposite trends in methylation observed between exercising fathers and high-fat diet fathers, as well as their respective offspring.

4.7.1 Muscle

As seen in figures 35 and 36 significant differences were identified for *Ogt* and *Oga* methylation in fathers and offspring. EFs were found to have a drastically higher level of methylation at *Ogt* compared to FF ($p<0.01$), while FF were significantly more methylated on *Oga* relative to CF and EF. The changes witnessed among fathers were found well maintained in the F_1 generation. Specifically, EFO had higher levels of methylation than CFO and FFO ($p<0.05$) for *Ogt*, while *Oga* was seen to be hypomethylated with respect to CFO and FFO ($p<0.01$).

Additionally, *H19* methylation for fathers and offspring was demonstrated to be remarkably similar. EF showed elevated methylated at the *H19* 5' DMICR compared to CF and FF ($p<0.005$ and 0.01 respectively). Furthermore, CFs were also seen to have higher methylation compared to FF ($p<0.01$).

Investigation of *Pdk4* revealed a significant reduction in the methylation within FF compared to CF and EF ($p<0.005$), while in offspring EFO demonstrated to be significantly higher than CFO and FFO ($p<0.01$ and $p<0.05$).

Glut4 methylation among fathers was found to be lowest in EF compared to CF and FF ($p<0.01$ and $p<0.0001$). Additionally, FFs demonstrated a statistically significant increase in methylation relative to CF ($p<0.05$). In offspring, strangely there was a reversal in Glut4 methylation compared to their respective fathers. FFO showed minimal methylation that was significantly lower than CFO ($p<0.01$), while EFO were additionally seen to be statistically higher than both FFO as well as CFO ($p<0.01$ and 0.05 respectively).

Finally, analysis of *Ptpn1* methylation in fathers revealed EFs were significantly higher than FF ($p<0.05$), while in offspring EFO demonstrated an increase in methylation in comparison to both CFO and FFO ($p<0.01$ and 0.001 respectively).

The validity of these findings are further substantiated by the respective gene expressions described previously, where methylation is clearly shown to represses gene transcription. The only exception appears with the gene *Glut4*, where offspring's expression and methylation exhibit transposable trends, indicating an ulterior means of gene regulation.

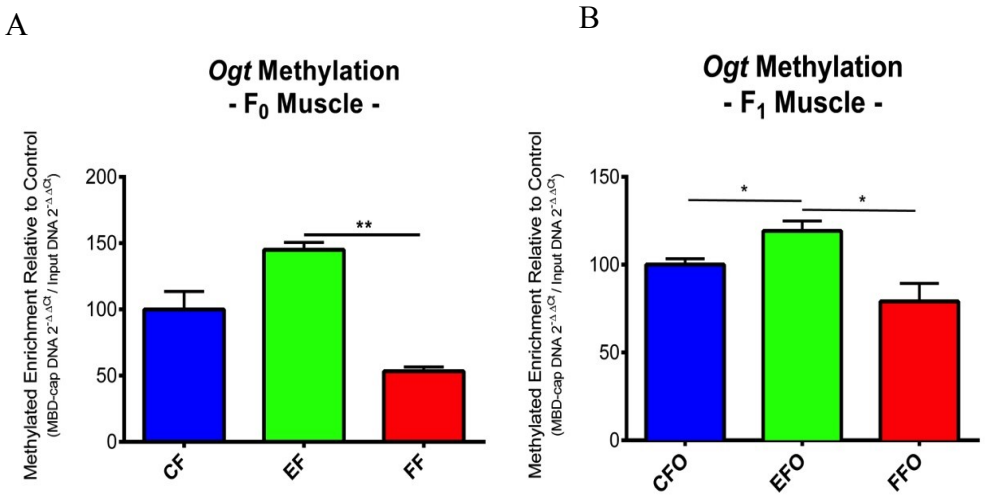

Figure 35. Promoter methylation for *Ogt* (genomic DNA) measured in the muscle. A – Father's (F_0) *Ogt* methylation (CF/EF/FF n=3/3/4 respectively). B – Offspring (F_1) *Ogt* methylation (CFO/EFO/FFO n=4/4/3 respectively). Significance calculated by two-tailed student's t-test **p<0.005 *p<0.05.

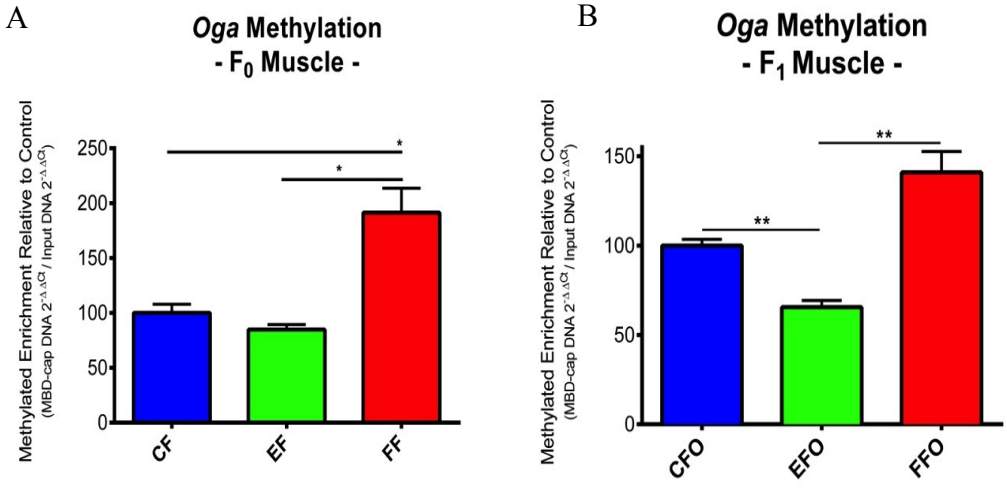

Figure 36. Promoter methylation for *Oga* (genomic DNA) measured in the muscle. A – Father's (F_0) *Oga* methylation (CF/EF/FF n=3/3/4 respectively). B – Offspring (F_1) *Oga* methylation (CFO/EFO/FFO n=4/4/3 respectively). Significance calculated by two-tailed student's t-test **p<0.005 *p<0.05.

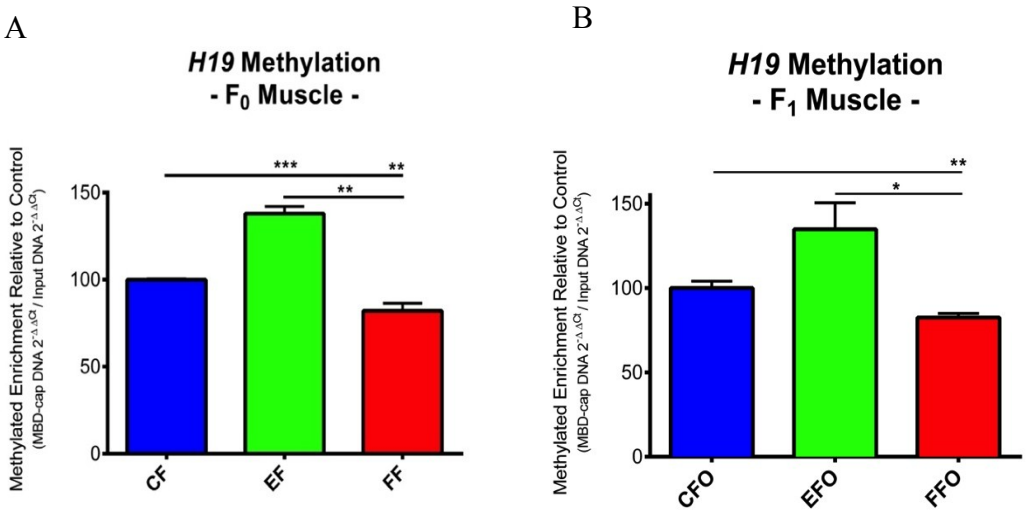

Figure 37. Promoter methylation for *H19* (genomic DNA) measured in the muscle. A – Father's (F_0) *H19* methylation (n=3). B – Offspring (F_1) *H19* methylation (n=4). Significance calculated by two-tailed student's t-test ***p<0.001 **p<0.005 *p<0.05.

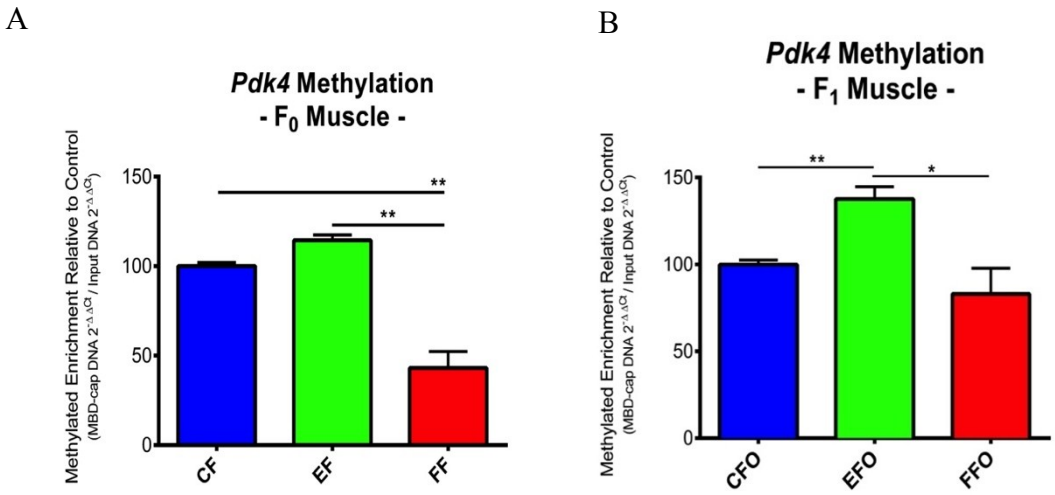

Figure 38. Promoter methylation for *Pdk4* (genomic DNA) measured in the muscle. A – Father's (F_0) *Pdk4* methylation (CF/EF/FF n=3/3/4 respectively). B – Offspring (F_1) *Pdk4* methylation (CFO/EFO/FFO n=4/4/3 respectively). Significance calculated by two-tailed student's t-test **p<0.005 *p<0.05.

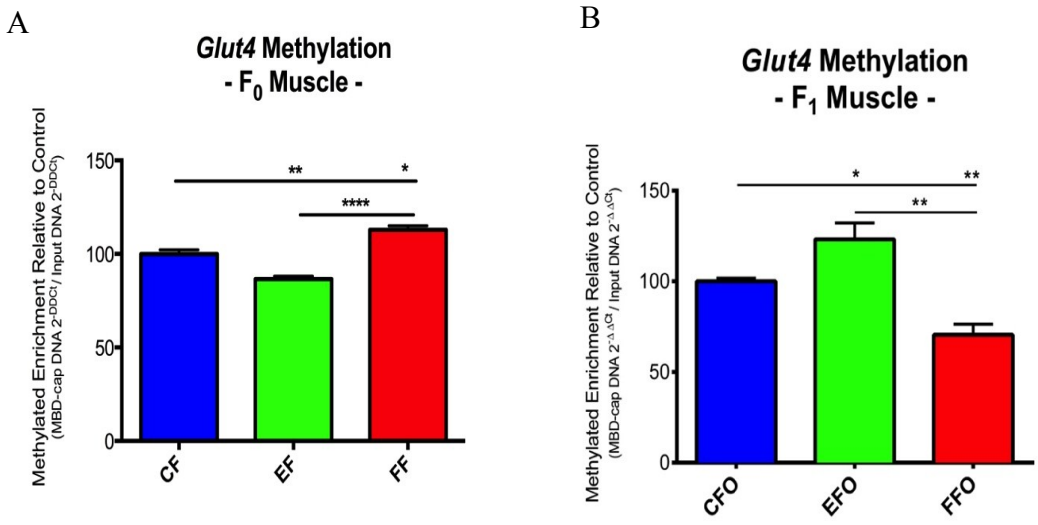

Figure 39. Promoter methylation for *Glut4* (genomic DNA) measured in the muscle. A – Father's (F_0) *Glut4* methylation (CF/EF/FF n=3/4/4 respectively). B – Offspring (F_1) *Glut4* methylation (CFO/EFO/FFO n=4/4/3 respectively). Significance calculated by two-tailed student's t-test ****p<0.0001 **p<0.005 *p<0.05.

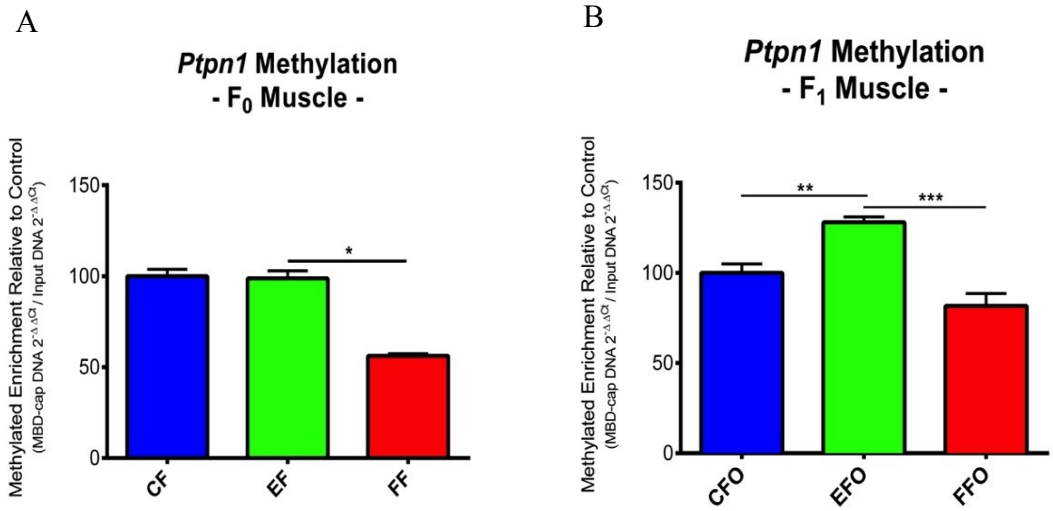

Figure 40. Promoter methylation for *Ptpn1* (genomic DNA) measured in the muscle. A – Father's (F_0) *Ptpn1* methylation (CF/EF/FF n=2/4/3 respectively). B – Offspring (F_1) *Ptpn1* methylation (n=4). Significance calculated by two-tailed student's t-test ***p<0.001 **p<0.005 *p<0.05.

4.7.2 Pancreas

Promoter-methylation of several genes examined in the pancreas were discovered to be conserved from fathers to offspring. Analysis with an unpaired student's t-test revealed the methylation of *Ogt* in fathers was statistically higher in EF compared to FF ($p<0.01$). Strangely, in fathers only negligible amounts of *Oga* were identified. In offspring, Ogt methylation was statistically reduced in FFO compared to CFO ($p<0.05$). *Oga* methylation was found to be lower in EFO compared to both CFO and FFO ($p<0.05$ and 0.01 respectively).

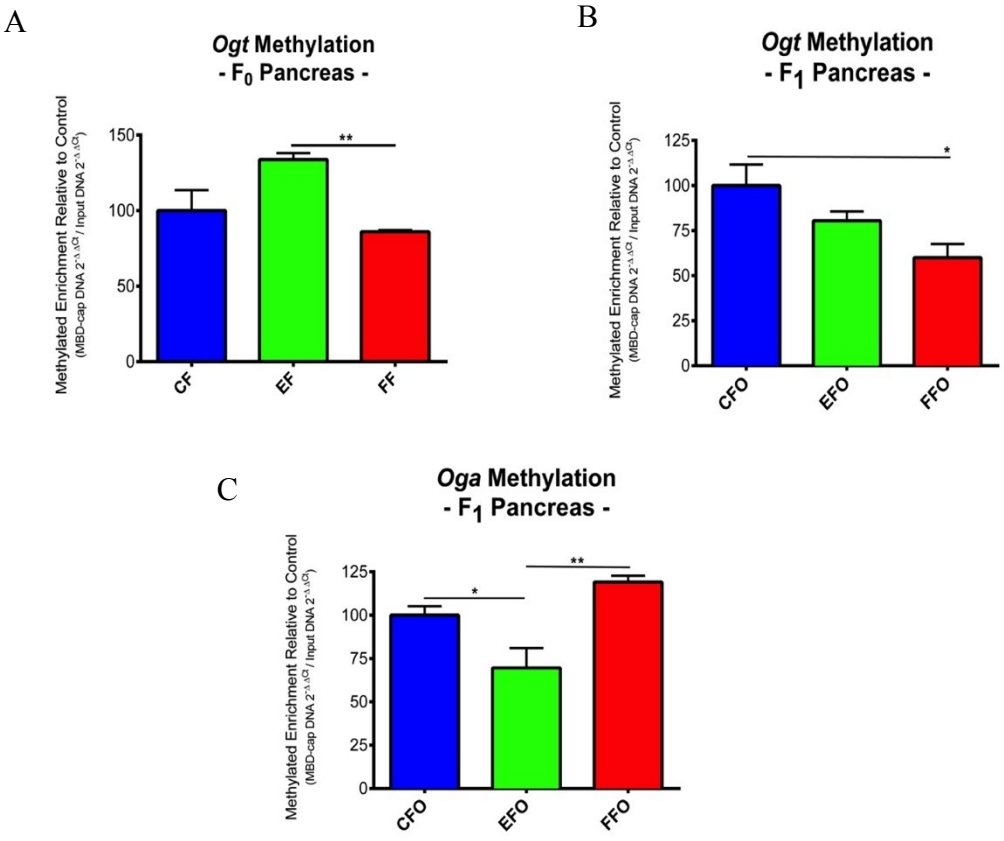

Figure 41. Promoter methylation for *Ogt* and *Oga* (genomic DNA) measured in the muscle. A – Father's (F_0) *Ogt* methylation (n=2); Father's Oga methylation was negligible. B – Offspring (F_1) *Ogt* methylation (CFO/EFO/FFO n=4/3/4 respectively). C – Offspring (F_1) *Oga* methylation (CFO/EFO/FFO n=3/4/4 respectively). Significance calculated by two-tailed student's t-test **p<0.005 *p<0.05.

Methylation of *H19* in FF was statistically higher than both CF and EF ($p<0.05$). This trend was carried to offspring, where FFO were demonstrated statistically increased compared to EFO ($p<0.05$).

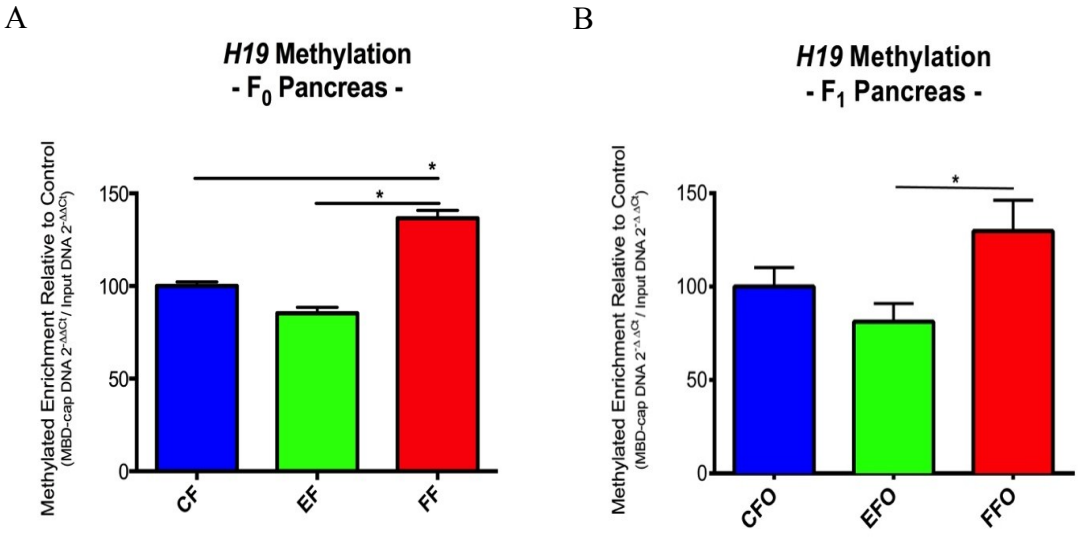

Figure 42. Promoter methylation for *H19* (genomic DNA) measured in the muscle. A – Father's (F_0) *H19* methylation (n=2). B – Offspring (F_1) *H19* methylation (CFO/EFO/FFO n=3/4/3 respectively). Significance calculated by two-tailed student's t-test *$p<0.05$.

Examination of *Pdk4*'s promoter region within pancreatic tissue revealed FFs were in a hypomethylated state compared to CF and EF ($p<0.01$). This was also seen among offspring, where FFO were highly similar to their hypomethylated fathers and were statistically lower than CFO and EFO ($p<0.01$ and 0.005). Furthermore, EFO were statistically higher than CFO ($p<0.005$).

Glut4 was found statistically reduced in FF compared to EF ($p<0.01$), while in offspring the FFO group was also statistically lower than EFO in addition to CFO ($p<0.005$). EFO also exhibited significantly less methylation compared to CFO ($p<0.01$).

Lastly, although no statistical differences were found to exist in Ptpn1 between fathers, FFO methylation was found significantly reduced compared to CFO and EFO ($p<0.005$), while EFO was additionally less than CFO ($p<0.01$).

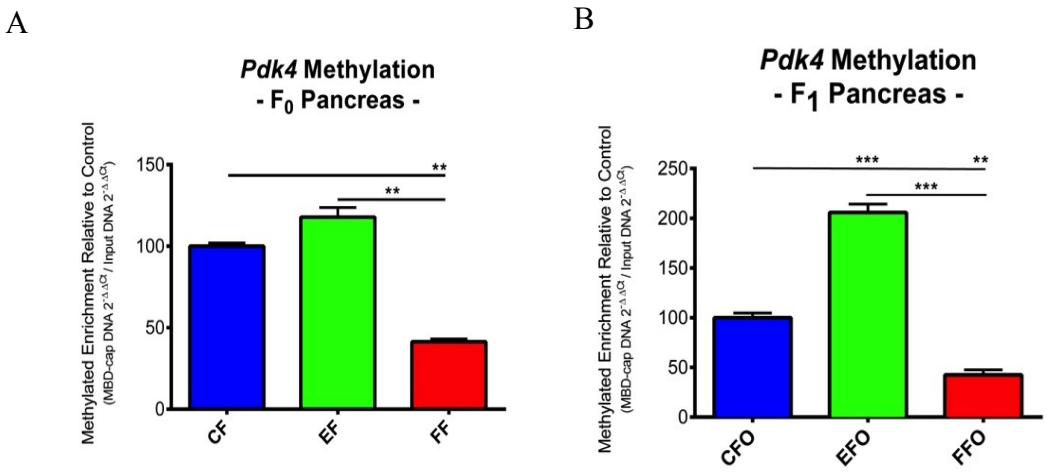

Figure 43. Promoter methylation for *Pdk4* (genomic DNA) measured in the muscle. A – Father's (F_0) *Pdk4* methylation (n=2). B – Offspring (F_1) *Pdk4* methylation (n=3). Significance calculated by two-tailed student's t-test ***p<0.001 **p<0.005.

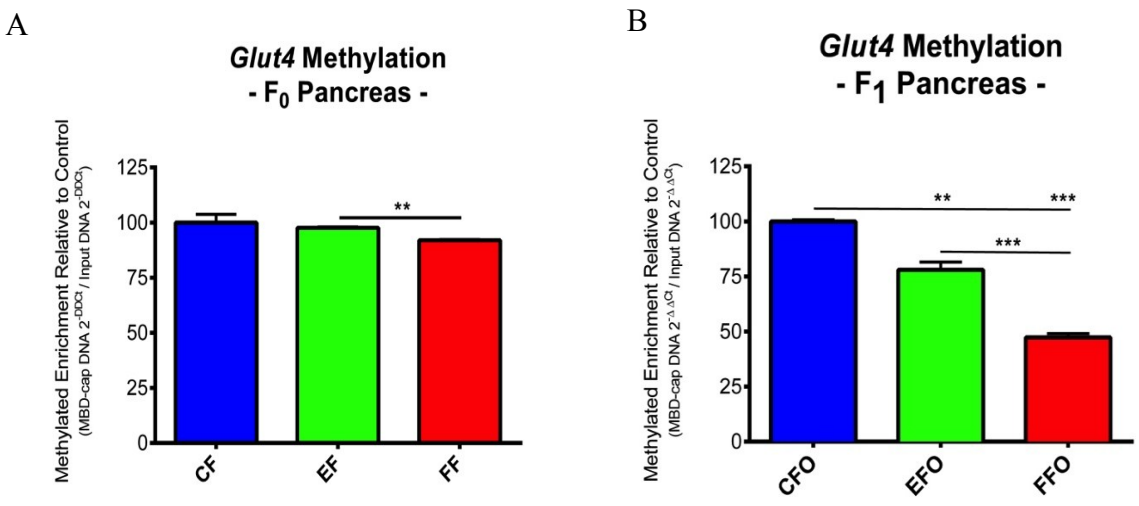

Figure 44. Promoter methylation for *Glut4* (genomic DNA) measured in the muscle. A – Father's (F_0) *Glut4* methylation (n=2). B – Offspring (F_1) *Glut4* methylation (CFO/EFO/FFO n=3/4/3 respectively). Significance calculated by two-tailed student's t-test ***p<0.001 **p<0.005.

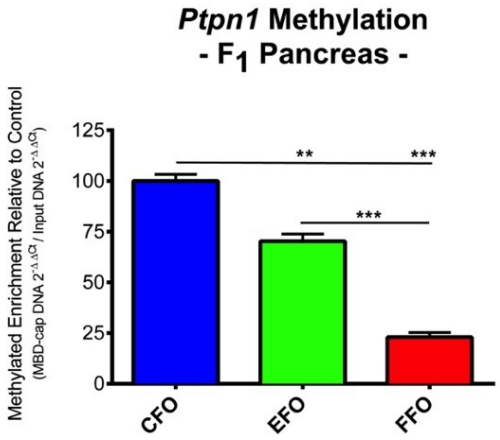

Figure 45. Promoter methylation for *Ptpn1* in offspring (F_1) (n=3). Significance calculated by two-tailed student's t-test ***p<0.001 **p<0.005.

4.7.3 Liver

Examination of hepatic *Ogt* in fathers revealed significantly higher methylation occurring in EF compared to FF ($p<0.01$). *Ogt*'s counterpart, *Oga*, was significantly more methylated in FF compared to CF and EF ($p<0.05$ and 0.01 respectively). Furthermore, EF exhibited a statistical reduction in methylation compared to CF ($p<0.05$). The exact same results were found in offspring *Ogt*, as well as *Oga*. The only exception however was the power of significance calculated for *Oga* in offspring, which was found to be $p<0.005$ for all comparisons described for fathers.

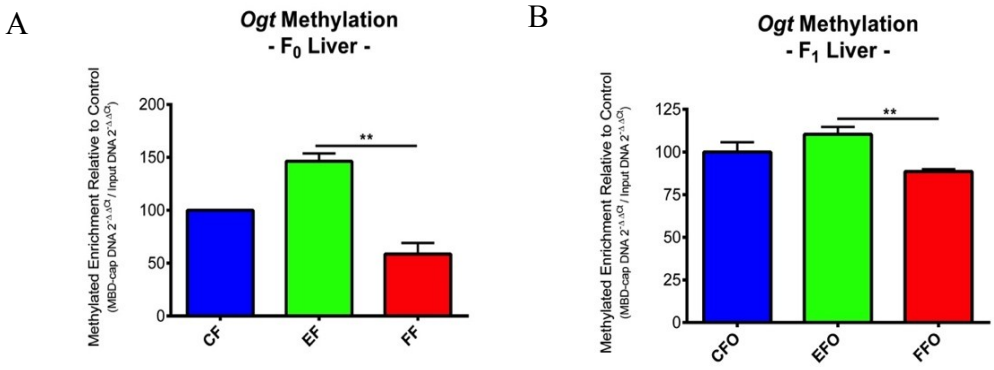

Figure 46. Promoter methylation for *Ogt* (genomic DNA) measured in the muscle. A – Father's (F_0) *Ogt* methylation (n=3). B – Offspring (F_1) *Ogt* methylation (CFO/EFO/FFO n=4/3/3 respectively). Significance calculated by two-tailed student's t-test **p<0.005.

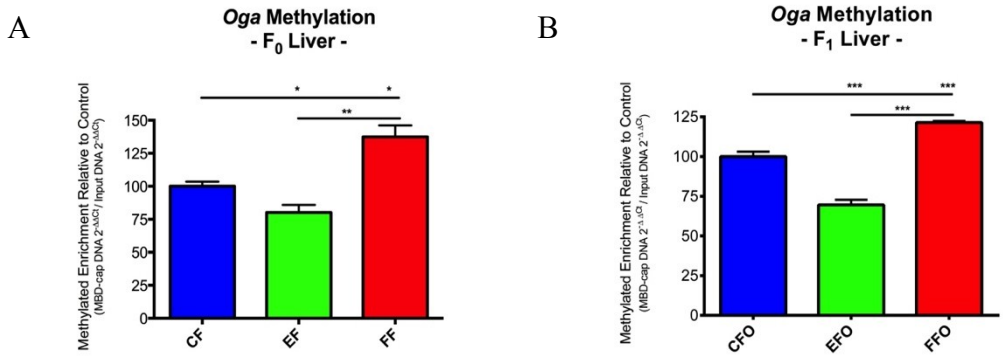

Figure 47. Promoter methylation for *Oga* (genomic DNA) measured in the muscle. A – Father's (F_0) *Oga* methylation (n=3). B – Offspring (F_1) *Oga* methylation (n=4). Significance calculated by two-tailed student's t-test ***p<0.001 **p<0.005 *p<0.05.

H19 in fathers and offspring was nearly identical, with the only differences lying in the power of statistical significance. In fathers, EFs were hypermethylated compared to CF and FF ($p<0.001$ and 0.0001 respectively). Additional significance was found upon comparison of CF and FF, where FFs were again less methylated ($p<0.01$). In offspring, these same trends were reported, however the powers of significance were $p<0.001$, 0.01, and 0.01 respectively.

Analyses made on *Pdk4* methylation demonstrated FF to be hypomethylated compared to CF and EF ($p<0.01$), while findings among offspring were the same, with FFO exhibited the smallest level of methylation.

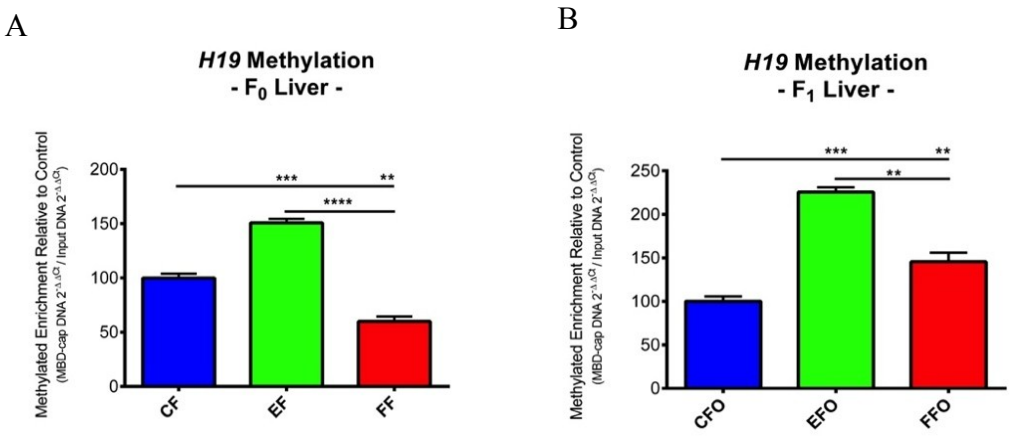

Figure 48. Promoter methylation for *H19* (genomic DNA) measured in the muscle. A – Father's (F_0) *H19* methylation (CF/EF/FF n=2/4/3 respectively). B – Offspring (F_1) *H19* methylation (CFO/EFO/FFO n=4/3/3 respectively). Significance calculated by two-tailed student's t-test ***p<0.001 **p<0.005 *p<0.05.

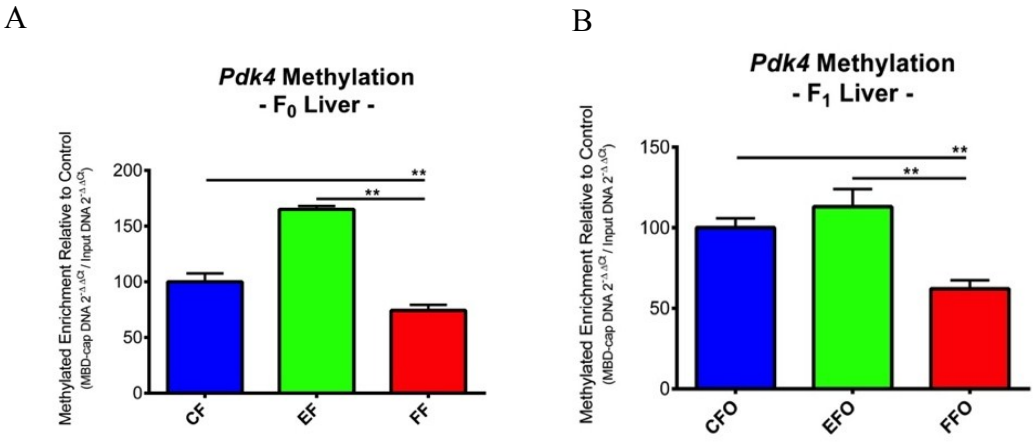

Figure 49. Promoter methylation for *Pdk4* (genomic DNA) measured in the muscle. A – Father's (F_0) *Pdk4* methylation (CF/EF/FF n=3/4/3 respectively). B – Offspring (F_1) *Pdk4* methylation (CFO/EFO/FFO n=4/3/4 respectively). Significance calculated by two-tailed student's t-test **p<0.005.

Glut4 methylation among fathers appeared lowest in FF ($p<0.005$ and 0.01). In offspring, the FFO group was found to be less methylated compared to CFO and EFO ($p<0.005$), and furthermore EFO was statistically higher than CFO ($p<0.05$).

Ptpn1 methylation patterns between fathers and offspring were remarkably similar to one another, with EF/EFO appearing statistically higher than FF/FFO ($p<0.05$).

Taken together, findings these are indicative of methylation-based transgenerational programming. This is evident by methylation patterns, which were highly conserved from fathers to offspring in several genes including *Ogt*, *Oga*, *Pdk4*, *Ptpn1*, and *H19*. Furthermore, these trends complemented respective gene expressions.

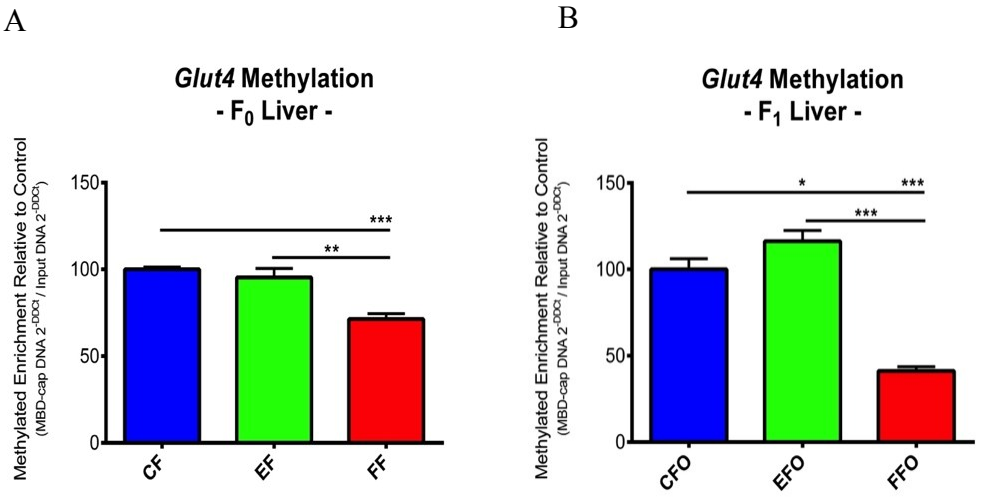

Figure 50. Promoter methylation for *Pdk4* (genomic DNA) measured in the muscle. A – Father's (F_0) *Pdk4* methylation (CF/EF/FF n=3/4/3 respectively). B – Offspring (F_1) *Pdk4* methylation (CFO/EFO/FFO n=4/3/4 respectively). Significance calculated by two-tailed student's t-test ***p<0.001 **p<0.005 p<0.05.

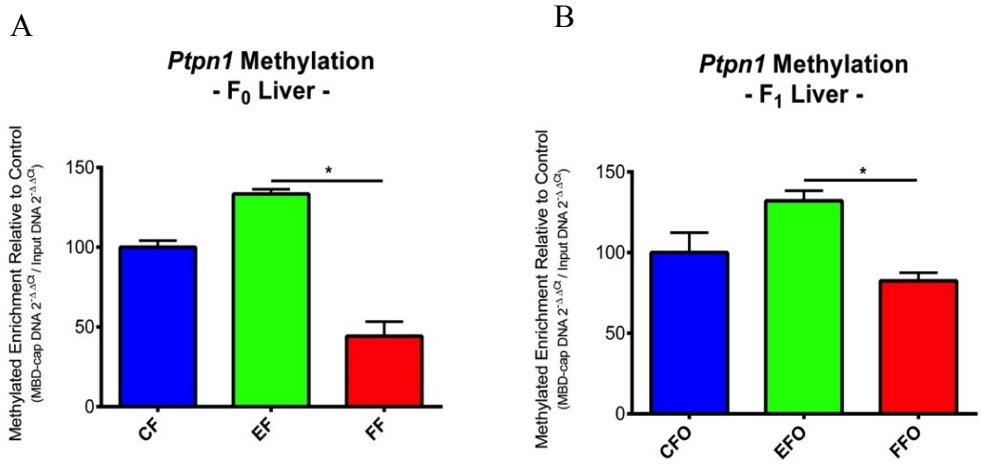

Figure 51. Promoter methylation for *Pdk4* (genomic DNA) measured in the muscle. A – Father's (F_0) *Pdk4* methylation (CF/EF/FF n=3/4/3 respectively). B – Offspring (F_1) *Pdk4* methylation (CFO/EFO/FFO n=4/3/4 respectively). Significance calculated by two-tailed student's t-test *p<0.05.

5.0 Discussion

The findings in this investigation clearly demonstrate that paternal diet and exercise are capable of producing epigenetic changes that subsequently alter the metabolic phenotype of male offspring. These changes appear to be linked to abnormal methylation patterns occurring at regulatory regions of several genes examined, all of which are known to be involved in metabolic homeostasis. To the best of our knowledge this is the first time paternal HFD and chronic exercise have been observed to cause transgenerational effects that directly modify the glucose and energy metabolism in male offspring within the F_1 generation of mice.

The transgenerational detriments observed in this study, which were associated with paternal nutrition, first became apparent at the time when birth weights were measured. Offspring born to fathers consuming a HFD were found to have a substantially lower birth weight compared to other cohorts. The significance of these findings are well described in multiple human investigations, which noted the same trend among infants born from diabetic (T2DM) fathers and non-diabetic mothers [104,105, 103]. Longitudinal studies have since followed thousands of these children well into adulthood to gain a better understanding of the long-term risks associated with birth weight [104,105, 103]. Common findings among these investigations indicate that low-birth weight is highly correlated to an increased risk for developing insulin resistance in young adulthood (1.8-fold increase; 1,608 children; $p=0.004$) [104,105, 103].

The results gathered from gene expression analysis and indirect calorimetry demonstrate that long-term free wheel running in fathers led to exercise-induced transgenerational programming within their offspring, which was manifested as a reduction in basal energy

expenditure. Therefore, when these offspring (i.e. EFO) were challenged with a high fat diet they were more prone to becoming obese (data not shown). Moreover, offspring whose father's consumed a HFD appeared to be epigenetically prepared for similar conditions, as seen by the diminished effects incurred when challenged with the same high-fat diet. These observations indicate that male offspring are programmed to thrive under the same living conditions as their respective fathers. Although the impacts of maternal obesity on offspring (male and female) have been documented in both mice and human studies alike [9,10,39,53,54,103,104,106,107], as far as we know this is the first account to document a transgenerational-based predisposition/preparedness existing within the father-to-son lineage.

As discussed in previous sections there have been several new reports by investigators implicating paternal 'epimutations', like DNA methylation, to be key players in the transgenerational pathogenesis of obesity and metabolic syndrome [12,16,18,19,39,107]. These allegations are well supported by findings reported here, which revealed a highly differentiated pattern in the methylation and gene expression between offspring sired by exercising fathers and those sired by fathers who consumed a HFD. The most notable molecular-based disparity between these cohorts was identified in the percent methylation found in the promoter regions of several metabolic genes including *Ogt*, *Oga*, *Ptpn1*, *Glut4*, *Pdk4*, *H19*, and *FoxO1*. Overall, these genes were primarily found to be hypomethylated in the male offspring born from fathers consuming a HFD. Some exceptions, however, were found to occur on *Oga*, *FoxO1*, and pancreatic *H19*; all of which were seen to be hypermethylated with respect to other groups of offspring. Interestingly, the genomic DNA in human (and mice) tumor cells is often found in a hypomethylated state [108]. One could speculate these findings (i.e. FFO hypomethylation) may be correlated not only to an increased risk for metabolic impairment, but also cancer.

Although the methylation patterns observed here are indicative of transgenerational inheritance it is crucial to note that no screening was performed to identify DNA sequence mutations (e.g. point mutation; single nucleotide polymorphism). Therefore, changes in gene expression cannot solely be attributed to mechanisms of epigenetic regulation. Furthermore, it can only be speculated that these epigenetic changes were also present within the germ line, considering at the time of this discussion sperm samples had not yet been subjected to methylation analysis.

The concurrent overexpression of *Ogt* and under expression of *Oga* in insulin sensitive tissues is a recipe for metabolic catastrophe that was observed in all tissues examined from HFD fathers and their offspring (FF and FFO, respectively). Under such conditions (i.e. elevated OGT and/or depressed OGA) excessive O-GlcNAcylation is likely to occur, a scenario which was recently implicated as the cause of T2DM-associated erectile dysfunction, via its' inhibition of nitric oxide synthetase; the enzyme responsible for eNOS formation and vasodilation [[109]]. Moreover, a disproportionate balance of O-GlcNAc cycling enzymes has been proven to cause metabolic impairment in all of the tissues studied here [[41,83,93,110,111]]. Beginning in the liver, following a high fat meal, increased O-GlcNAcylation of PGC-1α stimulates activity of host cell factor C1 (HCF-1; an epigenetic cell cycle regulator), which subsequently targets and activates cytosolic FOXO1 [[36,65,112]]. The now active, de-phosphorylated, FOXO1 translocates to the nucleus where it initiates transcription for a number of genes involved in mitochondrial biogenesis as well as gluconeogenesis. To summarize, in response to excess glucose in the liver, O-GlcNAc paradoxically facilitates hepatic glucose release, effectively triggering and propagating a hyperglycemic state [[36,65,112]].

At the level of the pancreas, there is now an increased flux of glucose through the HBP

(due to hepatic O-GlcNAc induced hyperglycemia). Consequently, the transcriptional initiation factors called NeuroD1 and pancreas-duodenum homeobox-1 (PDX-1) become excessively O-GlcNAcylated leading to increased expression of the insulin gene [93]. These events demonstrate how O-GlcNAc-induced hyperglycemia also facilitates the onset of a hyperinsulinemic state as well.

Finally, just as it was seen in the pancreas, the effects of hyperglycemia within skeletal muscle result in elevated UDP-GlcNAc levels, and yet again this leads to excessive O-GlcNAcylation [83]. As a result of O-GlcNAc's antagonistic effect on the insulin receptor substrates 1 and 2 (IRS1, IRS2), signal transduction by insulin is effectively severed in skeletal muscle [64]! This marks the third and final criterion for a diabetic phenotype: hyperglycemia, hyperinsulinemia, and insulin resistance.

While the activity levels for OGA or OGT were not investigated here, their respective gene and protein expressions indicate a high potential for being involved in transgenerational glucose impairment. This became evident upon analyzing promoter methylation patterns, which were demonstrated to be nearly identical between fathers and offspring, despite the fact offspring whose tissues were studied all consumed the same control diet (10% energy from fat).

Taken together, these data demonstrate that paternal nutrition and physical activity play an important role in shaping the glucose and energy metabolism of male progeny. Moreover, these potentially transgenerational changes are the product of parent-specific epimarkers (e.g. DNA methylation) that alter genomic activity through successive generations. These findings are well correlated to those made by Fullston et. al. (2013) discussed previously, which showed that paternal HFD was associated with a global reduction of DNA methylation in offspring that subsequently led to an impaired metabolic state [54].

Additionally, our results suggest an alteration in lipid metabolism within different cohorts of offspring. This became evident at the time they were challenged with a HFD and those offspring sired by exercising fathers suffered the greatest insult. These findings were consistent with those made by Carone et. al. (2010), although in the current study the specific mechanisms that affected offspring's susceptibility to developing impaired lipid metabolism were not explored [50].

It is important to note that although elevated O-GlcNAcylation has potentially disastrous effects within the insulin sensitive tissues described here, it may actually have clinical benefit in other tissues. For instance, high levels of O-GlcNAc in the brain serves a protective role by preventing hyperphosphorylation of Tau proteins, thereby inhibiting the formation of neurofibrillary tangles characteristic to the onset of Alzheimer's disease [84,113]. Such observations inspire the possibility of using 'O-GlcNAcylation modulation' as a means of preventing cognitive decline, although at the present no such proposals could be found.

While further research is needed to investigate the persistence of epigenetic programming within the germ line (e.g. F_2, F_3, and so on), these data shown here offer insight into abnormal epigenetic profiles associated with glucose impairment. We hope one day soon these observations will help contribute to the development of improved intervention techniques, as well as novel treatments that encompass all aspects of metabolic disease in humans. The purpose of this study, however, was not only to help develop new treatments for the ongoing fight against obesity and type 2 diabetes – it was also to find new avenues by which these overly prevalent diseases could be prevented and reversed.

ACKNOWLEDGEMENTS

We wish to thank the Gerald Hart laboratory at Johns Hopkins University, and the NHLBI P01HL107153 Core C4, for kindly providing the OGT and OGA primary antibodies used for Western Blotting.

References

1. Flegal KM, Carroll MD, Kit BK, Ogden CL. Prevalence of obesity and trends in the distribution of body mass index among US adults, 1999-2010 [original contribution]. *JAMA: The Journal of the American Medical Association*. 2012. http://jama.ama-assn.org. doi: 10.1001/jama.2012.39.

2. Trends in the prevalence of extreme obesity among US pr... [JAMA. 2012] - PubMed - NCBI. http://www.ncbi.nlm.nih.gov/pubmed/23268509.

3. Astrup A. Macronutrient balances and obesity: The role of diet and physical activity. *Public Health Nutr*. 1999;2(3A):341-347.

4. CDC - 2011 national diabetes fact sheet - publications - diabetes DDT. http://www.cdc.gov/diabetes/pubs/factsheet11.htm.

5. Cost of obesity approaching $300 billion a year - USATODAY.com. http://usatoday30.usatoday.com/yourlife/health/medical/2011-01-12-obesity-costs-300-bilion_N.htm.

6. Finkelstein EA, Trogdon JG, Cohen JW, Dietz W. Annual medical spending attributable to obesity: Payer-and service-specific estimates. *Health Aff (Millwood)*. 2009;28(5):w822-31. doi: 10.1377/hlthaff.28.5.w822; 10.1377/hlthaff.28.5.w822.

7. Diabetes statistics - american diabetes association®. http://www.diabetes.org/diabetes-basics/diabetes-statistics/.

8. Type 2 diabetes: Etiology and reversibility: Reversal of type 2 diabetes by diet alone. http://www.medscape.com/viewarticle/781719_3.

9. Dunn GA, Bale TL. Maternal high-fat diet effects on third-generation female body size via the paternal lineage. *Endocrinology*. 2011;152(6):2228-2236. doi: 10.1210/en.2010-1461; 10.1210/en.2010-1461.

10. Hattersley AT, Tooke JE. The fetal insulin hypothesis: An alternative explanation of the association of low birthweight with diabetes and vascular disease. *Lancet*. 1999;353(9166):1789-1792. doi: 10.1016/S0140-6736(98)07546-1.

11. Holliday R. Epigenetics: A historical overview. *Landes Biosciences*. 2006;1(2):76-80.

12. Epigenetic manifestation of metabolic ... [antioxid redox signal. 2012] - PubMed - NCBI. http://www.ncbi.nlm.nih.gov/pubmed/22229755.

13. Ding GL, Wang FF, Shu J, et al. Transgenerational glucose intolerance with Igf2/H19 epigenetic alterations in mouse islet induced by intrauterine hyperglycemia. *Diabetes*. 2012;61(5):1133-1142. doi: 10.2337/db11-1314; 10.2337/db11-1314.

14. Kouzarides T. Chromatin modifications and their function. *Cell*. 2007;128(4):693-705. doi: 10.1016/j.cell.2007.02.005.

15. Poston L. Intergenerational transmission of insulin resistance and type 2 diabetes. *Prog Biophys Mol Biol*. 2011;106(1):315-322. doi: 10.1016/j.pbiomolbio.2010.11.011.

16. Roche HM, Phillips C, Gibney MJ. The metabolic syndrome: The crossroads of diet and genetics. *Proc Nutr Soc*. 2005;64(3):371-377.

17. Permutt AM, Wasson J, Cox N. **Genetic epidemiology of diabetes**. *The Journal of Clinical Investigation*. 2005;115(6):1431-1439.

18. Wang J, Wu Z, Li D, et al. Nutrition, epigenetics, and metabolic syndrome. *Antioxid Redox Signal*. 2012;17(2):282-301. doi: 10.1089/ars.2011.4381; 10.1089/ars.2011.4381.

19. Gallou-Kabani C, Junien C. Nutritional epigenomics of metabolic syndrome: New perspective against the epidemic. *Diabetes*. 2005;54(7):1899-1906.

20. Slomko H, Heo H, Einstein F. **Minireview: Epigenetics of obesity and diabetes in humans**. *Endocrinology*. 2012;3(153):1025-1030.

21. Dolinoy DC, Faulk C. The use of animals models to advance epigenetic science. *ILAR Journal*. 2012;53(3/4):227-231.

22. Mathers JC, McKay JA. Epigenetics - potential contribution to fetal programming. *Advances in experimental medicine and biology*. 2009(646):119-123.

23. Bruce KD, Byrne CD. The metabolic syndrome: Common origins of a multifactorial disorder. *Postgrad Med J*. 2009;85(1009):614-621. doi: 10.1136/pgmj.2008.078014; 10.1136/pgmj.2008.078014.

24. Zimmet P, Boyko EJ, Collier GR, de Courten M. Etiology of the metabolic syndrome: Potential role of insulin resistance, leptin resistance, and other players. *Ann N Y Acad Sci*. 1999;892:25-44.

25. Pitsavos C, Panagiotakos D, Weinem M, Stefanadis C. **Diet, exercise and the metabolic syndrome**. *The Review of Diabetic Studies*. 2006;3:118-126.

26. Alberti KGMM, Zimmet PZ. Definition, diagnosis and classification of diabetes mellitus and its complications. part 1: Diagnosis and classification of diabetes mellitus. provisional report of a WHO consultation - alberti - 2004 - diabetic medicine - wiley online library. http://onlinelibrary.wiley.com/doi/10.1002/(SICI)1096-9136(199807)15:73.0.CO;2-S/abstract;jsessionid=38B196B21A982EC9233601853B539280.d01t02. Accessed 8/23/2013, 2013.

27. Beilby J. **Definition of metabolic syndrome: Report of the national heart, lung, and blood institute/american heart association conference on scientific issues related to definition**. *Clnical Biochemistry Review*. 2004;25(3):195-198.

28. **Standards of medical care in Diabetes—2012**. *Diabetes Care*. 2012;35(1):11-63.

29. What is type 2 diabetes? :: Diabetes education online. http://dtc.ucsf.edu/types-of-diabetes/type2/understanding-type-2-diabetes/what-is-type-2-diabetes/.

30. Spectrum of liver disease in type 2 diabetes and management of patients with diabetes and liver disease. http://care.diabetesjournals.org/content/30/3/734.extract#.

31. The role of the liver in type 2 diabetes - springer. http://link.springer.com/article/10.1023/B:REMD.0000021431.90494.0c#page-1.

32. Diabetes symptoms: When diabetes symptoms are a concern - MayoClinic.com. http://www.mayoclinic.com/health/diabetes-symptoms/DA00125.

33. Kawahito S. Problems associated with glucose toxicity: Role of hyperglycemia-induced oxidative stress. *World Journal of Gastroenterology*. 2009;15(33):4137. doi: 10.3748/wjg.15.4137.

34. Sheng L, Zhou Y, Chen Z, et al. NF-kappaB-inducing kinase (NIK) promotes hyperglycemia and glucose intolerance in obesity by augmenting glucagon action. *Nat Med*. 2012;18(6):943-949. doi: 10.1038/nm.2756; 10.1038/nm.2756.

35. Ebbert JO, Jensen MD. Fat depots, free fatty acids, and dyslipidemia. *Nutrients*. 2013;5(2):498-508. doi: 10.3390/nu5020498; 10.3390/nu5020498.

36. Matsumoto M, Pocai A, Rossetti L, Depinho RA, Accili D. Impaired regulation of hepatic glucose production in mice lacking the forkhead transcription factor Foxo1 in liver. *Cell Metab*. 2007;6(3):208-216. doi: 10.1016/j.cmet.2007.08.006.

37. DeFronzo RA, Tripathy D. Skeletal muscle insulin resistance is the primary defect in type 2 diabetes. *Diabetes Care*. 2009;32 Suppl 2:S157-63. doi: 10.2337/dc09-S302; 10.2337/dc09-S302.

38. Carone BR, Fauquier L, Habib N, et al. Paternally induced transgenerational environmental reprogramming of metabolic gene expression in mammals. *Cell*. 2010;143(7):1084-1096. doi: 10.1016/j.cell.2010.12.008; 10.1016/j.cell.2010.12.008.

39. Epigenetic regulation in obesity. [int J obes (lond). 2012] - PubMed - NCBI. http://www.ncbi.nlm.nih.gov/pubmed/21912396.

40. Chronic high-fat diet in fathers programs [bgr]-cell dysfunction in female rat offspring : Nature : Nature publishing group. http://www.nature.com/nature/journal/v467/n7318/abs/nature09491.html.

41. Kebede M, Ferdaoussi M, Mancini A, et al. Glucose activates free fatty acid receptor 1 gene transcription via phosphatidylinositol-3-kinase-dependent O-GlcNAcylation of pancreas-duodenum homeobox-1. *Proc Natl Acad Sci U S A*. 2012;109(7):2376-2381. doi: 10.1073/pnas.1114350109; 10.1073/pnas.1114350109.

42. Lee TF, Zhai J, Meyers BC. Conservation and divergence in eukaryotic DNA methylation. *Proc Natl Acad Sci U S A*. 2010;107(20):9027-9028. doi: 10.1073/pnas.1005440107; 10.1073/pnas.1005440107.

43. Antequera F. Structure, function and evolution of CpG island promoters. *Cell Mol Life Sci*. 2003;60(8):1647-1658. doi: 10.1007/s00018-003-3088-6.

44. Veenstra GJ, Wolffe AP. Constitutive genomic methylation during embryonic development of xenopus. *Biochim Biophys Acta*. 2001;1521(1-3):39-44.

45. Vu TH, Li T, Nguyen D, et al. Symmetric and asymmetric DNA methylation in the human IGF2-H19 imprinted region. *Genomics*. 2000;64(2):132-143. doi: 10.1006/geno.1999.6094.

46. Young LE, Beaujean N. DNA methylation in the preimplantation embryo: The differing stories of the mouse and sheep. *Anim Reprod Sci*. 2004;82-83:61-78. doi: 10.1016/j.anireprosci.2004.05.020.

47. Geiman TM, Muegge K. DNA methylation in early development. *Mol Reprod Dev*. 2010;77(2):105-113. doi: 10.1002/mrd.21118; 10.1002/mrd.21118.

48. Dominguez-Salas P, Moore SE, Cole D, et al. DNA methylation potential: Dietary intake and blood concentrations of one-carbon metabolites and cofactors in rural african women. *Am J Clin Nutr*. 2013;97(6):1217-1227. doi: 10.3945/ajcn.112.048462; 10.3945/ajcn.112.048462.

49. Sidoli S, Cheng L, Jensen ON. Proteomics in chromatin biology and epigenetics: Elucidation of post-translational modifications of histone proteins by mass spectrometry. *J Proteomics*. 2012;75(12):3419-3433. doi: 10.1016/j.jprot.2011.12.029; 10.1016/j.jprot.2011.12.029.

50. Carone BR, Fauquier L, Habib N, et al. Paternally induced transgenerational environmental reprogramming of metabolic gene expression in mammals. *Cell*. 2010;143(7):1084-1096. doi: 10.1016/j.cell.2010.12.008; 10.1016/j.cell.2010.12.008.

51. Soubry A, Schildkraut JM, Murtha A, et al. Paternal obesity is associated with IGF2 hypomethylation in newborns: Results from a newborn epigenetics study (NEST) cohort. *BMC Med*. 2013;11(1):29. www.refworks.com. doi: 10.1186/1741-7015-11-29.

52. Guerrero-Bosagna C. Epigenetic transgenerational actions of vinclozolin on promoter regions of the sperm epigenome. *ONE Alerts*. 2010. www.refworks.com. doi: 10.1371/journal.pone.0013100.

53. Godfrey KM, Barker DJ. Fetal programming and adult health. *Public Health Nutr*. 2001;4(2B):611-624.

54. Fullston T, Ohlsson Teague EMC, Palmer NO, et al. Paternal obesity initiates metabolic disturbances in two generations of mice with incomplete penetrance to the F2 generation and alters the transcriptional profile of testis and sperm microRNA content [research communication]. *The FASEB Journal*. 2013. http://www.fasebj.org. doi: 10.1096/fj.12-224048.

55. Hark AT, Tilghman SM. Chromatin conformation of the H19 epigenetic mark. *Hum Mol Genet*. 1998;7(12):1979-1985.

56. Srivastava M, Hsieh S, Grinberg A, Williams-Simons L, Huang SP, Pfeifer K. H19 and Igf2 monoallelic expression is regulated in two distinct ways by a shared cis acting regulatory region upstream of H19. *Genes Dev*. 2000;14(10):1186-1195.

57. Thorvaldsen JL, Fedoriw AM, Nguyen S, Bartolomei MS. Developmental profile of H19 differentially methylated domain (DMD) deletion alleles reveals multiple roles of the DMD in regulating allelic expression and DNA methylation at the imprinted H19/Igf2 locus. *Mol Cell Biol*. 2006;26(4):1245-1258. doi: 10.1128/MCB.26.4.1245-1258.2006.

58. Tremblay KD, Saam JR, Ingram RS, Tilghman SM, Bartolomei MS. A paternal-specific methylation imprint marks the alleles of the mouse H19 gene. *Nat Genet*. 1995;9(4):407-413. doi: 10.1038/ng0495-407.

59. Thorvaldsen JL, Fedoriw AM, Nguyen S, Bartolomei MS. Developmental profile of H19 differentially methylated domain (DMD) deletion alleles reveals multiple roles of the DMD in regulating allelic expression and DNA methylation at the imprinted H19/Igf2 locus. *Mol Cell Biol*. 2006;26(4):1245-1258. doi: 10.1128/MCB.26.4.1245-1258.2006.

60. Szabo PE, Tang SH, Silva FJ, Tsark WM, Mann JR. Role of CTCF binding sites in the Igf2/H19 imprinting control region. *Mol Cell Biol*. 2004;24(11):4791-4800. doi: 10.1128/MCB.24.11.4791-4800.2004.

61. Tremblay KD, Duran KL, Bartolomei MS. A 5' 2-kilobase-pair region of the imprinted mouse H19 gene exhibits exclusive paternal methylation throughout development. *Mol Cell Biol*. 1997;17(8):4322-4329.

62. BMC medical genetics | full text | IGF2/H19 hypomethylation in a patient with very low birthweight, preocious pubarche and insulin resistance. http://www.biomedcentral.com/1471-2350/13/42.

63. Jeoung NH, Harris RA. Pyruvate dehydrogenase kinase-4 deficiency lowers blood glucose and improves glucose tolerance in diet-induced obese mice. *AJP: Endocrinology and Metabolism*. 2008;295(1):E46 <last_page> E54. doi: 10.1152/ajpendo.00536.2007.

64. Whelan SA, Dias WB, Thiruneelakantapillai L, Lane MD, Hart GW. Regulation of insulin receptor substrate 1 (IRS-1)/AKT kinase-mediated insulin signaling by O-linked beta-N-acetylglucosamine in 3T3-L1 adipocytes. *J Biol Chem*. 2010;285(8):5204-5211. doi: 10.1074/jbc.M109.077818; 10.1074/jbc.M109.077818.

65. Kousteni S. FoxO1, the transcriptional chief of staff of energy metabolism. *Bone*. 2012;50(2):437-443. doi: 10.1016/j.bone.2011.06.034; 10.1016/j.bone.2011.06.034.

66. Kobayashi M, Kikuchi O, Sasaki T, et al. FoxO1 as a double-edged sword in the pancreas: Analysis of pancreas- and beta-cell-specific FoxO1 knockout mice. *Am J Physiol Endocrinol Metab*. 2012;302(5):E603-13. doi: 10.1152/ajpendo.00469.2011; 10.1152/ajpendo.00469.2011.

67. Tsou RC, Bence KK. The genetics of PTPN1 and obesity: Insights from mouse models of tissue-specific PTP1B deficiency. *Journal of Obesity*. 2012;2012:1 <last_page> 8. doi: 10.1155/2012/926857.

68. Dwbowden. Association of the PTPN1 gene with type 2 diabetes and insulin resistance. *Donald W Bowden*. 2009. http://www.discoverymedicine.com/Donald-W-Bowden.

69. Wallberg-Henriksson H, Zierath JR. GLUT4: A key player regulating glucose homeostasis? insights from transgenic and knockout mice (review). *Mol Membr Biol*. 2001;18(3):205-211.

70. Govers R, Coster AC, James DE. Insulin increases cell surface GLUT4 levels by dose dependently discharging GLUT4 into a cell surface recycling pathway. *Mol Cell Biol*. 2004;24(14):6456-6466. doi: 10.1128/MCB.24.14.6456-6466.2004.

71. The O-GlcNAc modification - essentials of glycobiology - NCBI bookshelf. http://www.ncbi.nlm.nih.gov/books/NBK20725/.

72. Increased expression of ß-N-acetylglucosaminidase in erythrocytes from individuals with pre-diabetes and diabetes. http://www.ncbi.nlm.nih.gov/pmc/articles/PMC2889787/.

73. Bond MR, Hanover JA. O-GlcNAc cycling: A link between metabolism and chronic disease. *Annu Rev Nutr*. 2013;33:205-229. doi: 10.1146/annurev-nutr-071812-161240; 10.1146/annurev-nutr-071812-161240.

74. Ruan HB, Singh JP, Li MD, Wu J, Yang X. Cracking the O-GlcNAc code in metabolism. *Trends Endocrinol Metab*. 2013;24(6):301-309. doi: 10.1016/j.tem.2013.02.002; 10.1016/j.tem.2013.02.002.

75. Copeland RJ, Bullen JW, Hart GW. Cross-talk between GlcNAcylation and phosphorylation: Roles in insulin resistance and glucose toxicity. *American Journal of Physiology: Endocrinology & Metabolism*. 2008;58(1):E17-E28. http://search.ebscohost.com/login.aspx?direct=true&db=a9h&AN=34067616&site=ehost-live. doi: 10.1152/ajpendo.90281.2008.

76. Two O-linked N-acetylglucosamine transferase genes of arabidopsis thaliana L. heynh. have overlapping functions necessary for gamete and seed development. http://www.genetics.org/content/161/3/1279.full.

77. Liu Y, Li X, Yu Y, et al. Developmental regulation of protein O-GlcNAcylation, O-GlcNAc transferase, and O-GlcNAcase in mammalian brain. *PLoS One*. 2012;7(8):e43724. www.refworks.com. doi: 10.1371/journal.pone.0043724.

78. Love DC, Krause MW, Hanover JA. O-GlcNAc cycling: Emerging roles in development and epigenetics. *Semin Cell Dev Biol*. 2010;21(6):646-654. doi: 10.1016/j.semcdb.2010.05.001.

79. Forsythe ME, Love DC, Lazarus BD, et al. Caenorhabditis elegans ortholog of a diabetes susceptibility locus: Oga-1 (O-GlcNAcase) knockout impacts O-GlcNAc cycling, metabolism, and dauer. *Proc Natl Acad Sci U S A*. 2006;103(32):11952-11957. doi: 10.1073/pnas.0601931103.

80. Hanover JA, Yu S, Lubas WB, et al. Mitochondrial and nucleocytoplasmic isoforms of O-linked GlcNAc transferase encoded by a single mammalian gene. *Arch Biochem Biophys*. 2003;409(2):287-297.

81. Zachara NE, Hart GW. Cell signaling, the essential role of O-GlcNAc! *Biochimica et Biophysica Acta (BBA) - Molecular and Cell Biology of Lipids*. 2006;1761(5–6):599-617. doi: http://dx.doi.org/10.1016/j.bbalip.2006.04.007.

82. Liu Y, Li X, Yu Y, et al. Developmental regulation of protein O-GlcNAcylation, O-GlcNAc transferase, and O-GlcNAcase in mammalian brain. *PLoS One*. 2012;7(8):e43724. www.refworks.com. doi: 10.1371/journal.pone.0043724.

83. McClain DA, Lubas WA, Cooksey RC, et al. Altered glycan-dependent signaling induces insulin resistance and hyperleptinemia. *Proc Natl Acad Sci U S A*. 2002;99(16):10695-10699. doi: 10.1073/pnas.152346899.

84. Lazarus BD, Love DC, Hanover JA. O-GlcNAc cycling: Implications for neurodegenerative disorders. *Int J Biochem Cell Biol*. 2009;41(11):2134-2146. doi: 10.1016/j.biocel.2009.03.008; 10.1016/j.biocel.2009.03.008.

85. Ngoh GA, Facundo HT, Zafir A, Jones SP. O-GlcNAc signaling in the cardiovascular system. *Circ Res*. 2010;107(2):171-185. doi: 10.1161/CIRCRESAHA.110.224675; 10.1161/CIRCRESAHA.110.224675.

86. Lazarus BD, Love DC, Hanover JA. Recombinant O-GlcNAc transferase isoforms: Identification of O-GlcNAcase, yes tyrosine kinase, and tau as isoform-specific substrates. *Glycobiology*. 2006;16(5):415-421. doi: 10.1093/glycob/cwj078.

87. Love DC, Kochan J, Cathey RL, Shin SH, Hanover JA. Mitochondrial and nucleocytoplasmic targeting of O-linked GlcNAc transferase. *J Cell Sci*. 2003;116(Pt 4):647-654.

88. Dias WB, Cheung WD, Wang Z, Hart GW. Regulation of calcium/calmodulin-dependent kinase IV by O-GlcNAc modification. *J Biol Chem*. 2009;284(32):21327-21337. doi: 10.1074/jbc.M109.007310; 10.1074/jbc.M109.007310.

89. Comtesse N, Maldener E, Meese E. Identification of a nuclear variant of MGEA5, a cytoplasmic hyaluronidase and a beta-N-acetylglucosaminidase. *Biochem Biophys Res Commun*. 2001;283(3):634-640. doi: 10.1006/bbrc.2001.4815.

90. Li J, Huang CL, Zhang LW, et al. Isoforms of human O-GlcNAcase show distinct catalytic efficiencies. *Biochemistry (Mosc)*. 2010;75(7):938-943.

91. ß-N-acetylglucosamine (O-GlcNAc) is part of the histone code. http://www.ncbi.nlm.nih.gov/pmc/articles/PMC2993388/. Accessed 8/23/2013, 2013.

92. Hanover JA. Epigenetics gets sweeter: O-GlcNAc joins the "histone code". *Chem Biol*. 2010;17(12):1272-1274. doi: 10.1016/j.chembiol.2010.12.001.

93. Issad T, Kuo M. O-GlcNAc modification of transcription factors, glucose sensing and glucotoxicity. *Trends Endocrinol Metab*. 2008;19(10):380-389. doi: 10.1016/j.tem.2008.09.001.

94. Hanover JA, Krause MW, Love DC. Post-translational modifications: Bittersweet memories: Linking metabolism to epigenetics through O-GlcNAcylation. *Nat Rev Mol Cell Biol*. 2012;13(5):312-321. doi: 10.1038/nrm3334; 10.1038/nrm3334.

95. Lehman DM, Fu DJ, Freeman AB, et al. A single nucleotide polymorphism in MGEA5 encoding O-GlcNAc-selective N-acetyl-beta-D glucosaminidase is associated with type 2 diabetes in mexican americans. *Diabetes*. 2005;54(4):1214-1221.

96. Wang Z, Park K, Comer F, Hsieh-Wilson L, Saudek CD, Hart GW. Site-specific GlcNAcylation of human erythrocyte proteins potential biomarker(s) for diabetes. *Diabetes*. 2009;58(2):309-317. http://search.ebscohost.com/login.aspx?direct=true&db=a9h&AN=36865252&site=ehost-live. doi: 10.2337/db08-0994.

97. Park K, Saudek CD, Hart GW. Increased expression of beta-N-acetylglucosaminidase in erythrocytes from individuals with pre-diabetes and diabetes. *Diabetes*. 2010;59(7):1845-1850. doi: 10.2337/db09-1086; 10.2337/db09-1086.

98. Chen Q, Chen Y, Bian C, Fujiki R, Yu X. TET2 promotes histone O-GlcNAcylation during gene transcription. *Nature*. 2013;493(7433):561-564. doi: 10.1038/nature11742; 10.1038/nature11742.

99. Livak KJ, Schmittgen TD. Analysis of relative gene expression data using real-time quantitative PCR and the 2(-delta delta C(T)) method. *Methods*. 2001;25(4):402-408. doi: 10.1006/meth.2001.1262.

100. Livak KJ, Schmittgen TD. Analysis of relative gene expression data using real-time quantitative PCR and the 2(-delta delta C(T)) method. *Methods*. 2001;25(4):402-408. doi: 10.1006/meth.2001.1262.

101. Even PC, Nadkarni NA. Indirect calorimetry in laboratory mice and rats: Principles, practical considerations, interpretation and perspectives. *Am J Physiol Regul Integr Comp Physiol*. 2012;303(5):R459-76. doi: 10.1152/ajpregu.00137.2012; 10.1152/ajpregu.00137.2012.

102. Rodbard HW, Bays HE, Gavin JR,3rd, et al. Rate and risk predictors for development of self-reported type-2 diabetes mellitus over a 5-year period: The SHIELD study. *Int J Clin Pract*.

2012;66(7):684-691. doi: 10.1111/j.1742-1241.2012.02952.x; 10.1111/j.1742-1241.2012.02952.x.

103. Elina Hyppönen, George Davey Smith, Chris Power. Parental diabetes and birth weight of offspring: Intergenerational cohort study. *BMJ*. 2003;326(7379):19-20. doi: 10.1136/bmj.326.7379.19.

104. Paternal weight plays important role in 'programming' diabetes in offspring through epigenetic changes - nutrition horizon. http://www.nutritionhorizon.com/news/Paternal-Weight-Plays-Important-Role-in-Programming-Diabetes-in-Offspring-through-Epigenetic-Changes.html.

105. Lindsay RS, Dabelea D, Roumain J, Hanson RL, Bennett PH, Knowler WC. Type 2 diabetes and low birth weight: The role of paternal inheritance in the association of low birth weight and diabetes. *Diabetes*. 2000;49(3):445-449.

106. Carone BR, Fauquier L, Habib N, et al. Paternally induced transgenerational environmental reprogramming of metabolic gene expression in mammals. *Cell*. 2010;143(7):1084-1096. doi: 10.1016/j.cell.2010.12.008; 10.1016/j.cell.2010.12.008.

107. Ding GL, Wang FF, Shu J, et al. Transgenerational glucose intolerance with Igf2/H19 epigenetic alterations in mouse islet induced by intrauterine hyperglycemia. *Diabetes*. 2012;61(5):1133-1142. doi: 10.2337/db11-1314; 10.2337/db11-1314.

108. Dolinoy DC, Faulk C. Introduction: The use of animals models to advance epigenetic science. *ILAR J*. 2012;53(3-4):227-231. doi: 10.1093/ilar.53.3-4.227; 10.1093/ilar.53.3-4.227.

109. Musicki B, Kramer MF, Becker RE, Burnett AL. Inactivation of phosphorylated endothelial nitric oxide synthase (ser-1177) by O-GlcNAc in diabetes-associated erectile dysfunction. *Proc Natl Acad Sci U S A*. 2005;102(33):11870-11875. doi: 10.1073/pnas.0502488102.

110. Wells,L., Vosseller,K., Hart G,W. A role for *N* -acetylglucosamine as a nutrient sensor and mediator of insulin resistance. *Cellular and Molecular Life Sciences*. 2003(2):222-228. doi: 10.1007/s000180300017.

111. Ande SR, Mishra S. Protein modification by β-N-acetyl glucosamine (O-GlcNAc) in insulin signaling and insulin resistance. *Recent Patents on Endocrine, Metabolic & Immune Drug Discovery*. 2010;4(2):161-171.

http://search.ebscohost.com/login.aspx?direct=true&db=a9h&AN=51992439&site=ehost-live.

112. Ruan HB, Han X, Li MD, et al. O-GlcNAc transferase/host cell factor C1 complex regulates gluconeogenesis by modulating PGC-1alpha stability. *Cell Metab*. 2012;16(2):226-237. doi: 10.1016/j.cmet.2012.07.006; 10.1016/j.cmet.2012.07.006.

113. Zeidan Q, Hart GW, Zeidan Q, Hart GW. The intersections between O-GlcNAcylation and phosphorylation: Implications for multiple signaling pathways [commentary]. *J Cell Sci*. 2009;123(1):13-22. http://jcs.biologists.org. doi: 10.1242/jcs.053678.

Appendix

Animal Care and Use Committee Letters of Approval and Amendments

The documentation on the following pages certifies that all experimental procedures performed on animals during this study were reviewed and approved by the Animal Care and Use Committee.

East Carolina University

1907-2007
CENTENNIAL

imal Care and
Committee
212 Ed Warren Life
Sciences Building
East Carolina University
Greenville, NC 27834

252-744-2436 office
252-744-2355 fax

May 24, 2010

Alexander Murashov, Ph.D.
Department of Physiology
Brody 6N-98
ECU Brody School of Medicine

Dear Dr. Murashov:

Your Animal Use Protocol entitled, "Effect of Paternal High Fat Diet and Exercise on Offspring Predisposure to Diabetes in Mice," (AUP #Q290) was reviewed by this institution's Animal Care and Use Committee on 5/24/10. The following action was taken by the Committee:

"Approved as submitted"

A copy is enclosed for your laboratory files. Please be reminded that all animal procedures must be conducted as described in the approved Animal Use Protocol. Modifications of these procedures cannot be performed without prior approval of the ACUC. The Animal Welfare Act and Public Health Service Guidelines require the ACUC to suspend activities not in accordance with approved procedures and report such activities to the responsible University Official (Vice Chancellor for Health Sciences or Vice Chancellor for Academic Affairs) and appropriate federal Agencies.

Sincerely yours,

Robert G. Carroll, Ph.D.
Chairman, Animal Care and Use Committee

RGC/jd

enclosure

East Carolina University

Animal Care and
Use Commitee
212 Ed Warren Life
Sciences Building
East Carolina University
Greenville, NC 27834

252-744-2436 office
252-744-2355 fax

June 22, 2012

Alexander Murashov, MD, Ph.D.
Department of Physiology
Brody 6N-98
ECU Brody School of Medicine

Dear Dr. Murashov:

The Amendment to your Animal Use Protocol entitled, "Effect of Paternal High Fat Diet and Exercise on Offspring Predisposure to Diabetes in Mice", (AUP #Q290) was reviewed by this institution's Animal Care and Use Committee on 6/22/12. The following action was taken by the Committee:

"Approved as amended"

****Please contact Dale Aycock prior to any hazard use**

A copy of the Amendment is enclosed for your laboratory files. Please be reminded that all animal procedures must be conducted as described in the approved Animal Use Protocol. Modifications of these procedures cannot be performed without prior approval of the ACUC. The Animal Welfare Act and Public Health Service Guidelines require the ACUC to suspend activities not in accordance with approved procedures and report such activities to the responsible University Official (Vice Chancellor for Health Sciences or Vice Chancellor for Academic Affairs) and appropriate federal Agencies.

Sincerely yours,

Scott E. Gordon, Ph.D.
Chairman, Animal Care and Use Committee

SEG/jd

enclosure

East Carolina University

mal Care and
se Commitee
212 Ed Warren Life
Sciences Building
East Carolina University
Greenville, NC 27834

252-744-2436 office
252-744-2355 fax

July 14, 2010

Alexander Murashov, M.D., Ph.D.
Department of Physiology
Brody 6N-98
ECU Brody School of Medicine

Dear Dr. Murashov:

The Amendment to your Animal Use Protocol entitled, "Effect of Paternal High Fat Diet and Exercise on Offspring Predisposure to Diabetes in Mice", (AUP #Q290) was reviewed by this institution's Animal Care and Use Committee on 7/14/10. The following action was taken by the Committee:

"Approved as amended"

A copy of the Amendment is enclosed for your laboratory files. Please be reminded that all animal procedures must be conducted as described in the approved Animal Use Protocol. Modifications of these procedures cannot be performed without prior approval of the ACUC. The Animal Welfare Act and Public Health Service Guidelines require the ACUC to suspend activities not in accordance with approved procedures and report such activities to the responsible University Official (Vice Chancellor for Health Sciences or Vice Chancellor for Academic Affairs) and appropriate federal Agencies.

Sincerely yours,

Robert G Carroll, Ph.D

Robert G. Carroll, Ph.D.
Chairman, Animal Care and Use Committee

Only C57BLc

393 → 4/19/11

RGC/jd

enclosure

East Carolina University

Animal Care and Use Commitee
212 Ed Warren Life Sciences Building
East Carolina University
Greenville, NC 27834

252-744-2436 office
252-744-2355 fax

September 18, 2012

Alex Murashov, MD, Ph.D.
Department of Physiology
Brody 6N-98
ECU Brody School of Medicine

Dear Dr. Murashov:

The Amendment to your Animal Use Protocol entitled, "Effect of Parental High Fat Diet and Exercise on Offspring and Predisposure to Diabetes in Mice", (AUP #Q290) was reviewed by this institution's Animal Care and Use Committee on 9/18/12. The following action was taken by the Committee:

"Approved as amended"

****Please contact Dale Aycock prior to any hazard use**

A copy of the Amendment is enclosed for your laboratory files. Please be reminded that all animal procedures must be conducted as described in the approved Animal Use Protocol. Modifications of these procedures cannot be performed without prior approval of the ACUC. The Animal Welfare Act and Public Health Service Guidelines require the ACUC to suspend activities not in accordance with approved procedures and report such activities to the responsible University Official (Vice Chancellor for Health Sciences or Vice Chancellor for Academic Affairs) and appropriate federal Agencies.

Sincerely yours,

SB McRae

Susan McRae, Ph.D.
Chair, Animal Care and Use Committee

SM/jd

enclosure